Memoirs of the Faculty of Engineering, Nagoya University
Vol. 41, No. 2 (1989)

DEVELOPMENT OF A NEW TYPE OZONIZER

CHOBEI YAMABE and KENJI HORII

Department of Electrical Engineering

(Received October 31, 1989)

Abstract

Fundamental studies of a new type ozonizer without dielectrics have been carried out. The rate constant k_1 for $O+O_2+O_2 \rightarrow O_3+O_2$ has been measured by the absorption measurements using a 253 nm line of a mercury lamp and is estimated about 2.2×10^{-34} cm^6 sec^{-1}. The ozone generation characteristics are also measured for various parameters, such as the charging voltage, gas mixture ratio, steepness of the waveform of the applied voltage and the gap spacing of the main electrodes so on.

A new type ozonizer with double discharge also has been proposed to improve the efficiency of the ozone generation. The mixtures of He/O_2 is effective to keep the discharge stable at atmospheric pressure and the maximum efficiency of the ozone generation of about 380 g/kWh has been obtained by a small-sized ozonizer. On the other hand, the efficiency of 400–450 g/kWh has been obtained by a large-sized one. The discharge volume for each ozonizer is about 23 cm^3 and 917 cm^3, respectively.

The superposition of the high frequency corona discharge (HFCD) during the main discharge is also effective to improve the efficiency of the ozone generation.

A simple electrical circuit which is able to obtain the applied voltage with the rapid rise time and control the delay time between the pre-discharge and the main-discharge is used. The effect of the series gap connected with the main electrodes on the ozone generation and the glow-to-arc transition is studied.

A coaxial cylindrical double discharge type ozonizer is made and the characteristics of the ozone generation are measured. It is confirmed that this device is able to operate stably in air at atmospheric pressure for the stored energy at least in the range of 0.05–0.8 J and the ozone of about 9 μg per one discharge is produced.

Contents

1. Characteristics of Ozone Generation by a New type Ozonizer

1. 1. Introduction

It is well known that the ozone is a very strong oxidizing agent and it follows to a fluorine for the force of oxidization among the oxidizing agents. For that reason, it has been used for the treatment of water and exhausted smoke, elimination of offensive order, bleaching, removal of organic matter and sterilization etc.. There is no trouble of the secondary contamination compared with chlorine which is used for the sterilization of drinking water because ozone resolves itself into oxygen finally, even though it would be used overmuch. The thermochemical reactions of ozone generation are given as follows.

$$O_2 \rightarrow O + O - 118\ kcal \qquad \text{(R-1)}$$

$$O + O_2 \rightarrow O_3 + 25\ kcal \qquad \text{(R-2)}$$

These equations being combined,

$$3O_2 \rightarrow 2O_3 - 68\ kcal \qquad \text{(R-3)}$$

That is, the energy of 34 kcal is required to generate 1 mole ozone and this energy corresponds to the ozone yield of about 1200 g/kWh. One of the biggest problems for the conventional ozonizer with a silent discharge is a large amount of power consumption (i.e. low ozone yield). The maximum ozone yield which has been obtained using silent discharge method is about 200 g/kWh with oxygen and about 90 g/kWh with air. It is an actual condition that these values are very small compared with the value of 1200 g/kWh. If these ozone yield are improved further, the rapid expansion of the applicable fields for the ozonizer will be expected.

As the oxygen is a negative gas and very sensitive for the electron attachment, the increasing of steepness of rise time of the applied voltage is useful[1),2)] for the establishment of uniform discharge and the improvement of ozone yield by the effective excitation of the oxygen molecules by electrons before the occurrence of the electron attachment.

A new type ozonizer without dielectrics between main electrodes has been made to investigate the possibility of the improvement of the ozone yield and the characteristics of the ozone generation.

1. 2. Experimental apparatus and procedure

The schematic diagram of the ozonizer is shown in Fig. 1. 1 (a). The capacity of an electronics boad used as a capacitor shown in Fig. 1. 1 is about 1600 pF. The thickness of the boad is about 1.6 mm. Both the anode and the cathode are made by copper tubes with the same diameter of 6 mm and about 25 cm long as shown in Fig. 1. 1 (b). The gap spacing is 5 mm. The mixtures of O_2/N_2, O_2/He, O_2/CO_2, O_2/Ar and O_2 only are used as the raw gas materials and their mixture ratio is varied properly. The repetition rate of the discharge is fixed at 1 Hz considering the exchange of the gas in the ozonizer. Both the main discharge current and the voltage across the main electrodes are measured by a low inductive resistance and C-R divider respectively. The generated ozone is measured chemically using Potassium Iodide solution. It has been known well that the ozone absorbs the light whose wavelength is about 250 nm as shown in Fig. 1. 2. Therefore the

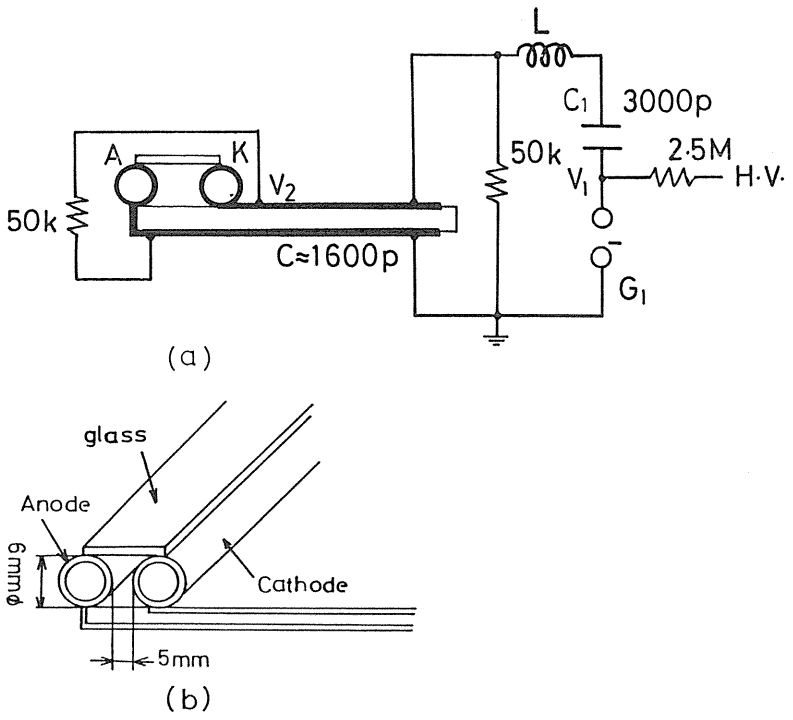

Fig. 1. 1 Schematic diagram of ozonizer

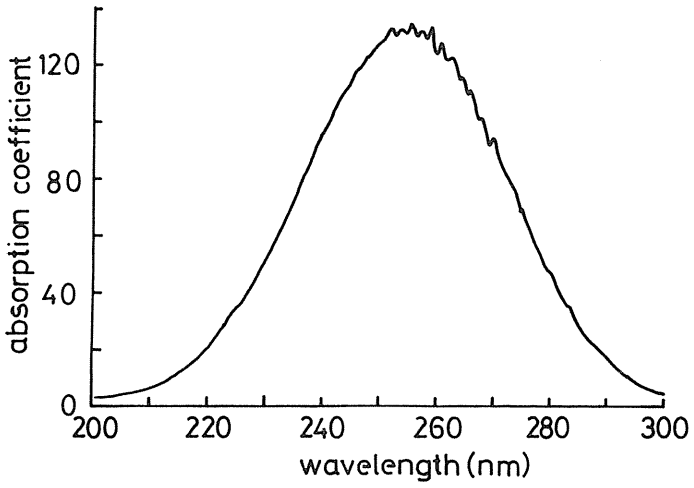

Fig. 1. 2 Absorption spectrum of ozone

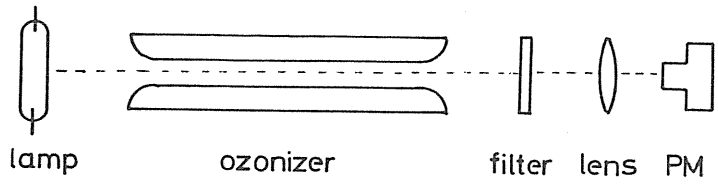

Fig. 1. 3 Block diagram for the absorption measurement at 253 nm

ozone generation with time is measured by the absorption measurement of the 250 nm emitted from a mercury lamp. The block diagram for the absorption measurement is shown in Fig. 1. 3. The 250 nm light is selected from the transmission light through the ozonizer by an interference filter ($\lambda_{max}=253$ nm, $\Delta\lambda_{1/2}=19.5$ nm) or monochrometer and its intensity with time is measured by a photomultiplier. It has been confirmed that the ozone which is generated directly by the irradiation of the mercury lamp is negligible small.

The following parameters which influence on the ozone generation are considered.

1) input energy into the discharge volume
2) gas composition in raw gas mixtures
3) humidity in the raw gas
4) steepness of the rise time of the applied voltage

The typical waveforms of the voltage across the main electrodes V_2 and main discharge current I are shown in Fig. 1. 4. In this case, O_2 only and $O_2/N_2=1/4$ mixture are used and the applied voltage V_1 on the capacitor C_1 is 20 kV. The steepness of the rise time of the applied voltage is about 0.1 kV/ns. The main discharge current builds up rapidly at near the peak of the voltage V_2 and the full width at half maximum of the current is about 30 ns.

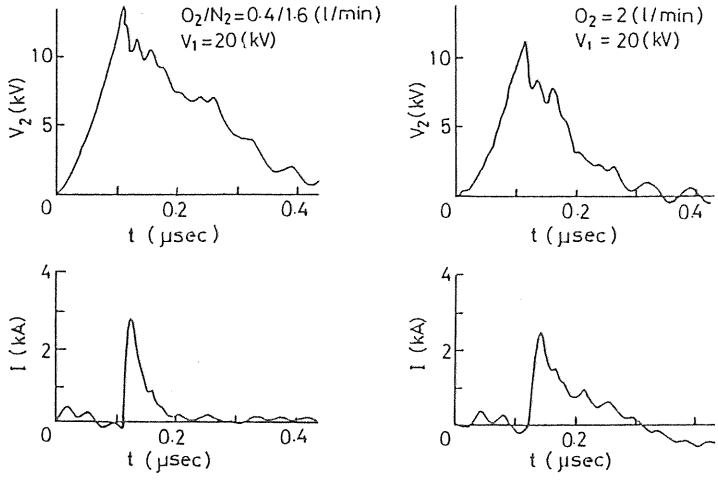

Fig. 1. 4 Typical waveforms of the voltage V_2 and main discharge current I in O_2/N_2 mixtures and O_2 only

1. 3. Experimental results

1. 3. 1 Effect of input energy on ozone generation

The amount of produced ozone per one discharge and the efficiency of ozone generation as a function of the input energy into the discharge volume are measured and the results are shown in Fig. 1. 5 (a) and (b). The input energy is calculated by the measured waveforms of the voltage V_2 and the current I. The ozone concentration increases with input energy and saturates at higher input energy due to the change of the discharge condition (i.e. glow-to-arc transition occurs) and NO_x generation by the discharge. That is, it seems that the dissociation of the oxygen does not occurs effectively by the change of the discharge condition. The influence of produced NO_x is discussed later. A maximum efficiency of ozone generation of about 20 g/kWh has been obtained at low input energy and the efficiency decreases at higher input energy. From these results, it is not always profitable for the increasing of the efficiency of the ozone generation to increase the input energy and it seems to be effective to generate a rather weak discharge.

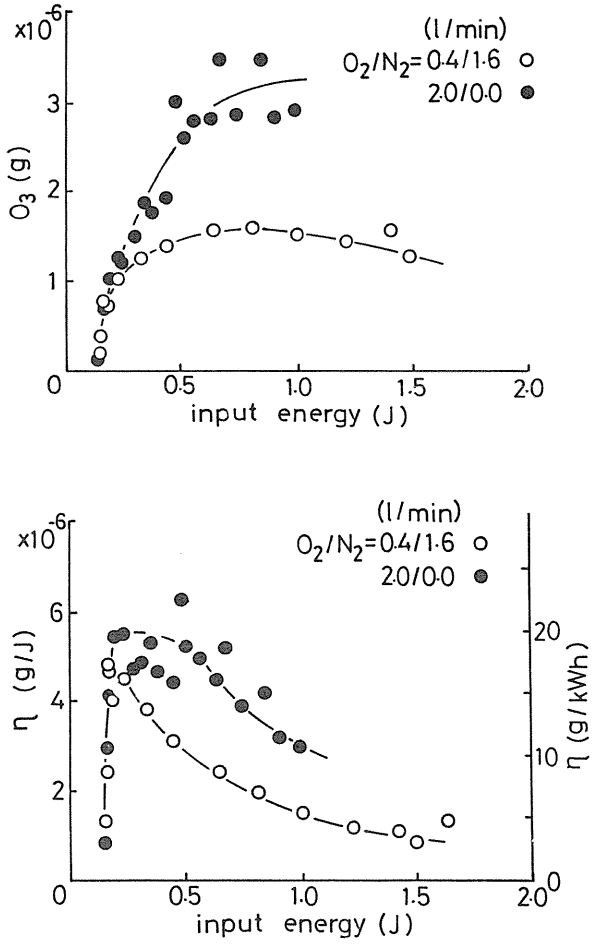

Fig. 1. 5 Amount of produced ozone per shot and efficiency of ozone generation vs. input energy

1. 3. 2. Effect of gas composition on ozone generation

The ozone concentration, the efficiency of the ozone generation and the spark onset voltage Vb are shown in Figs. 1. 6–1. 8 for the various gas mixtures of He/O_2, CO_2/O_2, N_2/O_2 and Ar/O_2. The ozone generation with both He/O_2 and CO_2/O_2 becomes maximum at the same mixture ratio of 1/1 and is two times larger compared with that with O_2 only. The nitrogen or argon being added, the ozone generation increases with oxygen concentration as shown in Fig. 1. 6. In case of mixtures with CO_2, the optimum percent of the oxygen for the efficiency of ozone generation shifts to the lower concentration of oxygen and appears at the oxygen concentration of about 20% as shown in Fig. 1. 7. The maximum value with CO_2 is about two times larger compared with the value with O_2 only. For the adding of nitrogen or argon, the efficiency of ozone generation increases with the oxygen concentration such as ozone concentration. The variation of the spark onset voltage Vb with oxygen concentration depends on the kind of gas mixtures as shown in Fig. 1. 8, that is, the spark onset voltage decreases for the nitrogen, increases for the argon and is about constant for the carbon dioxide with the oxygen respectively. According to the above results, it seems to be useful to mix the carbon dioxide or helium with the oxygen for increasing of the ozone concentration and the efficiency of ozone generation.

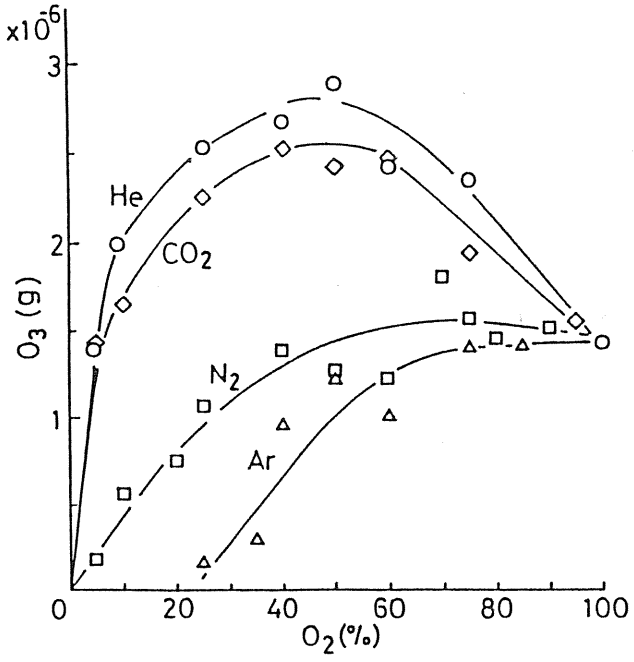

Fig. 1. 6 Amount of produced ozone per shot vs. percent of oxygen in various mixtures

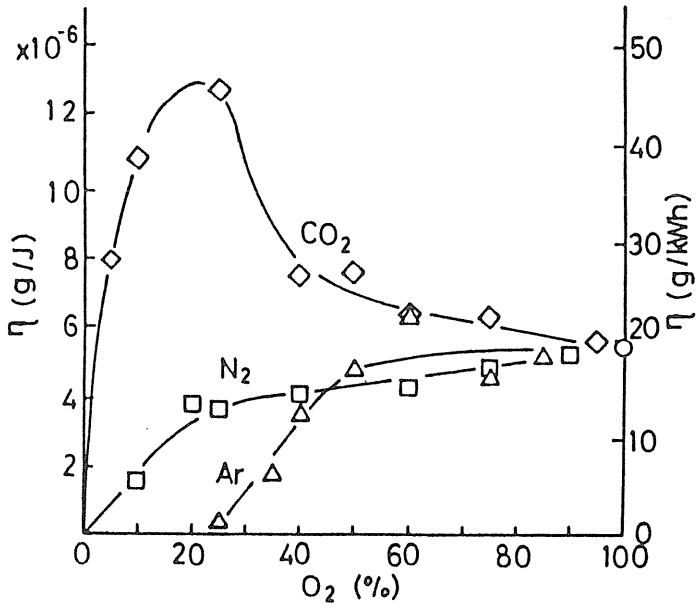

Fig. 1. 7 Efficiency of ozone generation vs. percent of oxygen in various mixtures

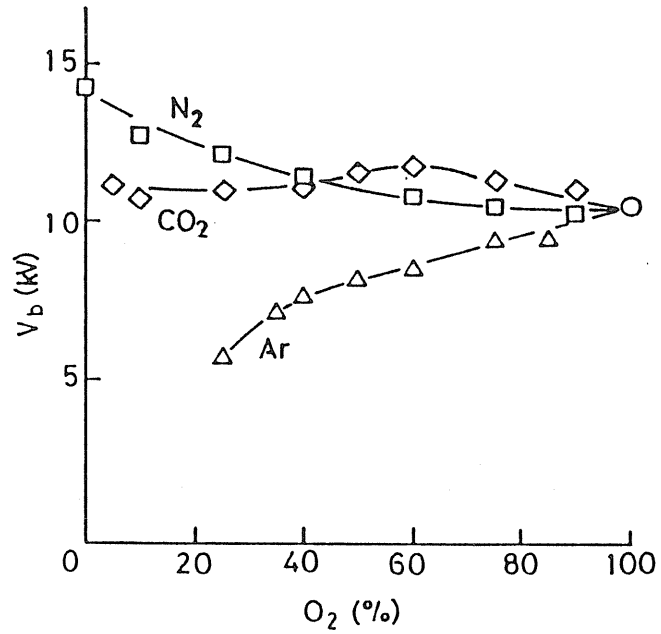

Fig. 1. 8 Spark onset voltage V_b vs. percent of oxygen in various mixtures

1. 3. 3 Effect of humidity in the raw gas

The influence of humidity in the raw gas (air) on the ozone generation has been measured for the next both cases (i) the raw gas is fed to the ozonizer after passing through the silica gel (ii) the raw gas is fed to the ozonizer directly from an air compressor. The results are shown in Fig. 1. 9. The ozone concentration with dried raw gas is about five times larger compared with that without treatment. But, the raw gas used except air in this experiment is fed directly from a tank to the ozonizer so it seems that the influence of the humidity on the ozone generation is relatively small.

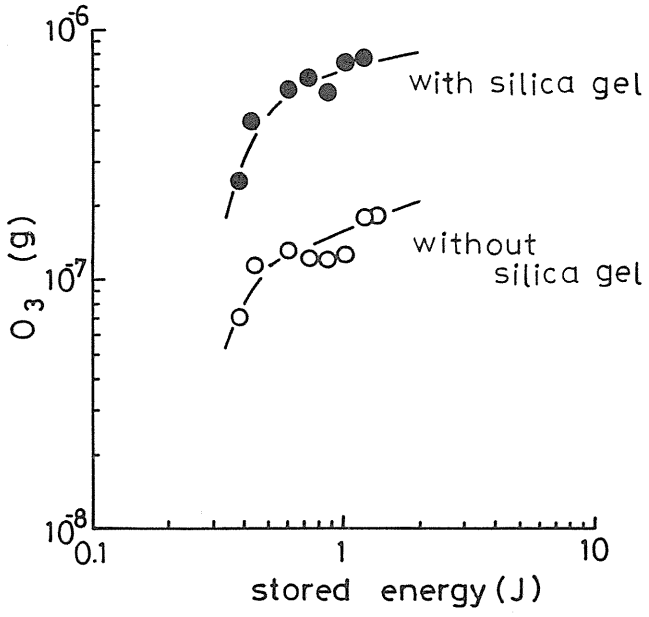

Fig. 1. 9 Affect of humidity on ozone generation

1. 3. 4 Effect of the steepness of rise time of applied voltage on the ozone generation and spark onset voltage

The inductance L shown in Fig. 1. 1 is used to vary the steepness of rise time of the applied voltage. The oxygen only (=2.0 l/min) and the mixture of O_2/N_2 (=0.4/1.6 l/min) are used as the raw gas at V_1=20 kV. The ozone concentration increases with the average steepness of the voltage Vb/t_1 as shown in Fig. 1. 10 and the spark onset voltage Vb decreases with the value of Vb/t_1 as shown in Fig. 1. 11. The time t_1 shows the time up to the peak of the voltage as shown in Fig. 1. 10. It is important for the increasing of the ozone concentration to make the steepness of rise time of the applied voltage increase from the above results.

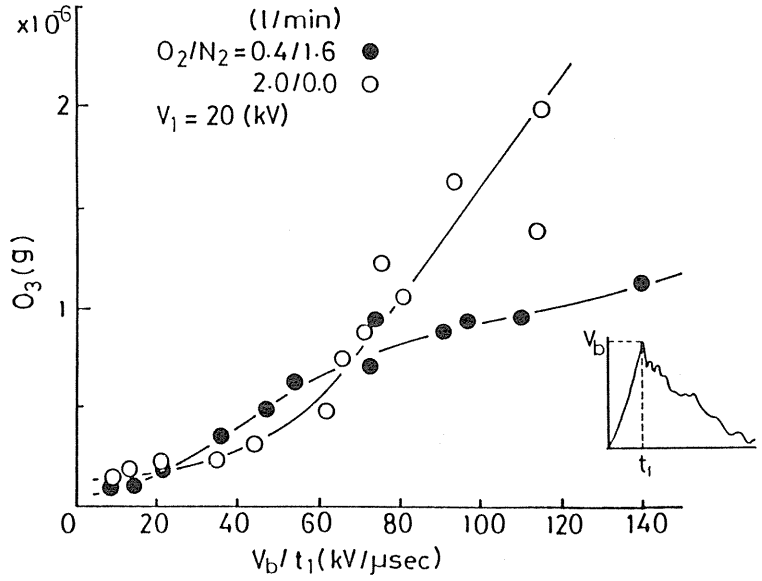

Fig. 1. 10 Ozone concentration vs. average steepness of rise time of applied voltage

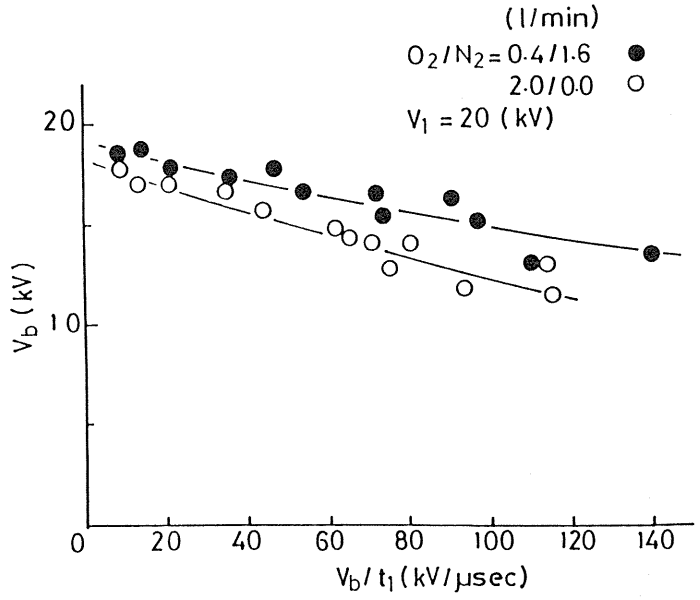

Fig. 1. 11 Spark onset voltage V_b vs. average steepness V_b/t_1

1. 3. 5. Measurements of the rate constant of the ozone generation

Assuming that the oxygen atoms are generated during the discharge and after the discharge, the ozone is mainly generated by the following reaction.

$$O + O_2 + M \rightarrow O_3 + M \qquad \text{(R-4)}$$

The variation of oxygen atoms with time is given by the following equation.

$$In[O]/[O]_i = -k_1^* t \qquad (1)$$

Where, $k_1^* = K_1[O_2][M]$, $[O]_i$ is the number of generated oxygen atoms at the end of discharge (t=0) and M is the third body. Assuming that all of oxygen atoms finally turn into the ozone molecules, the equation (1) is substituted by the following equation.

$$In[\{[O_3]_f - [O_3]\}/[O_3]_f] = -k_1^* t \qquad (2)$$

Where, $[O_3]_f$ is the ozone concentration at $t=\infty$.

The law of Lambert-Beer being applied to the intensity of transmittance light and the ozone concentration,

$$InIn[I_t/I_f] = -k_1^* t + c_1 \qquad (3)$$

$$In[In(I_t/I_f)/In(I_i/I_f)] = -k_1^* t + c_2 \qquad (4)$$

where, I_i, I_f and I_t are the intensity of the transmittance light at t=0, and t respectively. Consequently, the value of k_1^* can be obtained by the measurements of I_t and I_f. Typical observed waveforms of the discharge light and the transmittance light which is absorbed by the ozone in the mixture of O_2/He = 1/4 at V_1 = 8 kV are shown in Fig. 1. 12 (a) and

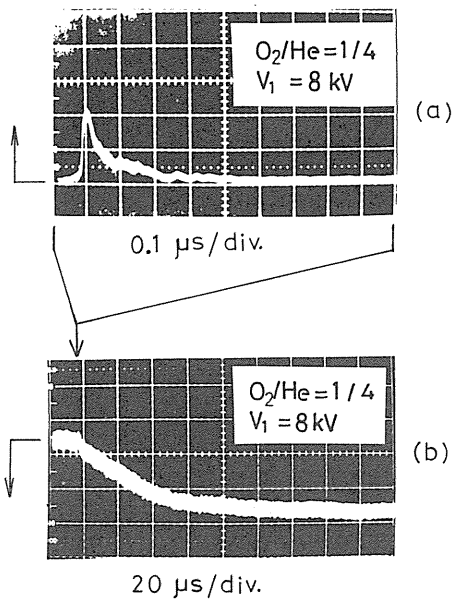

Fig. 1. 12 Typical waveforms of discharge light (a) and transmittance light through ozonizer at 253 nm (b) in mixture of O_2/He=1/4 at V_1=8 kV

(b). The experimental results for the variation of the intensity of the transmittance light with time are shown in Figs. 1. 13 and 1. 14. The results shown in Fig. 1. 13 have been obtained as a parameter of the applied voltage V_1 in the fixed mixture ratio of $O_2/He = 1/5$. The variation of the intensity of the transmittance light is almost same when the applied voltage V_1 is changed from 8 kV to 10 kV. These results show that the reactions between produced particles by the discharge can be neglected. The variation of the intensity of the transmittance light at $V_1 = 9$ kV is shown in Fig. 1. 14 for various mixtures of O_2/He. The value of k_1^* obtained from the slope of the lines in Fig. 1. 14 against the percent of the oxygen are shown in Fig. 1. 15. The k_1^* increases with the percent of the oxygen and is about 13.2×10^{-4} sec^{-1} at 100% oxygen. Assuming that the ozone generation depends on the reactions of (R-4) and (R-5), the rate constant k_1 is given by the following equation, $k_1 = k_1^* / [O_2][O_2] = 2.2 \times 10^{-34}$ $cm^6 sec^{-1}$. This value is about 0.3 times smaller compared with the value of 6.3×10^{-34} $cm^6 sec^{-1}$ obtained previously.[3)]

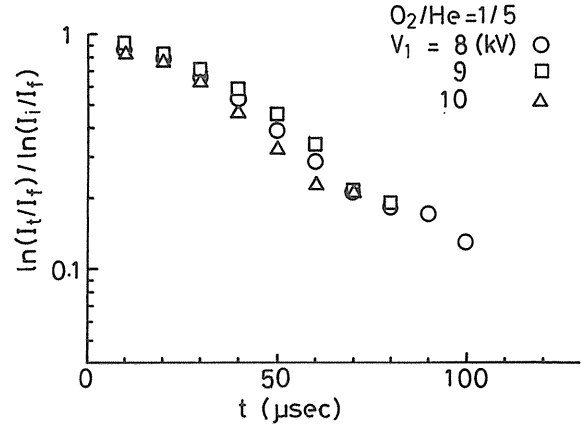

Fig. 1. 13 Variation of intensity of transmittance light with time for various voltage V_1 in O_2/He=1/5 mixtures

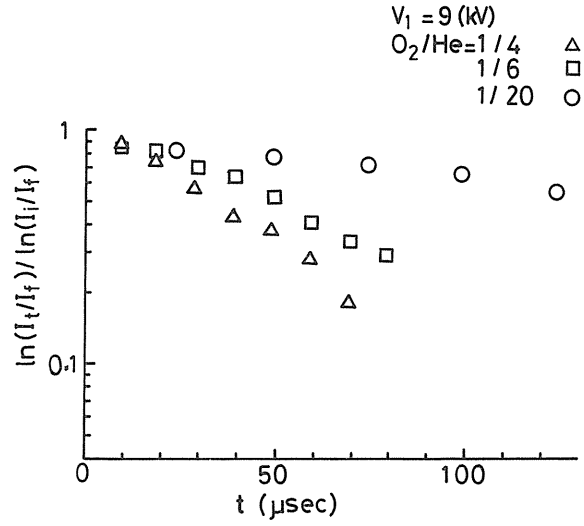

Fig. 1. 14 Variation of intensity of transmittance light with time for various O_2/He mixtures at V_1=9 kV

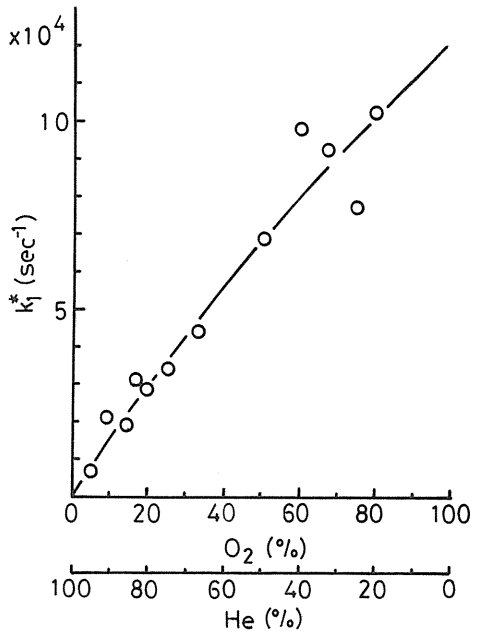

Fig. 1. 15 Values of k_1^* vs. percent of oxygen and helium

1. 4. Discussion

A comparison of the ozone generation characteristics in oxygen only and O_2/N_2 mixture is discussed here. The main ozone generation and destruction reactions in both oxygen only and O_2/N_2 mixtures are as follows.[4)]

$$O_2 + e \xrightarrow{k_0} 2O + e \qquad \text{(R-5)}$$

$$O + O_2 + O_2 \xrightarrow{k_1'} O_3 + O_2 \qquad \text{(R-6)}$$

$$O + O_3 \xrightarrow{k_2} 2O_2 \qquad \text{(R-7)}$$

$$e + O_3 \xrightarrow{k_3} O_2 + O + e \qquad \text{(R-8)}$$

$$O + O_2 + N_2 \xrightarrow{k_1''} O_3 + N_2 \qquad \text{(R-9)}$$

$$N_2 + e \xrightarrow{k_4} N_2^* + e \qquad \text{(R-10)}$$

$$N_2^* + O_2 \xrightarrow{k_5} 2O + N_2 \qquad \text{(R-11)}$$

$$N_2^* + N_2 \xrightarrow{k_6} N_2 + N_2 \qquad \text{(R-12)}$$

$$N_2^* + O_2 \xrightarrow{k_7} O_2 + N_2 \qquad \text{(R-13)}$$

$$N_2^* + O_3 \xrightarrow{k_8} O_2 + O + N_2 \qquad \text{(R-14)}$$

The rate constants k_0, k_3, and k_4 depend on the electron energy distribution, and k_1', k_2, k_5-k_8 depend on the gas temperature in the reaction volume. An excited nitrogen molecule N_2^* which has enough energy to dissociate a molecule. On the other hand, the characteristics of the ozone concentration in both oxygen only and $O_2/N_2 = 1/4$ are shown in Figs. 1. 5–1. 7. These results being compared, although the amount of oxygen in $O_2/N_2 = 1/4$ mixtures is one one fifth compared with that in oxygen only, both the oxygen concentration and the efficiency of ozone generation in O_2/N_2 mixtures are about a half and they are not proportional to the oxygen concentration. The decrease of the ozone concentration with the input energy appears at high input energy into the discharge volume in O_2/N_2 mixtures as shown in Fig. 1. 5 (a).

When the nitrogen is included in the raw gas, the excited nitrogen molecules N_2^* and NO_x are produced by the discharge. The excited nitrogen molecules N_2^* can dissociate the oxygen molecules in the reaction (R-11) and acts to increase the ozone concentration. On the other hand, the NO_x molecules seem to act to decrease the ozone concentration by the following reactions.[5)]

$$O + NO_2 \rightarrow NO + O_2 \qquad \text{(R-15)}$$

$$NO + O_3 \rightarrow NO_2 + O_2 \qquad \text{(R-16)}$$

The influence of N_2^* and NO_x on the ozone generation process is discussed. The molecules of $N_2(A^3\Sigma u^+)$ and $N_2(B^3\Pi_g)$ are thought to be the excited nitrogen molecules N_2^* which produce the atomic oxygen by the reactions of (R-10) and (R-11).[6)] These $N_2(A)$ and $N_2(B)$ molecules have larger energy than 5. 1 eV which is a dissociation energy of an oxygen molecule and the excitation probability of these $N_2(A)$ and $N_2(B)$ molecules by the collisions with electrons is high. A de-excitation of $N_2(A)$ occurs mainly by collisions with oxygen molecules and the oxygen molecules of the ground state $O_2(X)$ are excited to $O_2(B^3\Sigma_g^-)$ mainly by an electric transfer and the atomic oxygen is generated immediately by the dissociation of $O_2(B)$ as shown by the following reactions.[7)]

$$N_2(A) + O_2(X) \rightarrow N_2(X) + O_2(B) \qquad \text{(R-17)}$$

$$\rightarrow N_2(X) + O(1D) + O(3P) \qquad \text{(R-18)}$$

According to the previous results which have been obtained by the conventional ozonizer, the ozone concentration saturates and finally decreases to zero when the input power increases in air. It is considered that the destruction of the ozone occurs mainly by the generated NO_x molecules.[8)] The amount of NO_x generated by the discharge is measured as functions of the input energy and the ratio of O_2/N_2 respectively and these results are shown in Fig. 1. 16 and Fig. 1. 17. The measured ozone concentration is also shown in both figures. Both concentration of NO and NO_x increase rapidly at the input energy of about 0.7 J. At the low input energy (less than 0.7 J), the interaction between the ozone and NO_x molecules can be neglected in order to the rich of ozone concentration

compared with that of NO_x. But, when the ozone concentration saturates and the concentration of NO and NO_x becomes high enough, the interaction is not neglected and the ozone concentration decreases with the input energy. Although both concentration of NO and NO_x are maximum at the ratio of $O_2/N_2 = 1/4$ as shown in Fig. 1. 17, they are very small amount of values (i.e. 1 ppm for NO_x and 0.3 ppm for NO). In this case, the destruction of ozone by NO_x seems to be neglected due to the small concentration of NO_x compared with the ozone concentration. The ozone concentration of 1 μg corresponds to about 66 ppm.

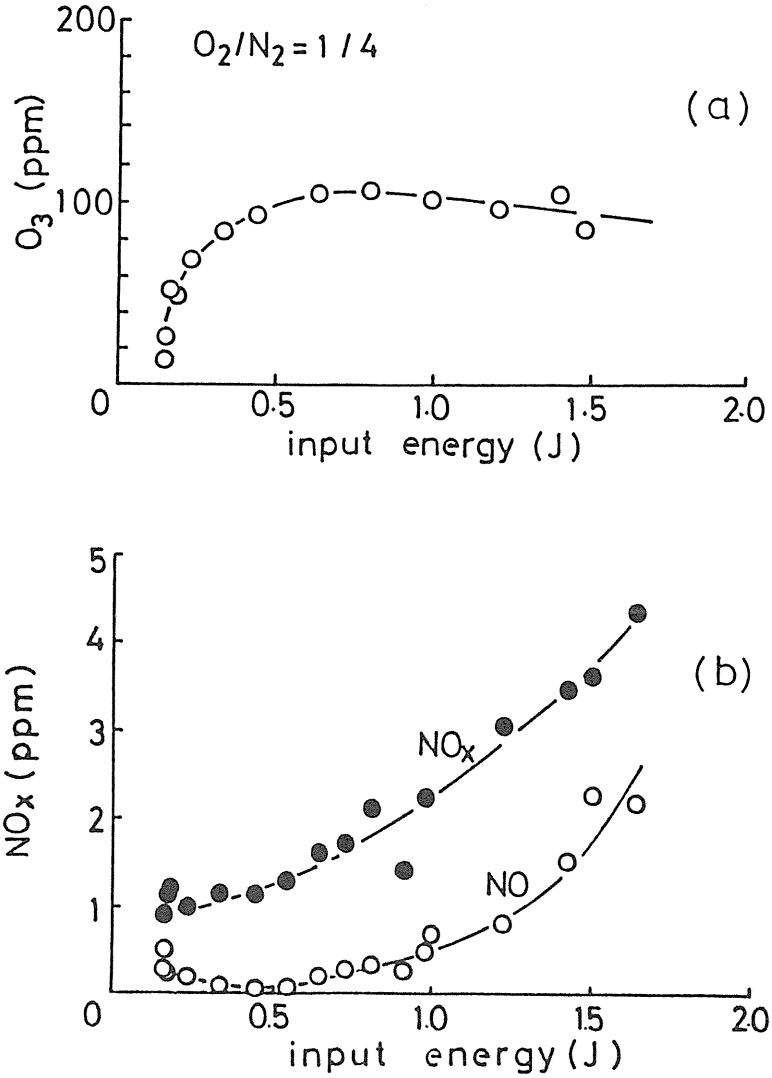

Fig. 1. 16 Ozone concentration vs. input energy (upper), and NO_x and NO concentration vs. input energy (lower) in $O_2/N_2=1/4$ mixtures

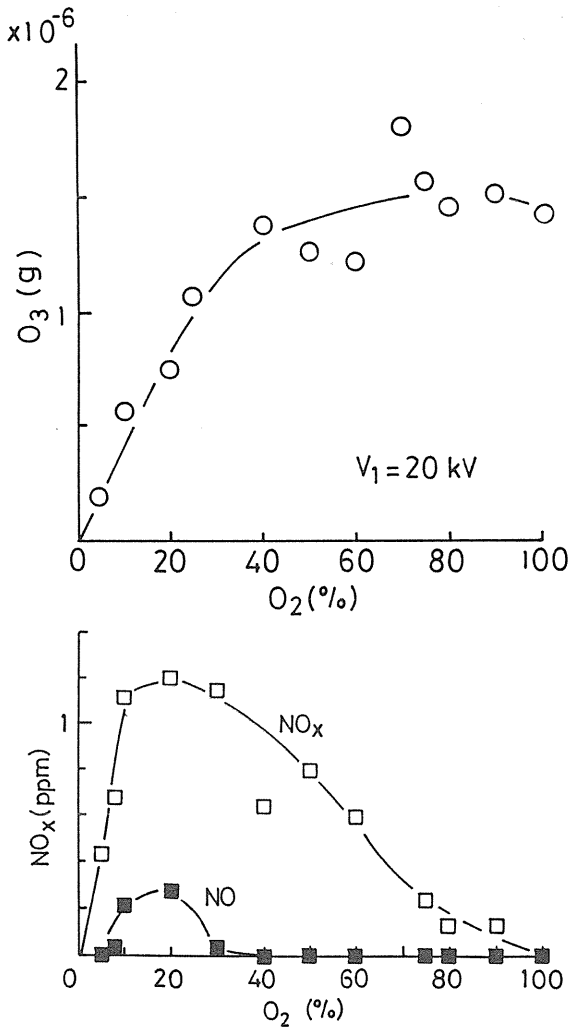

Fig. 1. 17 Ozone concentration vs. percent of oxygen (upper), and NO_x and NO concentration vs.

1. 5. Conclusions

The ozonizer without dielectrics between the main electrodes has been made to study the characteristics of the ozone generation in the various gas mixtures. Although the obtained ozone yield of about 20 g/kWh is lower compared with that of the conventional silent discharge type, it is expected that the ozone yield will be increased if the steepness of the rise time of the applied voltage is more increased. These results are reported later.

The rate constant k_1 for $O+O_2+O_2 \rightarrow O_3+O_2$ has been measured by the absorption method using the wavelength of 253 nm and is about 2.2×10^{-34} cm^6sec^{-1}.

2. *Ozone generation characteristics of a new type ozonizer with double discharge*

2. 1. *Introduction*

The ozone has many applications for such as the treatment of drinking water, the elimination of NO_x, the removal of offensive odor, bleaching, etc. which are mentioned in chapter 1. These applications with ozone cause no environmental problems, but at present, the production cost of ozone is much higher than that with chlorine. Therefore, it is very important to reduce the cost improving the efficiency of ozone production. Although the efficiency of ozone production by the conventional type ozonizers using silent discharge with a dielectric on the electrode has been made progress, it's value almost saturates. For that reason, the development of a new type ozonizer is required to overcome this saturation. The new type ozonizer using a discharge directly between metal electrodes was made and a double discharge method was applied to the new type ozonizer to increase the ozone generating volume and to keep the discharge glow.[9),10)] Some parameters such as rise time of the applied voltage, oxygen flow rate, etc. which make effect on the ozone generation have been changed to measure the characteristics of the new type ozonizer.

2. 2. *Experimental apparatus and procedure*

The schematic diagram of the new type ozonizer is shown in Fig. 2. 1. Both the cathode and the anode made by duralumin have a diameter of 12 cm for a small-sized device and the main gap spacing is 2.5 cm. The effective discharge volume for both devices is shown in Table 2. 1. The anode is the Rogowski shape and a trigger electrode covered with a Pylex glass tube (diameter: 4 mm, thickness: 1.2 mm) is put into a groove

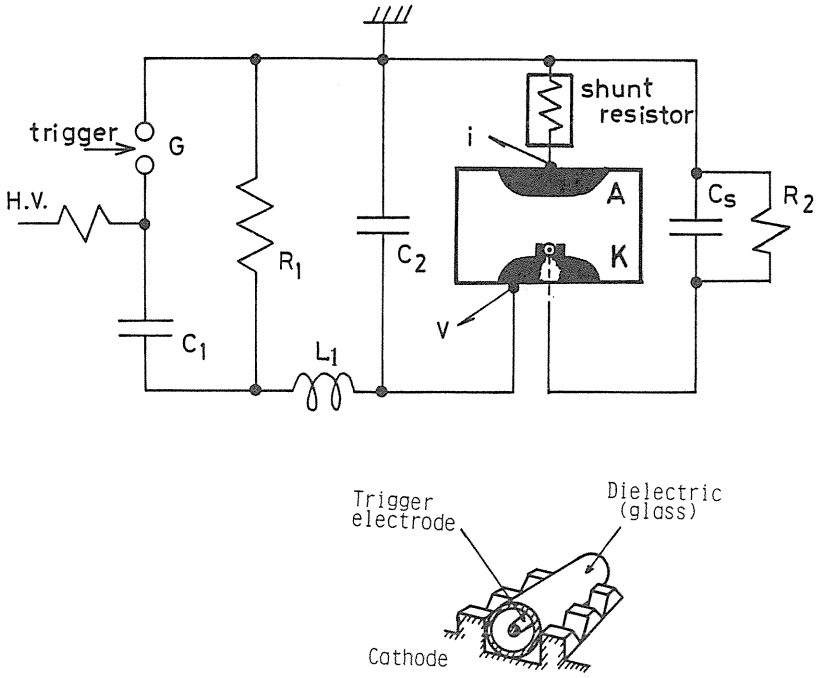

Fig. 2. 1 Schematic diagram of new type ozonizer and the shape of cathode

Table 2. 1 Parameters for small-sized and large-sized ozonizers

	type of size	
	small- sized	large-sized
gap spacing d (mm)	25	30
discharge area on anode(cm^2)	13	306
discharge volume (cm^3)	22.5	917

on the cathode and is earthed through a capacitor C_s. The size of the groove is 4.5 mm wide and 3 mm deep. Thirty two protrusions with the shape of trapezoid (upper side: 2 mm, lower side: 3 mm, height: 1.7 mm) are distributed on each side of the groove along the glass tube to prevent the glow-to-arc transition of the main discharge. The capacitor C_s is connected with the capacitor Ct of the glass tube in series and the applied voltage between the cathode and the trigger electrode is divided by these capacitors. Consequently, the applied voltage to the glass tube is reduced and its electrical destruction is prevented. It is also limited to flow more energy than needed through the trigger circuit. The electrical circuit for the pulse forming is composed of capacitor C_1 charged at V_1, inductance L_1, peaking capacitor C_2 and trigger gap G_1 pressurized with nitrogen gas. After the gap G_1 is closed, the capacitor C_2 is charged through the inductance L_1. During this procedure, a high electric field appears between the cathode K and the trigger electrode, then a pre-discharge which looks like a silent discharge occurs in the small gap between the surface of the glass tube and the cathode. At the same time, the weak discharge with uniform intensity along the surface of the glass tube appears. Before the main discharge occurs, the time variation of the voltage V_2 on the cathode is given by the following equation.

$$V_2 = C_1 V_1 (1 - \cos\omega t)/(C_1 + C_2) \tag{2.1}$$

where, $\omega = 1/\sqrt{LC}$ and $1/C \approx 1/C_1 + 1/C_2$.
In this case, the current which passes through the trigger circuit is small enough to be neglected. At the first stage of the main discharge, the current builds up rapidly in the low inductive circuit which is composed of capacitor C_2- anode- main discharge region- cathode- C_2. After the current builds up sufficiently, it is continued to supply the charge from the capacitor C_1 through the inductance L_1 gradually. The voltage V_2 and the main discharge current I are measured by a high voltage probe (Tektronix P6015) and a shunt respectively. Both the input energy and the injected charge into the discharge volume are calculated by these measured waveforms. Some kinds of mixtures, such as $CO_2/He/O_2$, He/O_2 and He/air are used for the ozone generation and the generated ozone is analyzed chemically by the Potassium Iodide solution.

2. 3. *Experimental results*

2. 3. 1. *Improvement of the ozone generation with He/O_2 mixtures*

Both $CO_2/He/O_2$ and $CO_2/N_2/O_2$ mixtures have been used for the ozone generation because this new type ozonizer comes from the application of TEA (Transversely Excited Atmospheric) CO_2 laser device.[10]

The generated ozone, injected charge into the discharge volume Q and the efficiency of ozone generation as a function of the applied voltage V_1 are measured with the mixtures of $CO_2/He/O_2 = 0.1/7.0/0.12$ l/min and $V_1 = 15-28$ kV. In this case, the lumped inductance L_1 is not used (i.e. only the inductance of the cable). The results are shown in Figs. 2. 2 and 2. 3. Both the generated ozone and the injected charge increase with the applied voltage V_1. The glow-to-arc transition is not observed in these experiments. Since only the diffuse glow discharge appears, the discharge volume is almost constant. The increase of the generated ozone seemes due to the increasing of the injected charge for the dissociation of the oxygen molecules. The efficiency of the ozone generation is nearly constant for the applied voltage because both the generated ozone and the input energy into the discharge volume increase with the applied voltage.

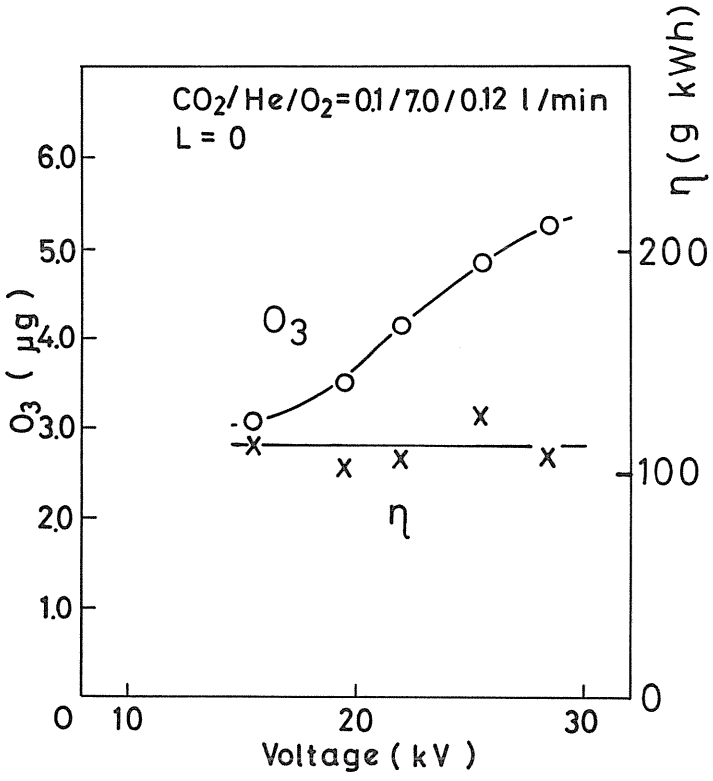

Fig. 2. 2 Generated ozone and efficiency vs. applied voltage

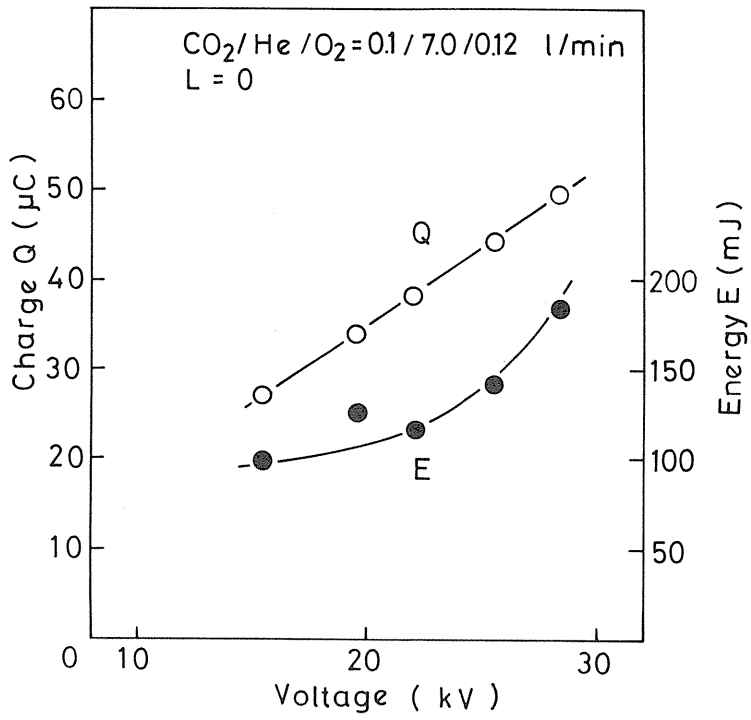

Fig. 2. 3 Injected charge Q and input energy E vs. applied voltage

Both the generated ozone and the glow-to-arc transition rate are measured at the oxygen flow rate of 0.07–0.3 l/min at constant mixture ratio of CO_2/He = 0.1/7.0 l/min and voltage V_1 = 19 kV. The definition of the glow-to-arc transition rate is as follows.

$$\text{glow-to-arc transition rate (\%)} = \frac{\text{total number of discharge with transition}}{\text{total number of discharge shots}} \times 100 \qquad (2.2)$$

The repetition of the discharge is 1 pps. The results are shown in Fig. 2. 4. According to the observation of the discharge, the stable glow discharge is obtained and the transition does not occur at all at the oxygen flow rate of 0.07 l/min. But, at larger than the flow rate of 0.15 l/min, the discharge tends to be unstable and the transition rate increases rapidly and is almost 100% at 0.3 l/min as shown in Fig. 2. 4. The generated ozone increases rapidly with the oxygen flow rate and is maximum at about 0.15 l/min. But, it decreases with the oxygen flow rate at larger than the value of 0.15 l/min. Since the

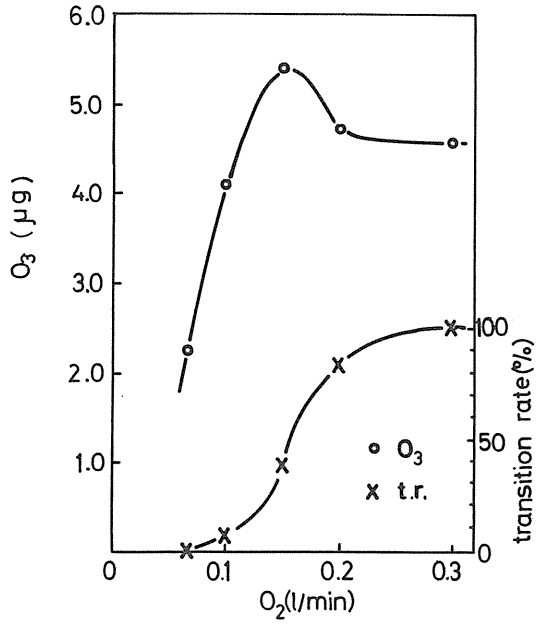

Fig. 2. 4 Generated ozone and glow-to-arc transition vs. oxygen flow rate

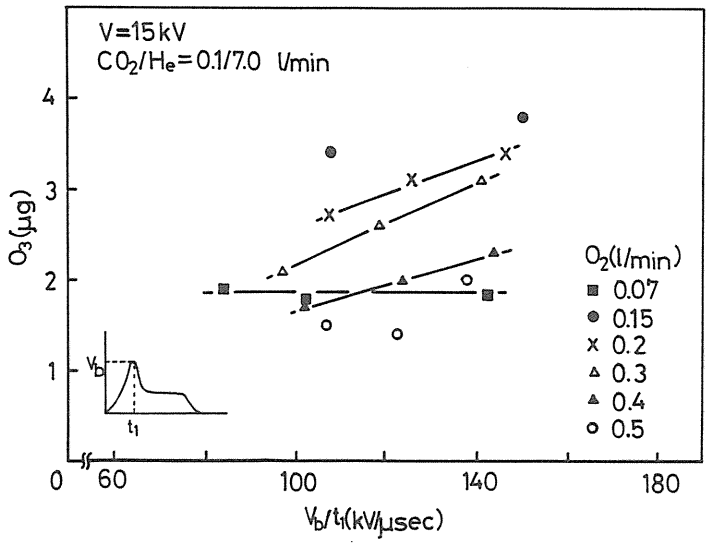

Fig. 2. 5 Generated ozone vs. steepness of the voltage V_b/t_1 for various oxygen flow rate at 15 kV

reduction of the ozone generation appears at the transition rate of about 50%, it seems that the discharge condition changes. That is, the transition from the stable diffuse glow discharge to the intensive arcing which concentrates on a point occurs and the effective discharge volume for the ozone generation reduces. The injected charge into the discharge volume decreases with the oxygen flow rate.

The generated ozone per one shot as the function of the steepness of the waveform of the applied voltage V_b/t_1 is shown in Fig. 2. 5 in the mixtures of $CO_2/He/O_2$. Here, the voltage V_b is the maximum value of the voltage applied across the main electrodes and the time t_1 is the duration between the starting point of the voltage and the maximum point as shown in Fig. 2. 5. The oxygen flow rate used here is in the range of 0.07–0.5 l/min and the steepness of the waveform is varied by changing the lumped inductance L_1 (=0, 5.1, 9.6 μH) in Fig. 2. 1. In this case, the charging voltage V_1 is fixed at 15 kV. The generated ozone increases with the steepness of the applied voltage due to the improvement of the discharge condition for the gas mixtures of $CO_2/He/O_2 = 0.1/7.0/X$, (X=0.15, 0.2, 0.3, 0.4 l/min). When the oxygen flow rate X increases, the generated ozone decreases. At X=0.15 l/min, the transition does not appear at all with the largest steepness (i.e. $L_1 = 0$ μH), but it appears with the lower steepness ($L_1 = 9.6$ μH) and the transition rate is almost 100% at $X > 0.2$ l/min with the various steepness. On the other hand, in case that only the uniform glow discharge is obtained ($X = 0.07$ l/min), the generated ozone is almost constant with the steepness. Generally, the generated ozone increases with the steepness except the case of $X = 0.07$ l/min because the transition is hard to appear with larger steepness as shown in Fig. 2. 6 due to the better uniformity of the discharge. The experimental results mentioned above are considered by both the applied voltage across the main electrodes and the main discharge current. The breakdown voltage V_b becomes large and the duration t_1 becomes long with the oxygen flow

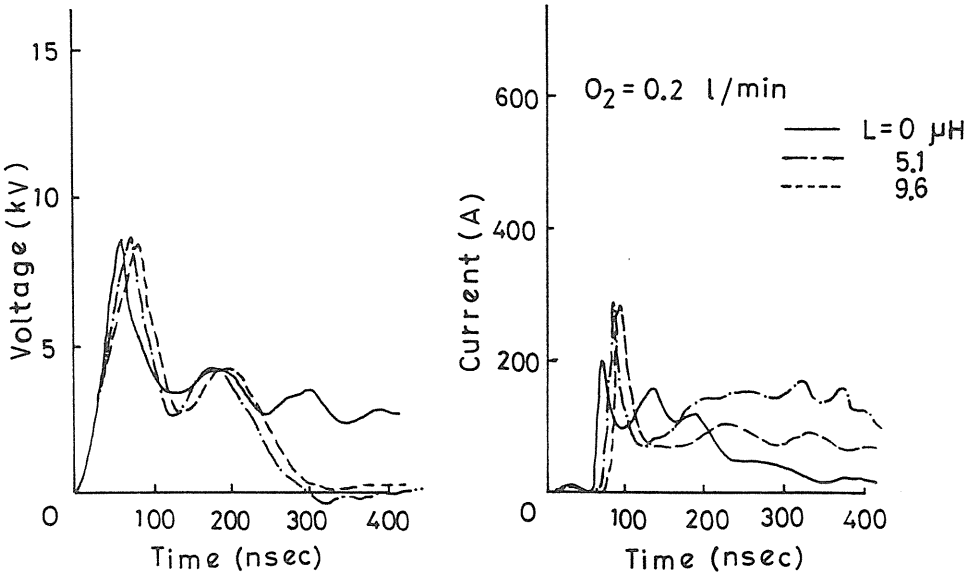

Fig. 2. 6 Voltage and current waveforms for various inductance at 15 kV

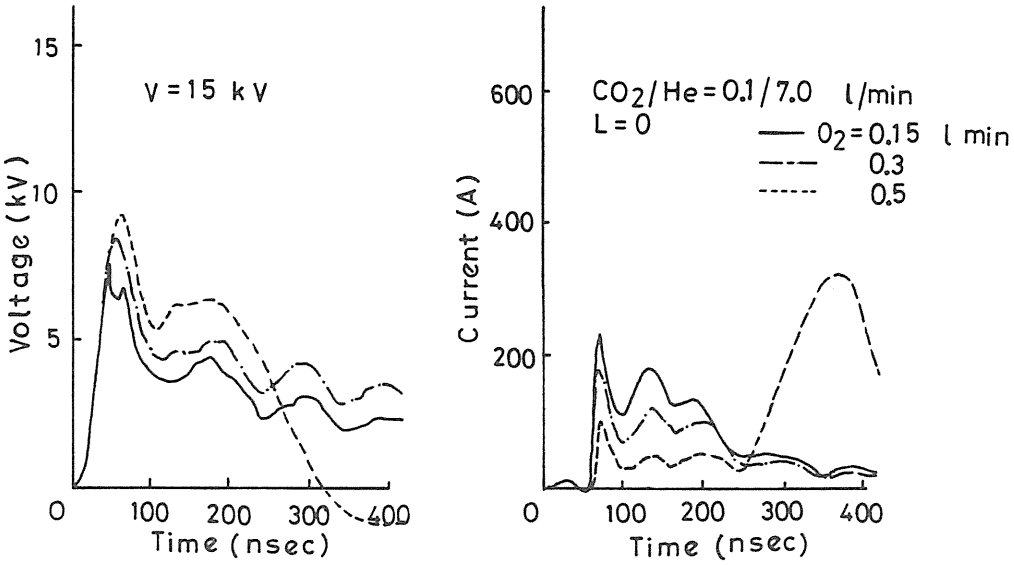

Fig. 2. 7 Voltage and current waveforms for various oxygen flow rate at 15 kV

rate as shown in Fig. 2. 7. In the waveforms of the main discharge current, the peak which appears at about 80 ns decreases with the oxygen flow rate. Since the oxygen molecules are the negative gas, the initial electrons produced prior to the main discharge are caught by the oxygen molecules and the breakdown voltage increases. The peak of the current becomes small due to the reduction of the conductivity of the plasma across the main electrodes when the oxygen flow rate increases and the tail of the waveform of the voltage becomes large due to the increasing of the voltage applied to the plasma. It is observed that the transition appears at 200–250 ns at X = 0.5 l/min in Fig. 2. 7. The duration of the voltage t_t increases with the inductance L_l and the steepness becomes slow. The peak current with $L_l = 0\,\mu H$ is smaller compared with that with $L_l = 5.1$ and $9.6\,\mu H$. The initial electrons seem to be produced much more with $L_l = 5.1$ and $9.6\,\mu H$, though the transition occurs.

The mixtures of $He/O_2 = 7.0/0.5$ l/min is used and the capacitance C_l and the charging voltage V_l are varied in the range of 200–3300 pF and 11–42.5 kV respectively for the measurements of the ozone generation. Both the generated ozone and the glow-to-arc transition rate as a function of the stored energy on the capacitor C_l are shown in Figs. 2. 8 and 2.9 for a parameter of the capacitance C_l at fixed gap spacing of 25 mm. The generated ozone increases with the stored energy, and at the same stored energy, the generated ozone with larger capacitance is less than that with smaller capacitance due to the increasing of the transition rate when the capacitance C_l is large as shown in Fig. 2. 9. The typical waveforms of the glow-to-arc transition with the capacitance of $C_l = 3300$ pF are shown in Fig. 2. 10. The main current does not pass through the main electrodes so much before the arcing at $V_l = 11$ kV, but the arcing appears following the glow discharge at $V_l = 22$ kV. The charge on the capacitor C_l is enough large for arcing at higher voltage and the condition of the production of the initial

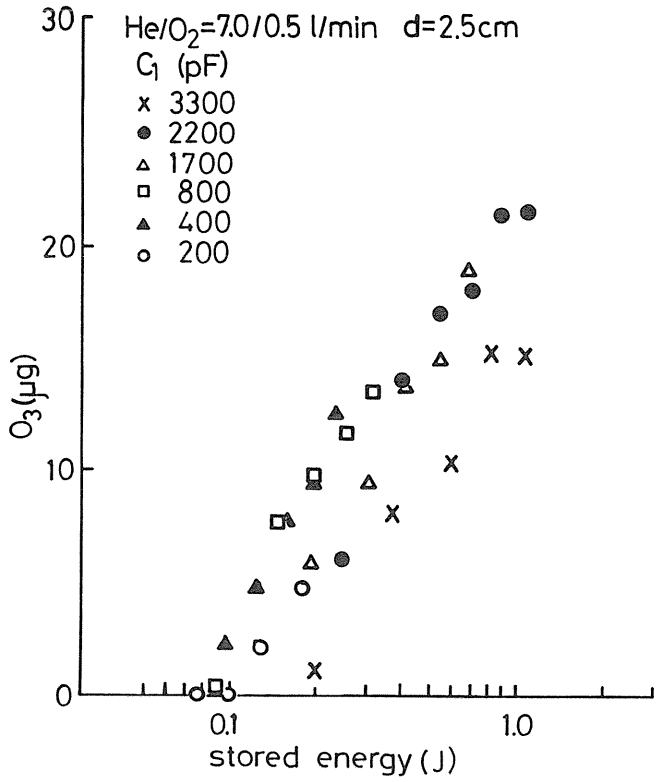

Fig. 2. 8 Generated ozone vs. stored energy

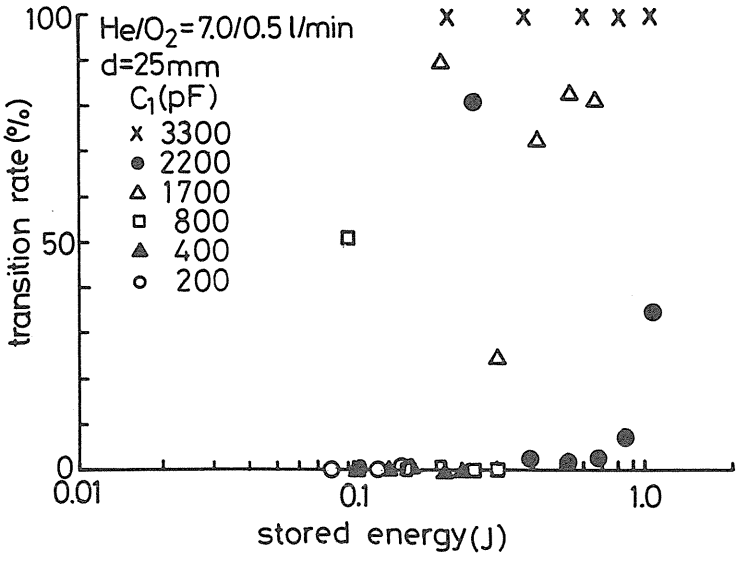

Fig. 2. 9 Glow-to-arc transition rate vs. stored energy

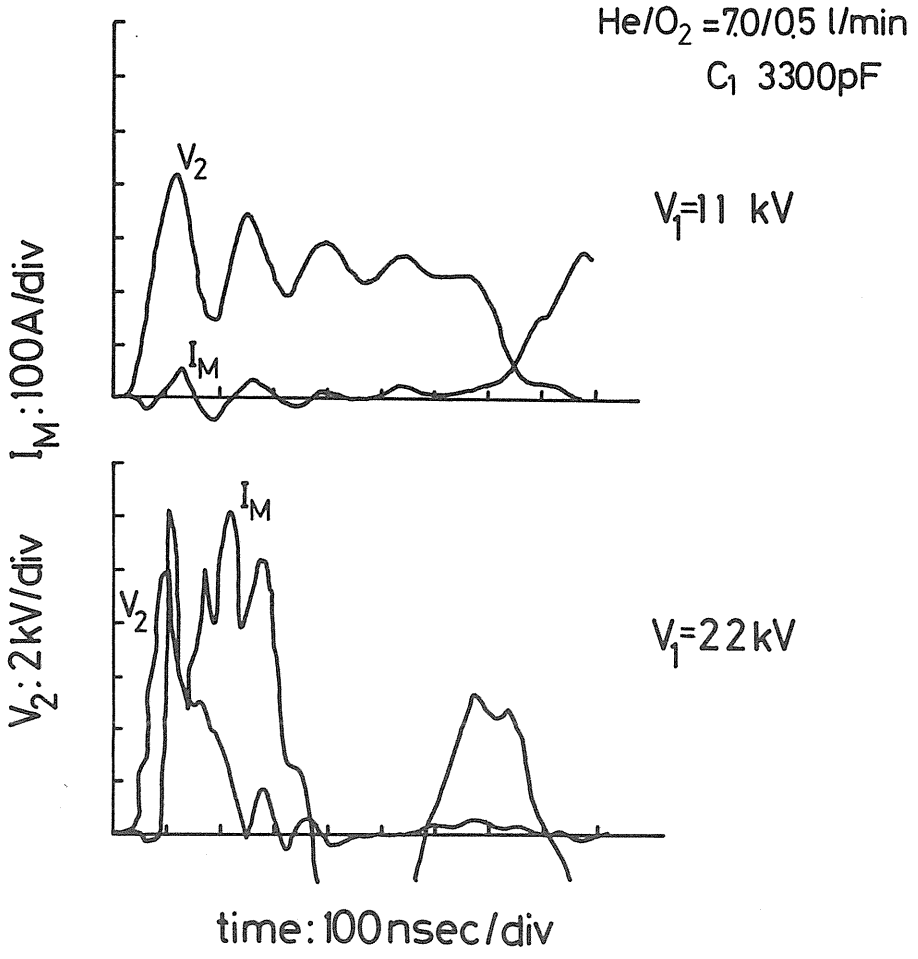

Fig. 2. 10 Typical waveforms of glow-to-arc transition with C_1=3300 pF for different voltage

electrons is not suitable due to the affection of the initial electrons by the trigger current at lower voltage. The reason that the transition is hard to appear at smaller capacitance is due to the small amount of charge stored on the capacitor C_1 and the difference voltage between V_1 and V_b is larger at higher voltage V_1 and the main discharge current passes through for a short time. The waveforms of discharge current are shown in Fig. 2. 11 for the different capacitors (C_1 = 3300 pF and C_1 = 400 pF) but the same stored energy of 0.15 J.

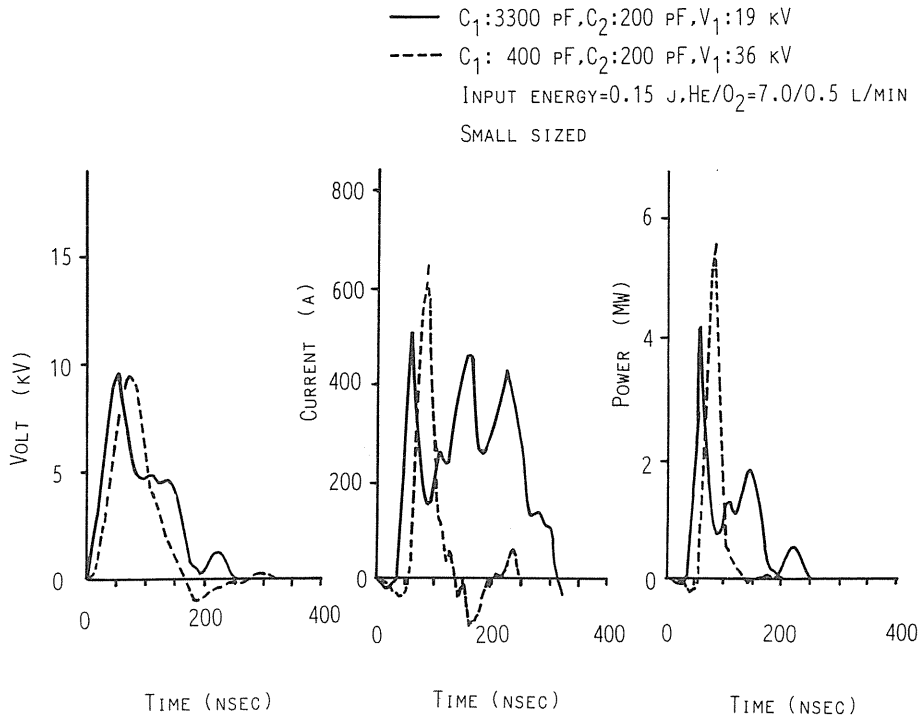

Fig. 2. 11 Waveforms of voltage and current for different capacitance but the same stored energy of 0.15 J

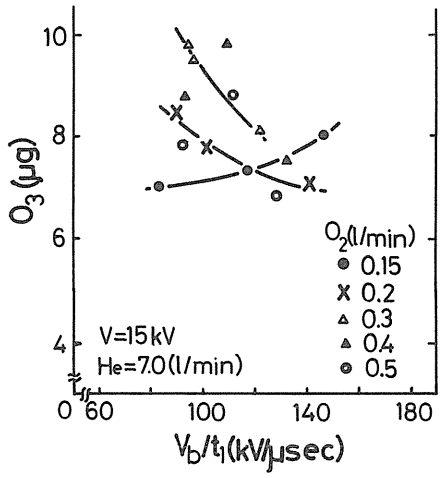

Fig. 2. 12 Ozone concentration vs. steepness V_b/t_1 in He/O_2 mixtures at 15 kV

The ozone generation is carried out for the variation of the oxygen flow rate (0.15–0.5 l/min) and of the steepness of the applied voltage (V_b/t_1) which is changed by the lumped inductance L_1 (= 0, 5.1, 9.6 μH) at the both charging voltage V_1 = 15 kV and 11 kV and the flow rate of helium of 7.0 l/min. In case of V_1 = 15 kV, the measured ozone concentration with He/O_2 mixtures is more than two times larger compared with that of $CO_2/He/O_2$ mixtures (which is shown in Fig. 2. 6) as shown in Fig. 2. 12. The characteristics of the ozone concentration as the function of the steepness has three different kinds of tendency for the following oxygen flow rate, $X < 0.2$, $0.2 \leqq X < 0.4$, and $X \geqq 0.4$ l/min. In case of $X < 0.4$ l/min, the glow-to-arc transition is not observed at any steepness. Although it appears at $X \geqq 0.4$ l/min, it is apt to keep uniform discharge (i.e. the transition rate is minimum) at the steepness of about 0.11 kV/ns (for L = 5.1 μH). The glow-to-arc transition affects on the ozone generation due to the drastic decreasing of the discharge volume at the transition time. The relation between the ozone concentration and the steepness is very complicate as shown in Fig. 2. 12. In case of X = 0.15 l/min, the larger the steepness is, the more ozone concentration is obtained. On the other hand, at X = 0.2, 0.3 l/min, the ozone concentration decreases with the steepness monotonously, and at X=0.4, 0.5 l/min the ozone concentration is maximum at which the transition is minimum (i.e. the decreasing of the ozone concentration at larger steepness seems to be due to the reduction of the discharge volume by the glow-to-arc transition.). At $X \leqq 0.3$ l/min, although the discharge volume is almost constant with no transition, the amount of generated ozone changes with the steepness. Therefore, another influence on the ozone generation except the transition must be considered. The relations between the amount of generated ozone, the injected charge into the main discharge volume and the oxygen flow rate as the parameter of the inductance are shown in Fig. 2. 13. The injected charge is calculated for the region with no transition from the main discharge current. At both L_1=0, 5.1 μH, the injected charge decreases with the oxygen flow rate and saturates. In case of L_1 = 9.6 μH, the charge is nearly constant up to X = 0.3 l/min and decreases at $X > 0.3$ l/min. At X = 0.15 l/min, the charge increases with decreasing the inductance L_1 and at both X = 0.2 and 0.3 l/min, the results are opposite. The amount of ozone has a relation with the charge injected into the discharge volume. The reason for these results is discussed later by considering the waveforms of the discharge current and voltage. The ratio of produced ozone molecules $[O_3]$ to oxygen molecules $[O_2]$ and the injected charge as a function of the oxygen flow rate are shown in Fig. 2. 14 as a parameter of the inductance. Both the ratio $[O_3]/[O_2]$ and the injected charge decrease with the oxygen flow rate. Qualitatively, the number of electrons attached by the oxygen molecules increase in the discharge region and the useful electrons for the dissociation of the oxygen molecules decrease relatively compared with the oxygen molecules. Consequently, it seems that the oxygen atoms produced by the dissociation decrease. The maximum efficiency of the ozone generation is about 380 g/kWh when the various parameters are changed. At the charging voltage of V_1 = 11 kV, the discharge conditions are always diffuse glow discharge for the oxygen flow rate X = 0.15 l/min, the glow-to-arc transition for X = 0.2 and 0.3 l/min with the large steepness (L_1 = 0 μH), and always arcing for $X \geqq 0.4$ l/min even though with smaller steepness (L_1 = 5.1, 9.6 μH) and very weak discharge with large steepness. The generated ozone as a function of the steepness is shown in Fig. 2. 15 as the parameter of the oxygen flow rate. The ozone generation decreases at V_b/t_1 = 0.08 kV/ns for any oxygen flow rate, and the reduction of it is remarkable for $X \geqq 0.3$ l/min. For X = 0.4 and 0.5 l/min at largest steepness, the generated ozone is not at all due to the very weak discharge (i.e. the dissociation of the oxygen molecules does not occur at all.). Both the relations between the generated

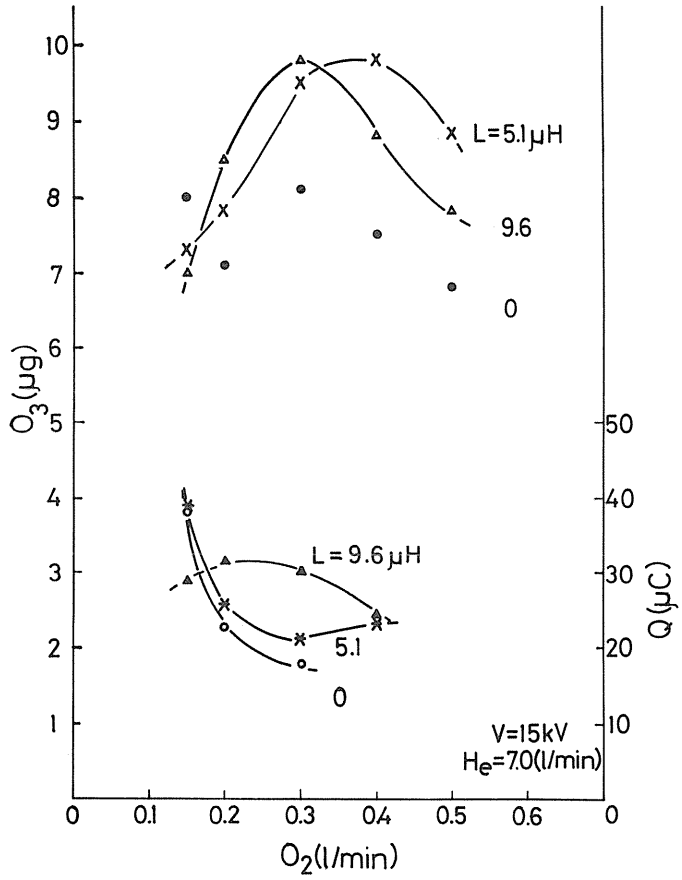

Fig. 2. 13 Generated ozone and injected charge vs. oxygen flow rate for various inductance at 15 kV

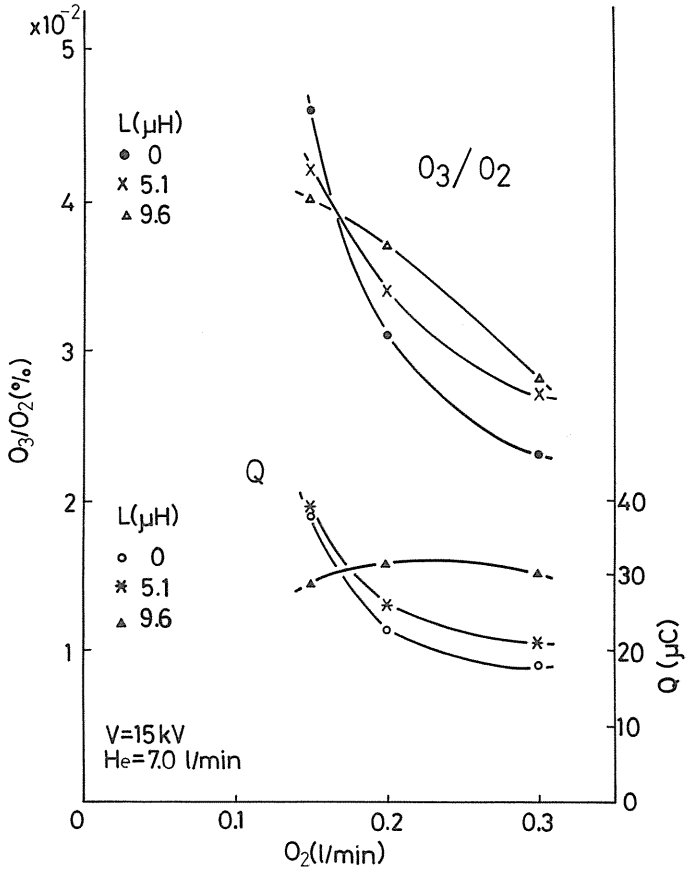

Fig. 2. 14 Ratio of $[O_3]/[O_2]$ and injected charge vs. oxygen flow rate for various inductance

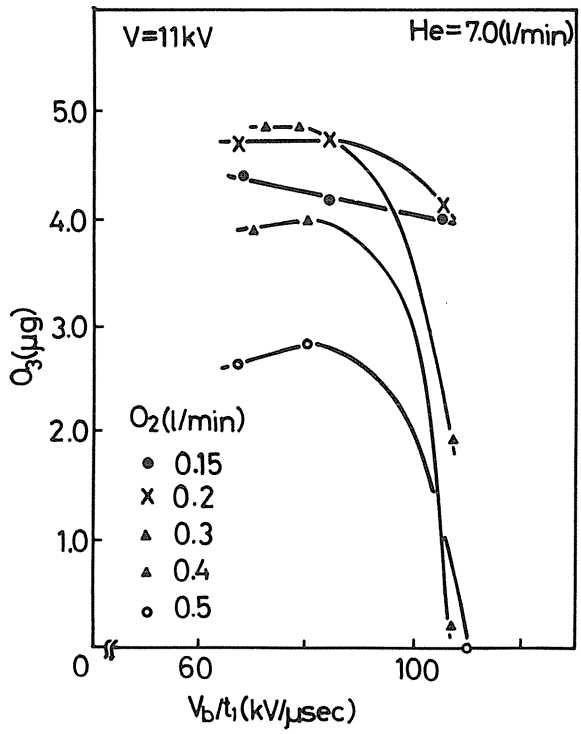

Fig. 2. 15 Generated ozone as a function of steepness V_b/t_1 for various oxygen flow rate with very weak discharge

ozone and the oxygen flow rate and the injected charge into the discharge volume and the oxygen flow rate are shown in Figs. 2. 16 and 2. 17. Here, the injected charge is calculated from the voltage and current waveform of the main discharge as the charge injected before the occurrence of the transition. From these results, the injected charge and the generated ozone have a strong relation. In Fig. 2. 17, the charge with $L_1 = 0\,\mu H$ at $X = 0.3$ l/min is much smaller than that with $L_1 = 5.1$ and $9.6\,\mu H$ and this looks like the tendency of the ozone generation in Fig. 2. 16. The experimental results mentioned above are considered by the waveforms of the applied voltage across the main electrodes, the main discharge current and the trigger current. The discharge voltage and current waveforms measured both at $V_1 = 11\,kV$ and $L_1 = 0\,\mu H$ (the oxygen flow rate X is a parameter), and $V_1 = 15\,kV$ and $X = 0.3$ l/min (the inductance L_1 is a parameter) are shown in Figs. 2. 18 and 2. 19. At $V_1 = 11\,kV$, the breakdown voltage and the time until the breakdown t_1 are almost same for the different values of X and the voltage in the tail of the waveform (i.e. the applied voltage to the sheath and the discharge column) increases with the oxygen flow rate. The discharge current decreases with the oxygen flow rate and hardly flows at $X = 0.5$ l/min. On the other hand, at $V_1 = 15\,kV$, the peak current of the discharge with $L_1 = 0\,\mu H$ is much smaller than that with L_1=5.1, $9.6\,\mu H$ as shown in Fig. 2. 19. The number of initial electrons with $L_1 = 0\,\mu H$ is less than that with

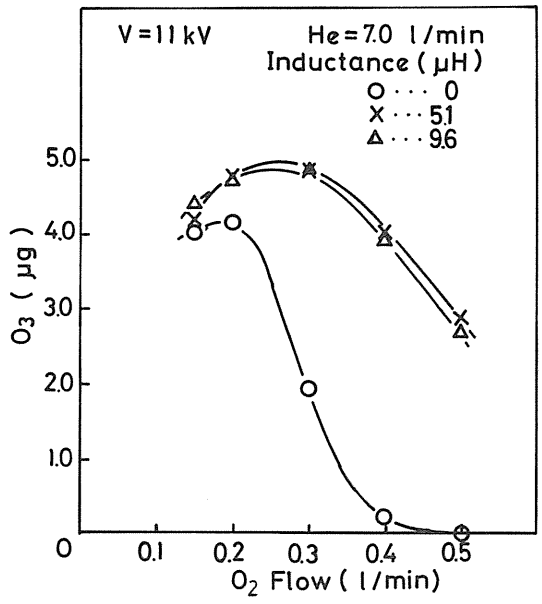

Fig. 2. 16 Generated ozone vs. oxygen flow rate for various inductance with very weak discharge

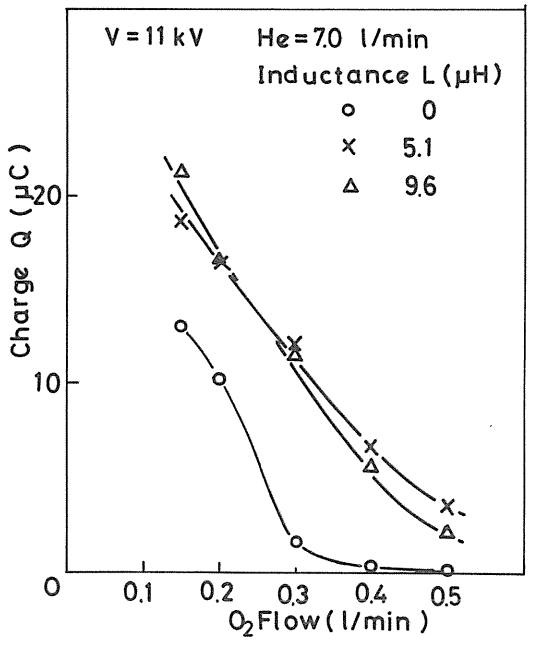

Fig. 2. 17 Injected charge vs. oxygen flow rate for various inductance with very weak discharge

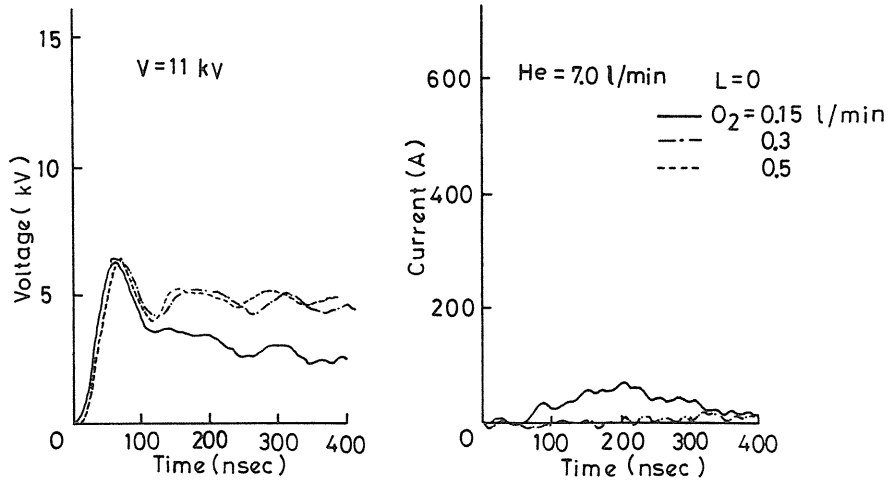

Fig. 2. 18 Discharge voltage and current waveforms at V_1=11 kV and L_1=0

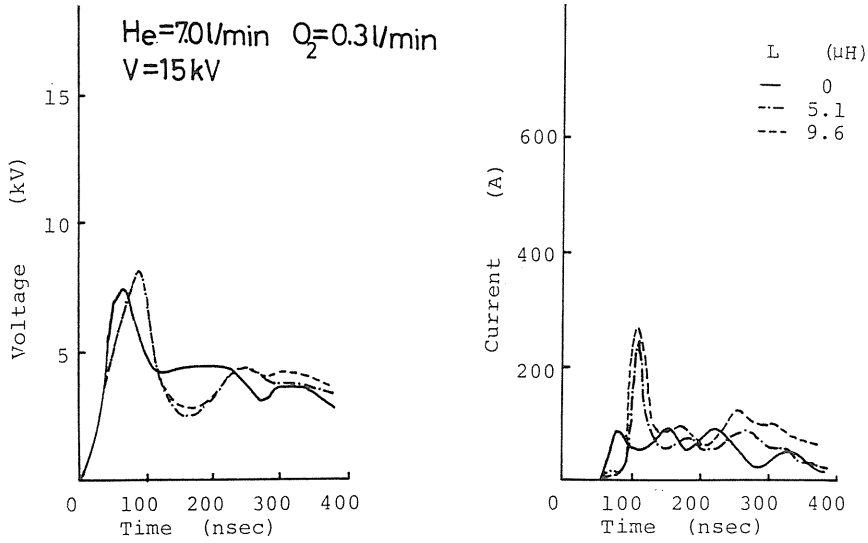

Fig. 2. 19 Discharge voltage and current waveforms for various inductance at 15 kV and X=0.3 l/min

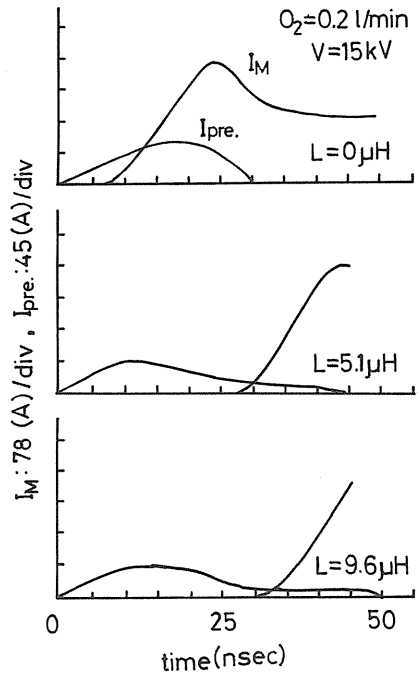

Fig. 2. 20 Trigger current and main discharge current for various steepness of voltage at X=0.2 l/min

$L_1 = 5.1$, 9.6 μH. Both the waveforms of the trigger current and the main discharge current are shown in Fig. 2. 20 for the various steepness of the applied voltage (i.e. different inductance are used to change the steepness) at $X = 0.2$ l/min. For the large steepness (in case of $L_1 = 0$ μH), since the discharge current starts to flow immediately after the trigger current starts, the initial electrons produced before the main discharge occurs are not so much. For the lower steepness (in case of $L_1 = 5.1$ and 9.6 μH), since the main discharge occurs at 25–30 ns after the trigger current starts, the initial electrons before the main discharge are much more compared with the former case. In this case, the large steepness is not so good for the production of the initial electrons. But at the lower oxygen flow rate, the relation between the initial electrons and the injected charge is opposite, that is, the injected charge into the discharge volume increases with the steepness as shown in Fig. 2. 21. The peak current is roughly same for the change of the inductance.

The characteristics of ozone generation for the different main gap spacing d are studied. The breakdown voltage V_b as a function of the main gap spacing is shown in Fig. 2. 22. Here, the mixtures of $He/O_2 = 7.0/0.5$ l/min and $L_1 = 0$ μH. The solid line in the figure shows the average electric field Eav of about 4 kV/cm. The gap spacing is fixed here at $d = 35$ mm and the characteristics of ozone generation are measured to compare with the results obtained at 25 mm. The amount of generated ozone as a function of the charging voltage V_1 is shown in Fig. 2. 23 as a parameter of the main gap spacing d. Though the generated ozone with $d = 25$ mm is much larger than that with $d = 35$ mm at $V_1 \leqq 22$ kV, the latter is about one and half times larger compared with the former at $V_1 \geqq 25$ kV. From Fig. 2. 22, the breakdown voltage for $d = 35$ mm and $d = 25$ mm is about 22 kV and 15 kV respectively. Since the difference of the voltage between the charging voltage V_1 and the breakdown voltage V_b is about 5 kV for $d = 35$ mm and

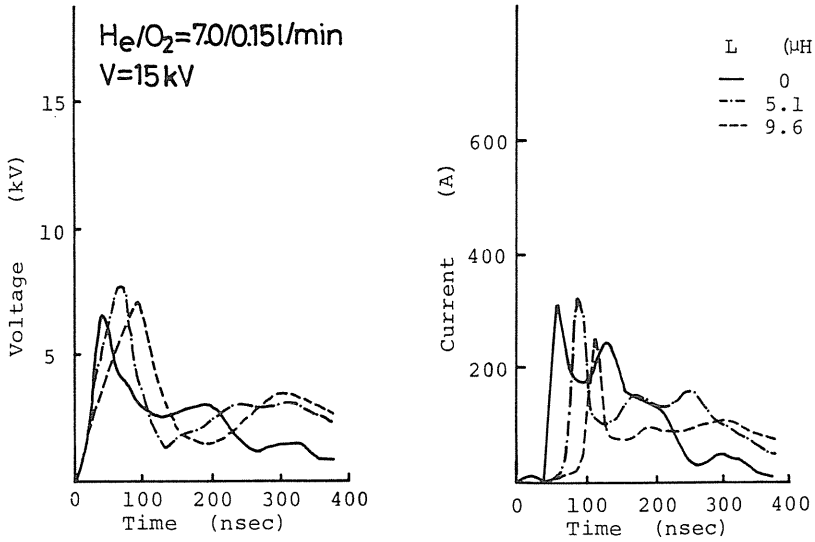

Fig. 2. 21 Voltage and current with time in $He/O_2=7/0.15$ l/min at V=15 kV for various inductance

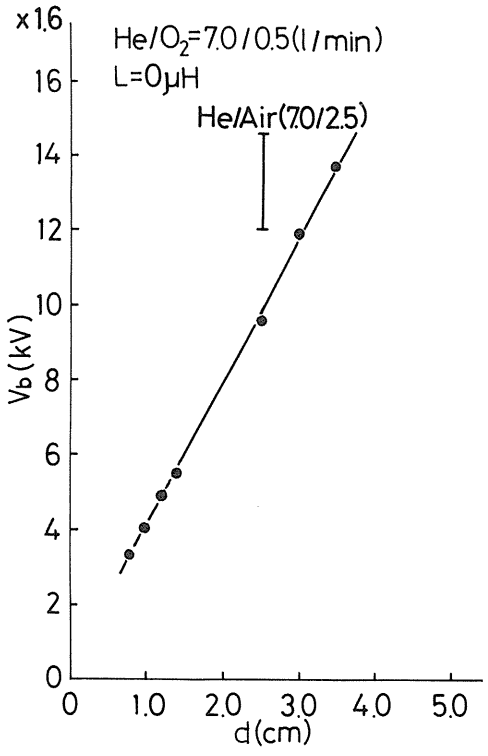

Fig. 2. 22 Breakdown voltage V_b as a function of main gap spacing with $L_1=0$

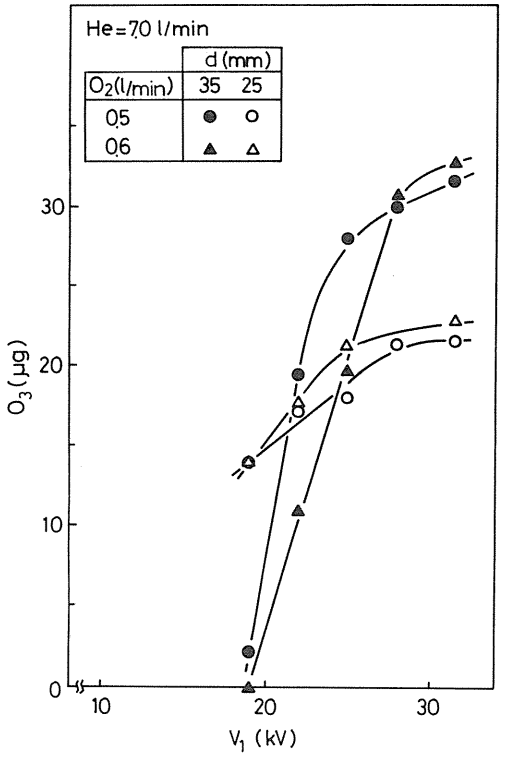

Fig. 2. 23 Generated ozone as a function of the charging voltage for the different gap spacing

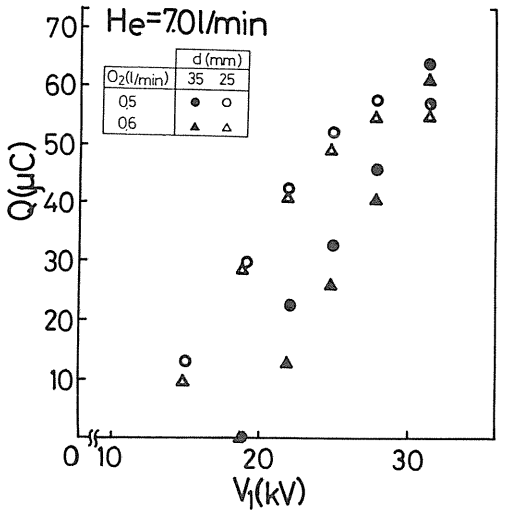

Fig. 2. 24 Injected charge Q as a function of the charging voltage for different oxygen flow rate and gap spacing

about 10 kV for d = 25 mm at V_1 = 19 kV, the injected charge during the discharge with 25 mm is much larger and more effective for the ozone generation. The injected charge Q as a function of the charging voltage is shown in Fig. 2. 24 as parameters of the oxygen flow rate and gap spacing. According to these results, the charge is hardly injected for d = 35 mm at V_1 = 19 kV and the charge for d = 25 mm saturates at $V_1 \geqq 25$ kV. The measured maximum efficiency for the ozone generation is about 340 g/kWh with d=25 mm and about 350 g/kWh with d = 35 mm.

2. 3. 2. Improvement of ozone generation by high frequency corona discharge (HFCD)

It is one of the most important point for the development of the ozonizer with high ozone concentration that the glow-to-arc transition is suppressed. During the process of this transition, the growth of the streamer like discharge with an intensive light which appears from the protrusion with the shape of a trapezoid of the cathode plays the important part. If this occurrence of the streamer like discharge from the protrusion or it's growth is suppressed the glow-to-arc transition will be prevented. It has been developed to be able to prevent the transition due to the large number of electrons produced near the glass tube by the superposition of HFCD during the main discharge. The circuit enclosed by the broken line shown in Fig. 2. 25 is that of HFCD which is composed of the inductance L_2, capacitor C_3 and gap G_2. The capacitor C_3 is charged at V_3 by another power source and one of the terminals of gap G_2 is at the same potential V_3. After gap G_1 in the main circuit is fired, the negative potential of the cathode and the other terminal of gap G_2 connected with the cathode increases its absolute value with time. Therefore, the potential difference between the terminals of G_2 becomes large and gap G_2 fires automatically at some potential difference. The timing of this firing is controlled by changing the nitrogen pressure of gap G_2. As the potential of the cathode drops to the voltage maintaining the atmospheric glow discharge when the main discharge occurs, it is impossible to fire gap G_2 after the discharge. That is, the controllable delay time between the firing of G_1 and G_2 is until the breakdown of the main gap at most. Following the firing of G_2, the corona discharge (HFCD) occurs near the tips of trapezoid (or the glass tube) on the cathode again and produces many electrons until the end of the main discharge. The period of HFCD depends on the L_2-C_3 oscillation. The typical voltage across the main electrodes V_2, main discharge current I and corona current I_c (pre-discharge or pre-discharge plus HFCD) are shown in Fig. 2. 26 for both cases with HFCD(a) and without HFCD(normal operation)(b). The operating parameters are $V_1 = 47$ kV, $CO_2/N_2/He = 1/1/10$ l/min for both operations and $C_3 = 500$ pF, $V_3 = 30$ kV for HFCD operation. In the normal operation(b), the corona current is used for the preionization and its amplitude is relatively small and it continues up to about 1 μs before

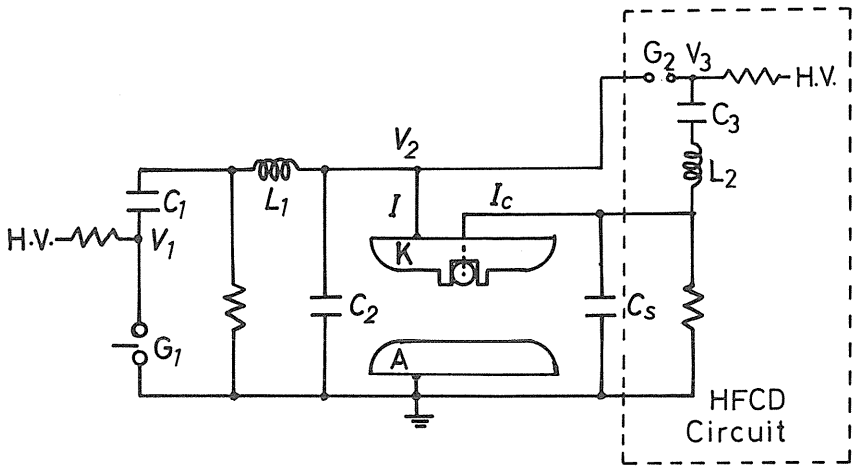

Fig. 2. 25 Electrical circuit for HFCD operation enclosed by broken line

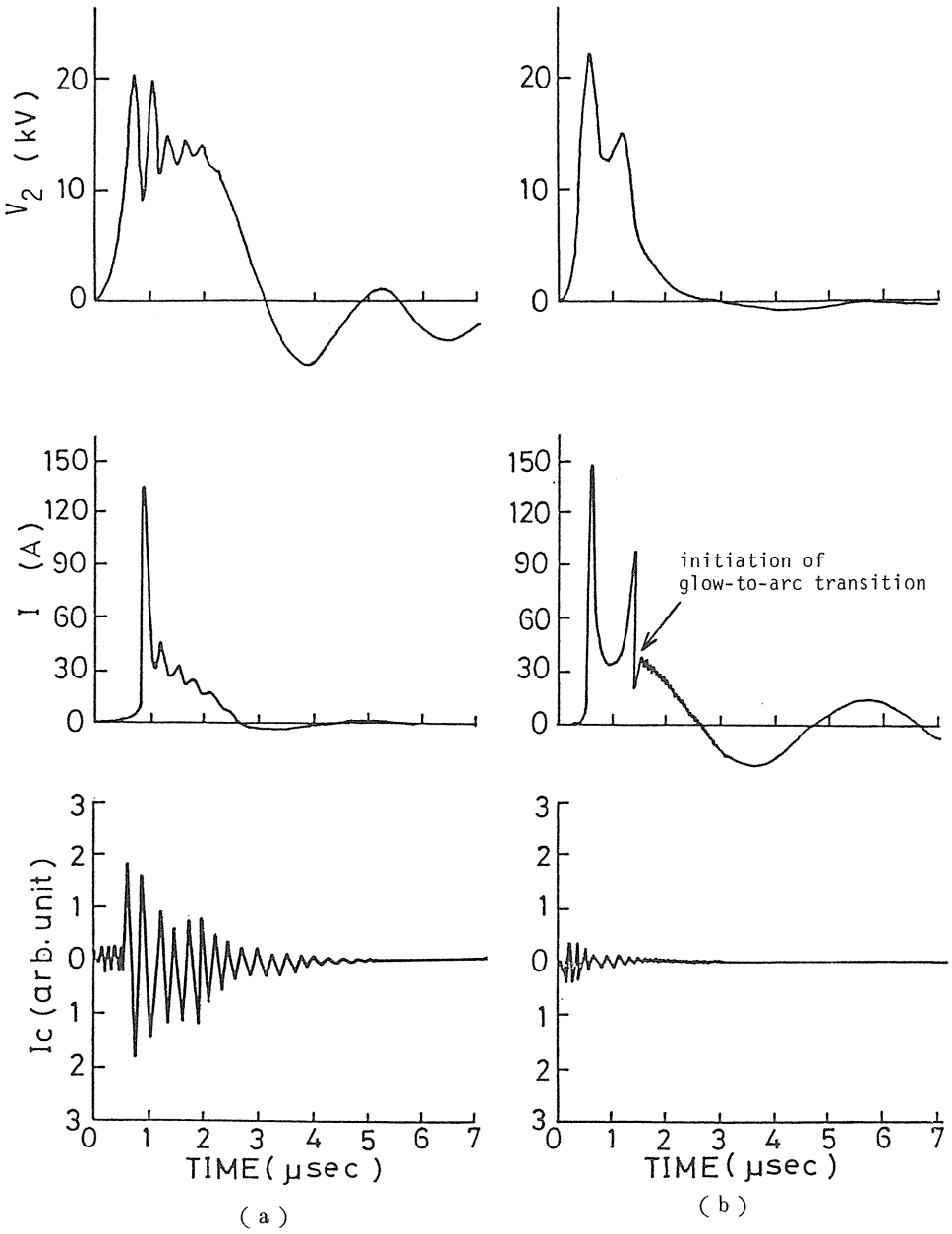

Fig. 2. 26 Typical waveforms of voltage V_2 (upper), main discharge current (middle) and corona current I_c with and without HFCD

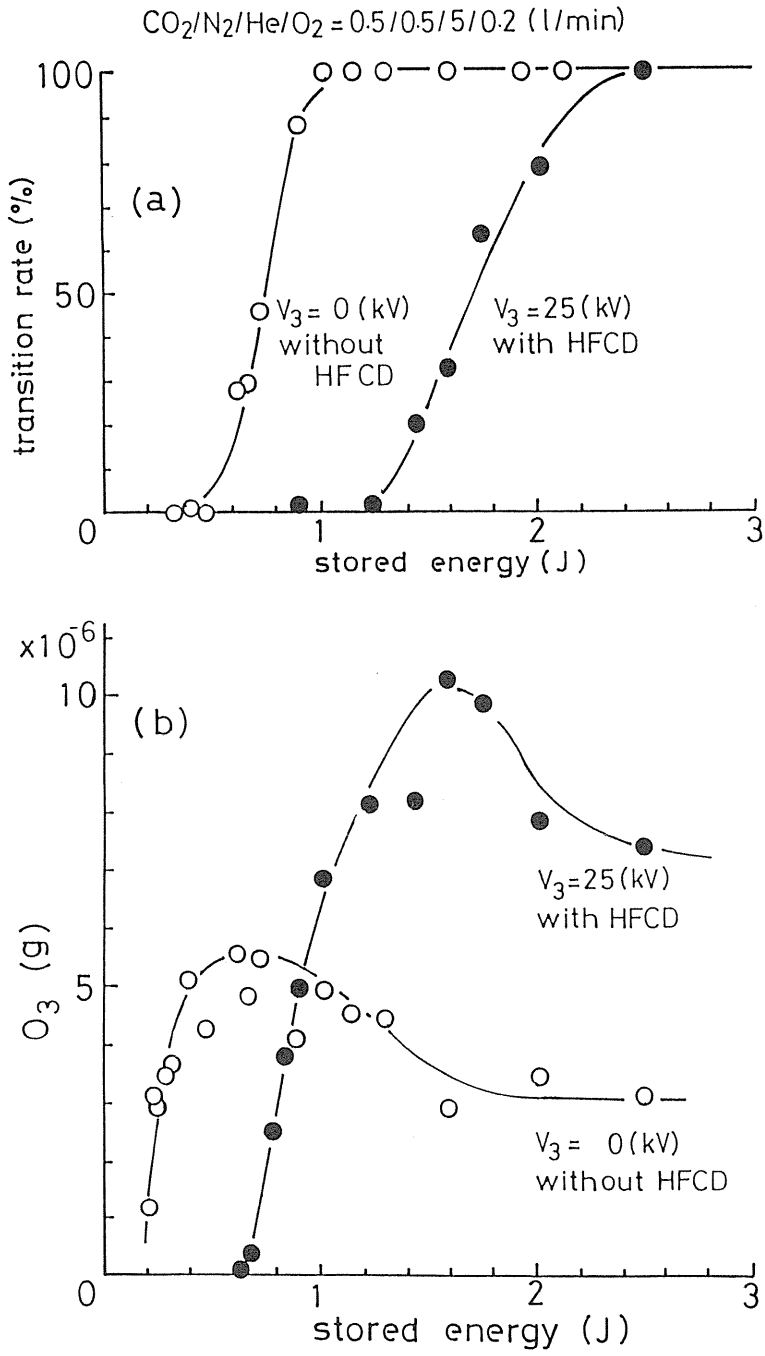

Fig. 2. 27 Glow-to-arc transition rate and ozone concentration vs. stored energy in $CO_2/N_2/He/O_2$=0.5/0.5/5/0.2 l/min with and without HFCD

the build up of the main discharge current. On the other hand, in the case of HFCD operation(a), HFCD current whose period is about 230 ns is superposed on the corona current for the preionization. The amplitude of HFCD current is about four times larger than that of the corona current with the normal operation and HFCD continues until the end of the main discharge current for about 3.5 μs. The second peak of the main discharge current I in the normal operation shows the start of the glow-to-arc transition and the current oscillates after this transition and the voltage V_2 decreases to zero rapidly and it shows the short circuit of the main electrodes. On the contrary, HFCD operation prevents the transition so that the glow discharge is maintained, and the oscillations synchronized with the period of HFCD current are observed on the waveforms of the voltage V_2 and the current I. According to the observation of the discharge by the time integrated photographs, the length of the fine discharges with the intensive light which comes from the tips of the trapezoids on the cathode is diminished and the spatial uniformity of the discharge is improved, when the voltage V_3 is increased. The glow-to-arc transition and ozone concentration against the stored energy in the mixture of $CO_2/N_2/He/O_2 = 0.5/0.5/5.0/0.2$ l/min as shown in Fig. 2. 27. The voltage V_3 is fixed at 25 kV for HFCD operation. The threshold of the stored energy for the occurrence of the glow-to-arc transition increases up to about three times by HFCD superposition comparing with the normal operation (without HFCD), and it is possible to increase the ozone concentration still more, since the uniform discharge is obtained at larger stored energy. But when the stored energy is increased further, the ozone concentration starts to decrease at the glow-to-arc transition rate of about 50%. In this case, the voltage V_3 has to be increased to prevent the transition. The ozone yield against input energy ($= \int IVdt$) for both with HFCD and without HFCD is shown in Fig. 2. 28. The ozone yield decreases with the input energy. From these results, it is useful for the increase of the

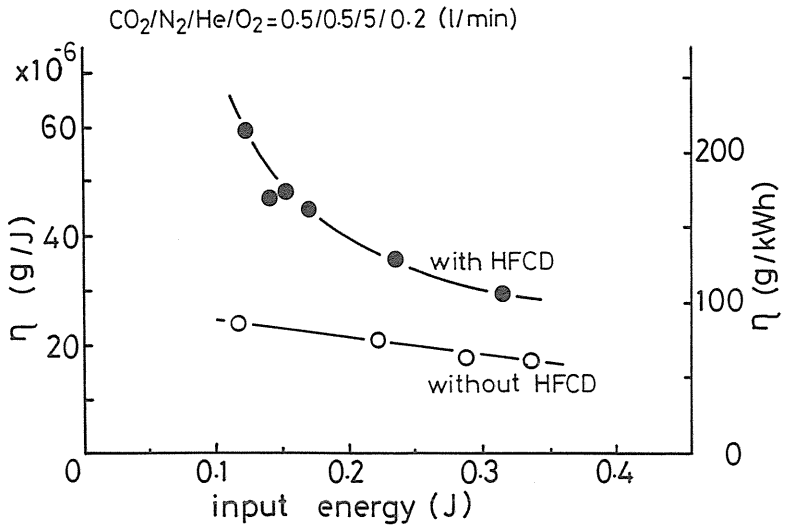

Fig. 2. 28 Efficiency of ozone generation vs. input energy with and without HFCD

Table 2. 2 Various conditions in the experiments

case	oxygen flow rate (l/min)	with or without HFCD
A	0.5	without
B	0.6	without
C	0.5	with
D	0.6	with

ozone yield to make a weak glow discharge instead of the increase of the input energy. The ozone yield obtained with HFCD is 2–2.5 times larger than that without HFCD at the same input energy. The maximum ozone yield obtained in the mixture of $CO_2/N_2/He/O_2$ is about 220 g/kWh. Following the mixtures of $CO_2/N_2/He/O_2$, the mixtures of He/O_2 is used for the improvement of the ozone generation. The parameters in the circuit in Fig. 2. 25 are $C_1 = 2200$ pF, $C_2 = 200$ pF, $C_3 = 18000$ pF, $L_1 = 0$ and 4 μH. The experiments are carried out for the following four cases shown in Table 2. 2. The charging voltage on the capacitor C_3 is 5 kV constant. The amount of the generated ozone per one shot and the transition rate as a function of the charging voltage V_1 are shown in Figs. 2. 29 and 2. 30. The difference of the amount of generated ozone between the case A and B (without HFCD) and cases C and D (with HFCD) is not so much as shown in Fig. 2. 29. In cases A and B, the ozone concentration increases with the charging voltage up to $V_1 = 20$ kV, and saturates at $V_1 > 20$ kV. The efficiency of the ozone generation is maximum at $V_1 = 19$ kV and decreases at $V_1 > 19$ kV. The transition rate tends to increase at $V_1 = 15$ kV and 31.5 kV. The saturation of the ozone concentration is due to the lack of the uniformity of the discharge. The effect of the suppression of the transition by the HFCD operation is not so much except at $V_1 = 15$ kV. Though the improvement of the discharge by the HFCD is remarkable at $V_1 = 15$ kV, the ozone concentration is not improved at all due to the decreasing of the main discharge current as shown in Fig. 2. 29. The reason why the effect of the HFCD is not observed so much is that the transition is very small (i.e. the discharge is considerably uniform) without HFCD operation and the charging voltage on the capacitor C_3 is low. The maximum efficiency of the ozone generation is about 410 g/kWh with HFCD and about 340 g/kWh without HFCD at the oxygen flow rate of 0.6 l/min and $V_1 = 15$ kV. The mechanism of the suppression of the glow-to-arc transition by the HFCD superposition is the mitigation of the electric field by the electron avalanche produced around the protrusions with the shape of a trapezoid by the HFCD operation and the streamer like discharge is diffused around the protrusions, even though the intensive filamentary discharge progress from the cathode.

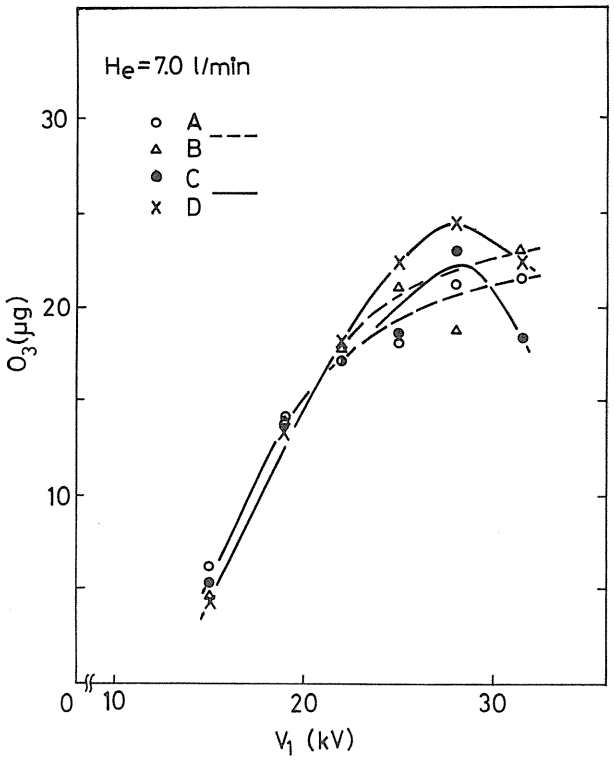

Fig. 2. 29 Generated ozone vs. charging voltage for four different conditions

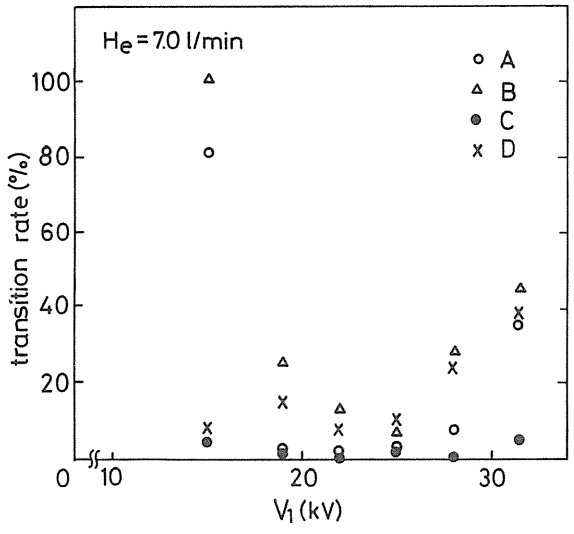

Fig. 2. 30 Glow-to-arc transition rate vs. charging voltage for four different conditions

2. 3. 3. Ozone generation in He/air mixtures

The experiment has been done in He/air ($He/N_2/O_2 = 7.0/2.0/0.5$ l/min) mixtures using the small-sized ozonizer and the frequency of the discharge f is O.2 Hz. The electrical circuit is the same one shown in Fig. 2. 1. The condition of the main discharge is as follows.

i) The discharge is not observed at $V_1 < 19$ kV.

ii) The glow-to-arc transition rate is 100% at $V_1 = 19$ kV

iii) The transition rate is 0% at $V_1 = 22$ kV, 20% at 28 kV and 54% at 31.5 kV.

The amount of produced ozone (μg/shot) as a function of the changing voltage V_1 is shown in Fig. 2. 31. The amount of produced ozone in He/air mixtures is less than half of that obtained in He/O_2 mixtures. Both the reduced electric field E/p and the injected electric charge into the discharge volume are also shown in Fig. 2. 32 as a function of V_1. Though the breakdown voltage V_b in He/air mixtures is larger than that in He/O_2 mixtures, but the injected electric charge is almost same. In He/air mixtures, the energy of electrons is transfered to the nitrogen molecules and the nitrogen molecules react with the excited helium atoms He^* because the ionization potential of nitrogen molecule (= 15.58 eV) is closely to the metastable state of the helium (= 19.8 eV) compared with the ionization potential of the oxygen (= 12.2 eV) and the dissociation of the oxygen might be affected. The maximum efficiency of the ozone generation in He/air mixtures is about 120 g/kWh.

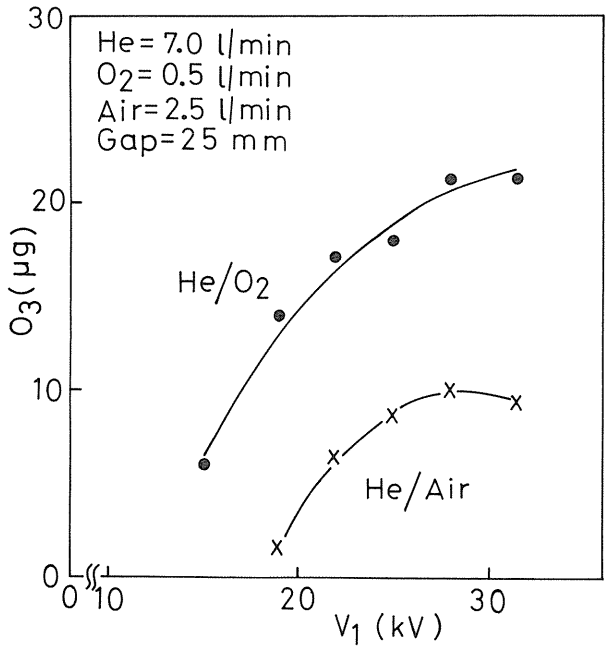

Fig. 2. 31 Generated ozone per shot as a function of applied voltage V_1 in He/O_2 and He/air mixtures at gap spacing of 25 mm

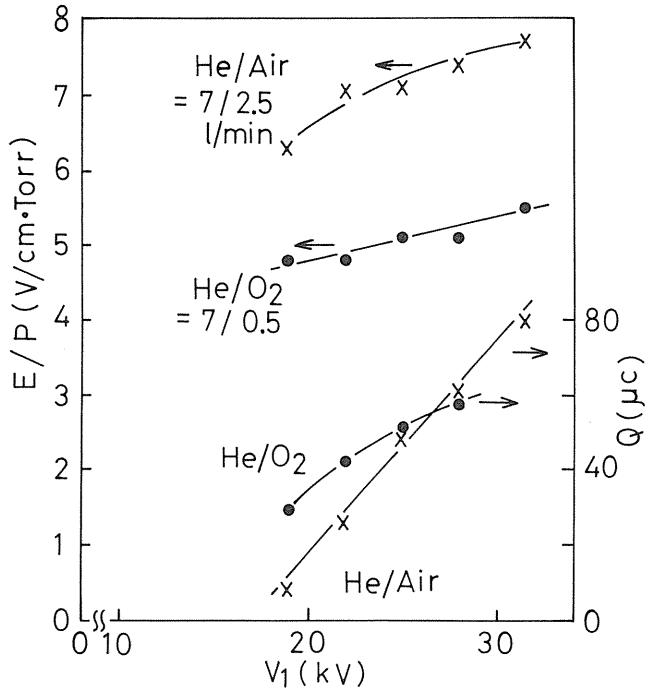

Fig. 2. 32 Reduced electric field E/P (electric field to pressure) and injected electric charge Q as a function of applied voltage V_1 in He/O_2 and He/air mixtures

3. Improvement of the efficiency of the ozone generation by a large-sized ozonizer[11]

3. 1. Introduction

It is considered for the making of the ozone with high ozone concentration that the discharge volume per one shot is increased.

The large-sized double discharge type ozonizer is used to increase the discharge volume and its characteristics of the ozone generation are measured. The obtained results are compared with the results by the small-sized ozonizer.

3. 2. Experimental apparatus of the large-sized ozonizer and procedure

The diagram of the large-sized ozonizer is shown in Fig. 3. 1 and the comparison of the size such as the main gap spacing, area of the discharge and the discharge volume between the large-sized and the small-sized ozonizer is summarized in Table 2. 1 as mentioned before. A cathode of 90 mm width and 700 mm length is made of aluminum and has ten parallel grooves on its surface. The cross-section of each groove is 4.5 mm wide and 3 mm deep. Many protrusions with the shape of trapezoid are distributed along each groove to increase the threshold of the glow-to-arc transition. A trigger electrode T covered with a Pyrex glass tube is put each groove in along the electrode. The outer diameter and thickness of the glass tube are 4 mm and 1.2 mm, respectively. The mixtures of He/O_2 is used and the voltage across the main electrodes V_2 and the main discharge

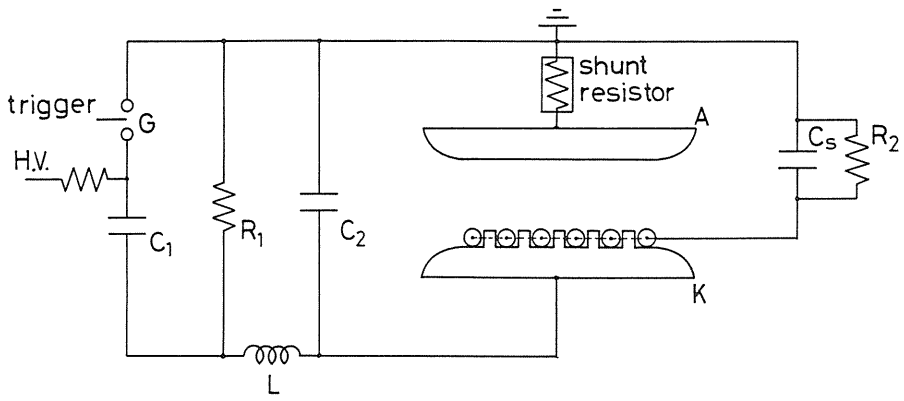

Fig. 3. 1 Schematic diagram of a large-sezed ozonizer

current are measured by the high voltage probe (Tektronix P6015) and the coaxial type shunt (Tokyo transformer Co.) respectively. The oxygen flow rate, charging voltage V_1 and the capacitance C_1 are changed as parameters. After the total number of 60 shots (discharge frequency is 0.2 Hz), the produced ozone is absorbed by Potassium Iodide solution and is measured chemically.

3. 3. Experimental results

The glow-to-arc transition rate does not change so much for the various parameters and is about 30–40%. The amount of generated ozone per shot as a function of the stored energy is shown in Fig. 3. 2 as a parameter of the oxygen flow rate. The amount of generated ozone per shot increases with the stored energy for the oxygen flow rate.

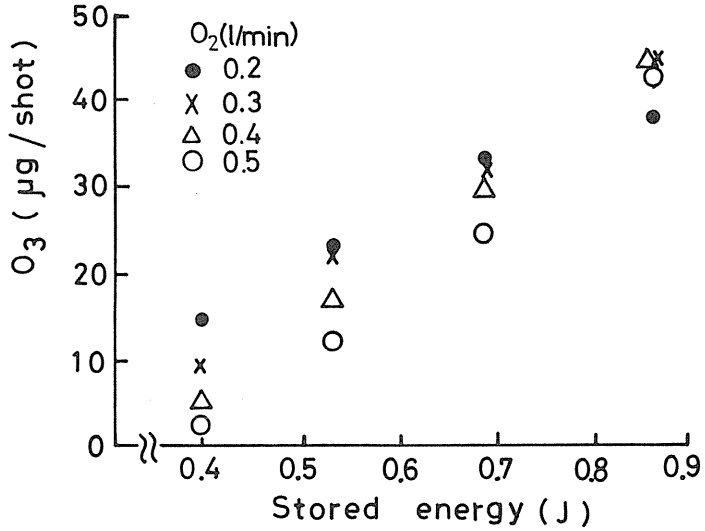

Fig. 3. 2 Generated ozone vs. stored energy for the parameter of oxygen flow rate

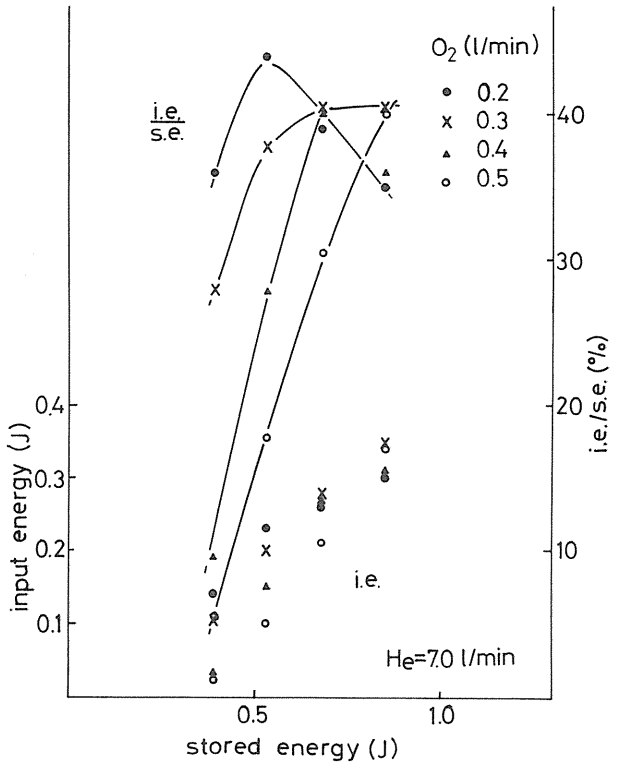

Fig. 3. 3 Input energy and the ratio of input energy injected into the discharge volume to stored energy vs. stored energy for various oxygen flow rate

The amount of generated ozone with the large oxygen flow rate is less than that with the small oxygen flow rate at the low stored energy due to the negative gas of the oxygen molecules. At the higher stored energy, the difference of the amount of generated ozone per shot for the various oxygen flow rate reduces. In the case of the oxygen flow rate of 0.2 l/min, the amount of generated ozone saturates, though the stored energy increases. The reduction of the injected charge into the discharge volume is suspected at the higher stored energy. Both the input energy and the injected energy ratio into the discharge volume as a function of the stored energy are shown in Fig. 3. 3. The injected energy ratio is defined as the ratio of the input energy into discharge volume (i.e.) to the stored energy (s.e.). Though both the input energy and the injected energy ratio increase with the stored energy in case of the oxygen flow rate of 0.4 and 0.5 l/min, the injected energy ratio saturates with 0.3 l/min and has a maximum value with 0.2 l/min. The efficiency of the ozone generation as a function of the input energy is shown in Fig. 3. 4 as a parameter of the oxygen flow rate. The efficiency is almost constant value of 400–450 g/kWh with the input energy. The amount of generated ozone as a function of the input energy is shown in Fig. 3. 5 for the different size of ozonizer (that is, the small-sized ozonizer and the large-sized ozonizer). The amount of generated ozone is not directly proportional to the discharge volume. There is no difference for the ozone generation at less than the input energy of 0.2 J, but the ozone generation with the small-sized ozonizer saturates at larger than that of 0.2 J. These results will be discussed later.

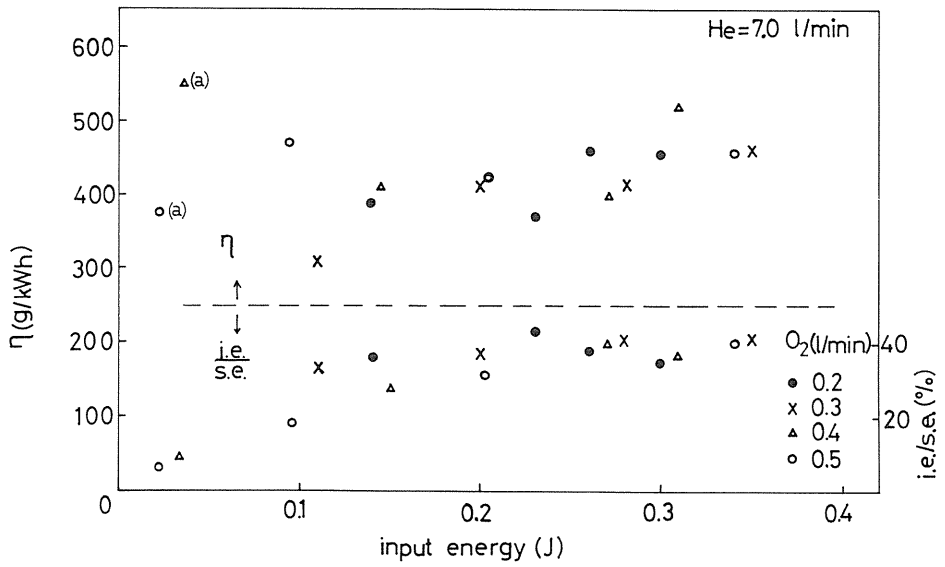

Fig. 3. 4 Efficiency of ozone generation and the ratio of input energy to stored energy vs. input energy for various oxygen flow rate

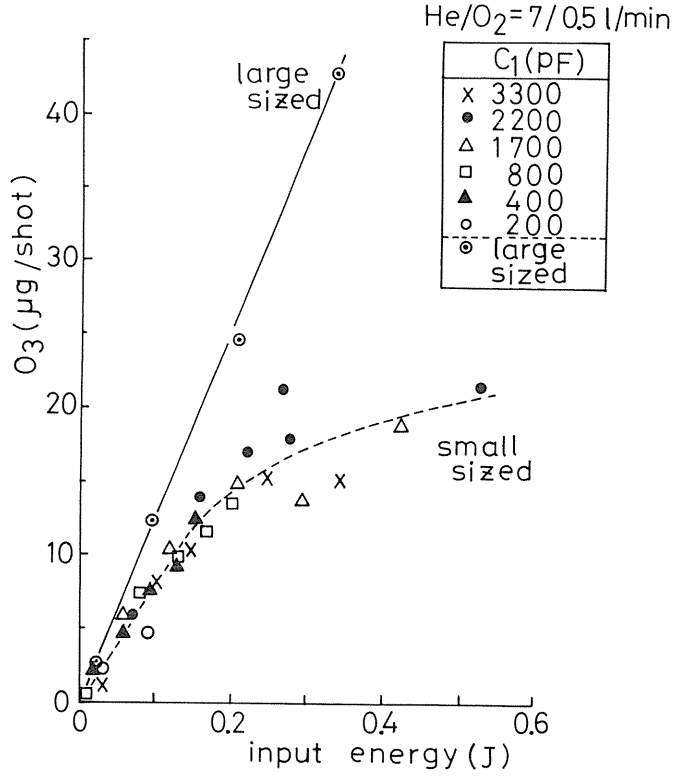

Fig. 3. 5 Generated ozone vs. input energy measured by both small-sized and large-sized ozonizers

3. 4. Discussion

As mentioned above, both efficiency of 400–450 g/kWh (obtained by the large-sized ozonizer whose discharge volume is 917 cm^3) and 300–350 g/kWh (obtained by the small-sized ozonizer whose discharge volume is 23 cm^3) are obtained. In these cases, the same electrical parameters except the applied voltage are used and the difference of the efficiency seems due to the difference of the input energy density into the discharge volume. The efficiency as a function of the input energy density is shown in Fig. 3. 6 for two different size of ozonizers. The capacitance of $C_1 = 200–3300$ pF and the charging voltage of $V_1 = 11–42.5$ kV are used for the small-sized ozonizer. The amount of generated ozone is measured chemically after the total number of discharges of about two hundred with the repetition rate of 0.2 Hz. The efficiency increases with the decreasing of the input energy density. The energy density for the small-sized ozonizer is about 10–100 times larger compared with that for the large-sized ozonizer, and the improvement by the large-sized ozonizer due to the decreasing of the input energy density. On the other hand, the input energy density of the conventional type ozonizers for the commercial is the order of 10^{-2} J/cm^3 and this seems to be one of the reasons for the saturation of efficiency of the conventional ozonizer. The waveforms of the applied voltage across the main electrodes, the main discharge current which are obtained with both the large-sized and the small-sized ozonizer are shown in Fig. 3. 7 at the same input energy into the discharge volume (= 0.2 J). In this case, the difference of the energy density is about forty times. From the measured voltage waveform and the gap spacing d, the average electric field E at the breakdown is estimated to be 4.0 kV/cm for the small-sized ozonizer

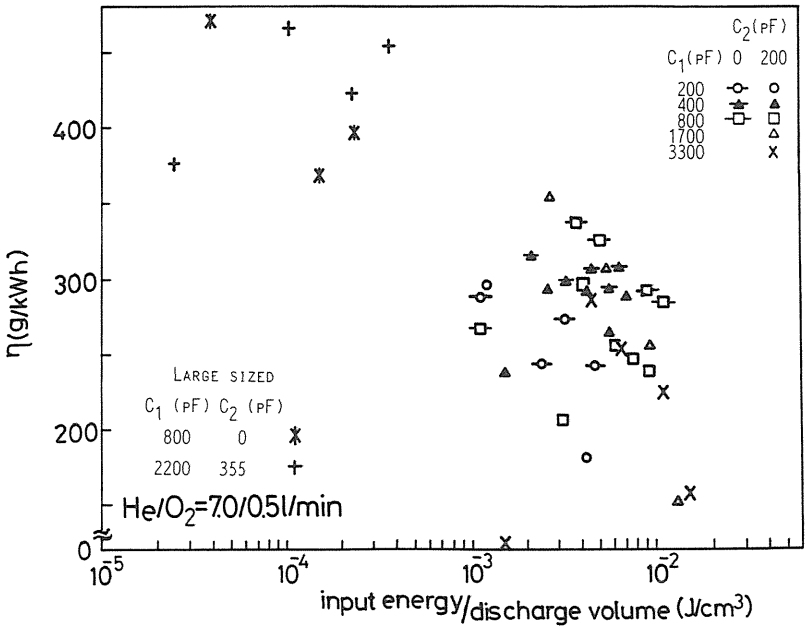

Fig. 3. 6 Efficiency of ozone generation vs. input energy density for both sizes of ozonizer

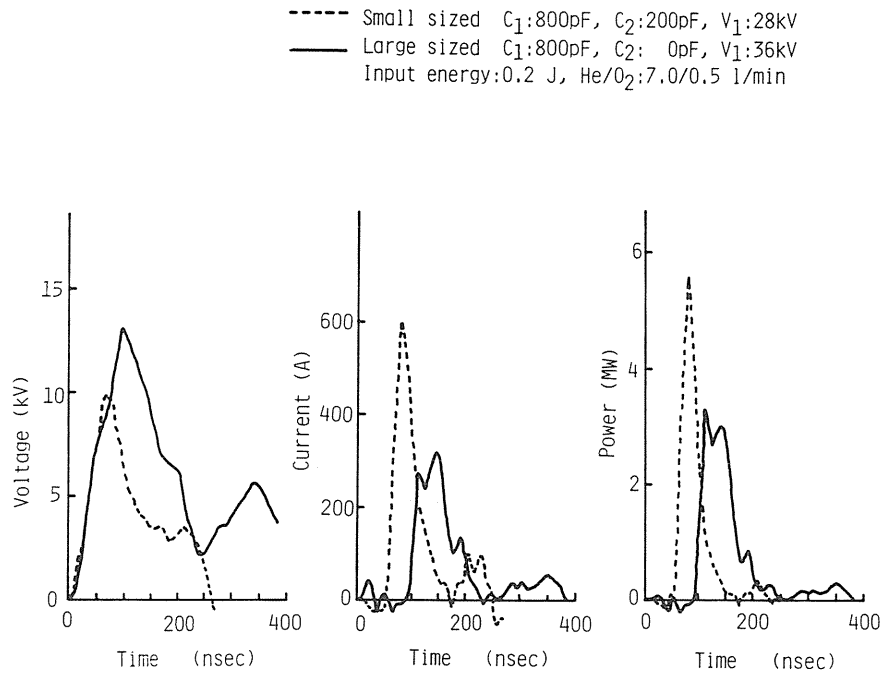

Fig. 3. 7 Voltage across the main electrodes and main discharge current at the same input energy

and 4.3 kV/cm for the large-sized one. The energy density ϱ is given by the following equation.

$$\varrho = \int E \cdot J dt \tag{3.1}$$

Where, E is the average electric field and J is the current density at time t. Assuming that the change of the current density J with time is enough faster than that of the average electric field E, the difference of the energy density is due to the difference of the current density. The efficiency as a function of the injected charge density into the main discharge region is shown in Fig. 3. 8. The efficiency of the ozone generation increases with the decreasing of the injected charge density. One of the reasons for the decreasing of the efficiency with the current density is the destruction of the ozone molecule by the atomic oxygen as shown by the following reaction.

$$O + O_3 \rightarrow 2O_2 \tag{R-19}$$

The probability P that the oxygen molecules are dissociated by the discharge is shown by the following equation.

$$P = \sigma \cdot N_e / S \tag{3.2}$$

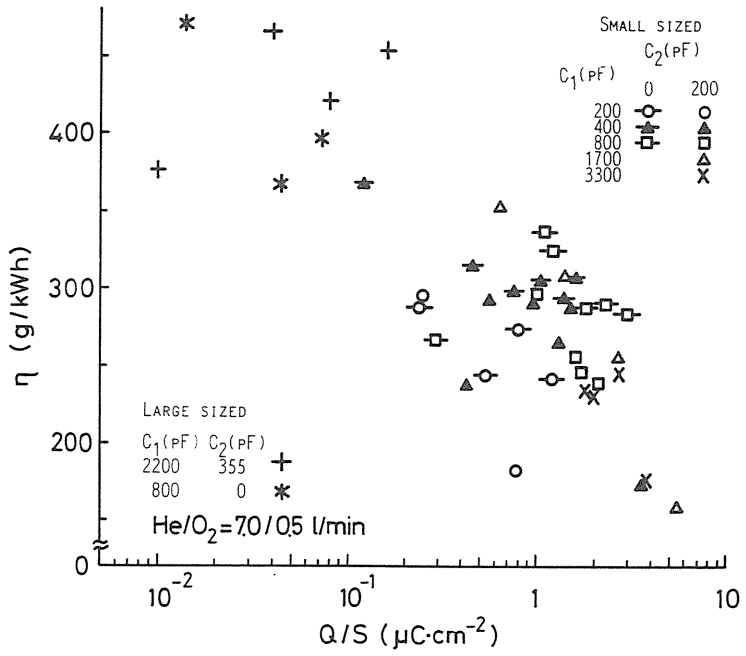

Fig. 3. 8 Efficiency of ozone generation vs. electric charge density for both sizes of ozonizer

Table 3. 1 Comparison of the probability of dissociation of oxygen molecule and the number density ratio of atomic oxygen and oxygen molecules in the discharge volume

size	small-sized	large-sized
probability(P)	1.3×10^{-3}	4.6×10^{-5}
$[O]/[O_2]$	2.6×10^{-3}	9.2×10^{-5}

Where, σ is the cross section of the dissociation, N_e is the total number of electrons and S is the area of the discharge. Both the probability and the ratio of the number of atomic oxygen to the number of oxygen molecule ($[O]/[O_2]$) are shown in Table 3. 1 for two different size of ozonizer. Assuming that is nearly equal to $10^{-16}\,cm^2$. The dissociation probability of the large-sized ozonizer is two order of magnitude smaller than that of the small-sized ozonizer and the ratio of the number of atomic oxygen is proportional to the dissociation probability. From these results, the dissociation probability of the oxygen molecules is large at high current density and the number of atomic oxygen increases, and the reaction of destruction of ozone molecule occurs frequently and finally the efficiency decreases. This phenomena will be find in the results of the saturation of the ozone generation obtained by the small-sized ozonizer. It has been reported by Kogelschatze et al[12] that the efficiency decreases when the number of atomic oxygen increases in the discharge region.

4. Possibility of the improvement of the efficiency of ozone generation with small-sized ozonizer

The reason that the efficiency of ozone generation with the small-sized ozonizer is inferior to that with the large-sized one is due to the larger input energy density, that is, higher current density and the following two reasons are considered for that (Fig. 4. 1).

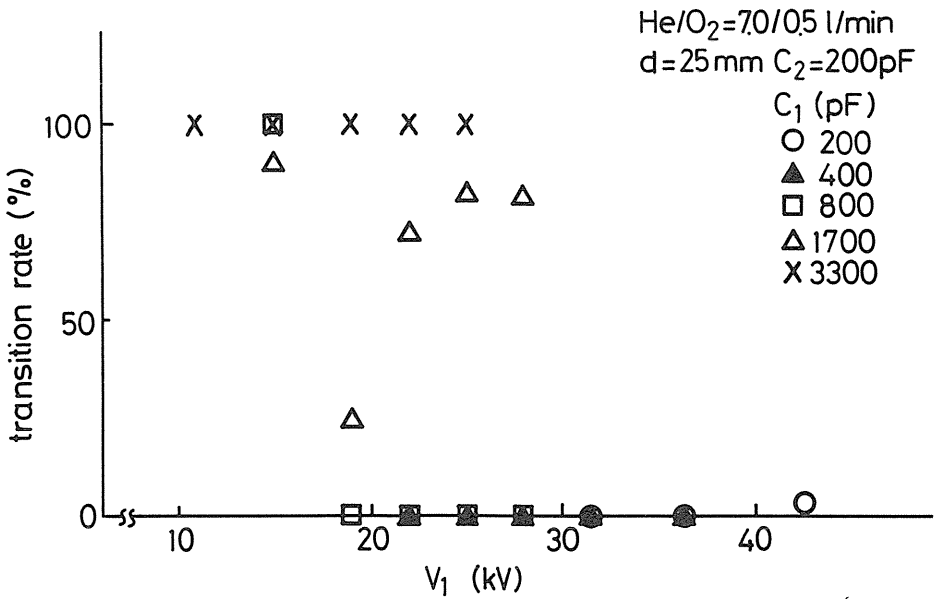

Fig. 4. 1 Glow-to-arc transition rate as a function of applied voltage V_1 for various capacitance C_1 at constant gap spacing of d=25 mm and C_2=200

i) In case of small capacitance C_1, since the distributed capacitance of the coaxial cable plays a role as a capacitance C_2 effectively and influences on the voltage V_2 applied across the main electrodes, and higher charging voltage on the capacitor C_1 is needed for the occurrence of the main discharge.
ii) The glow-to-arc transition appears at lower charging voltage.
For that reason, it is necessary for the establishment of the high efficiency with the small-sized ozonizer that the distributed capacitance of the feeder (or cable) has to be reduced as possible as we can and the stable discharge has to be maintained at lower charging voltage with lower capacitance C_1. Since there is a limitation for the reduction of the distributed capacitance of the cable, the minimum value of the capacitance C_1 is also limited. Therefore, it is considered to get a stable discharge at low charging voltage. In the large-sized ozonizer whose glow-to-arc transition is low at low charging voltage, both measured capacitances of C_s and C_g in the trigger circuit which influence on the production of the initial electrons are 800 pF and 330 pF respectively. On the other hand, since the values of C_s and C_g for the small-sized ozonizer are 800 pF and 16 pF, the ratio of C_s/C_g is larger compared with that of the large-sized ozonizer and almost of the applied voltage V_2 is applied to the trigger electrode. But about 70% of the voltage V_2 is applied to the trigger electrode in the large-sized ozonizer. From these results, when the value of C_s in the small-sized ozonizer is changed to 44 pF, the transition is not observed at $V_1 = 15$ kV and the measured ozone production is about two times larger (~430 g/kWh) compared with that obtained with $C_s = 16$ pF. In this case, the experimental parameters are $C_1 = 800$ pF and He/O_2=7.0/0.5 l/min. In the case of large ratio of C_s/C_g, the initial electrons are produced non-uniformly at around the edges of the trapezoid and the non-uniformity of the electric field is rather intensified and it introduces the occurrence of the transition.

5. Generation of atmospheric diffuse glow discharge in mixtures with oxygen[13)]

5. 1. Introduction

The method which is applied for the ozone generation by discharge between metal electrodes with relative long gap spacing (2–3 cm) has been reported in place of conventional ozonizer. The glow-to-arc transition comes into question after the establishment of atmospheric glow discharge. As the efficiency of the ozone generation is affected by the appearance of this transition, it is important for improvement to obtain an anti-transition. In the ozonizer using discharge between metal electrodes (i.e. no dielectrics is used between main electrodes), the phenomena of macroscopic discharge influence the ozone generation greatly and the characteristics of the ozone generation is complicated with instability of discharge. The macroscopic discharge phenomena and characteristics of the ozone generation are reported here.

5. 2. Experimental apparatus and procedure

The block diagram of the electrical circuit for this experiment is the same shown in Fig. 2. 1. The detail explanation of this circuit is mentioned in the references 9)-10). The amount of generated ozone is measured by the ozone monitor (Ebara Jitsugyo Co.LTD, EG-2001D) using uv absorption method.

5. 3. Experimental results and discussion

The amount of generated ozone (μg[O_3]/shot) as a function of the applied voltage V_1 on the capacitor C_1 (= 850 pF) is measured for the parameter of He/O_2 mixture ratio. In this case the total flow rate is fixed at 3 l/min and another parameters are as follows. The gap spacing d = 1 cm, the repetition rate of discharge f = 1 Hz, the inductance L = 0 μH, and the capacitance C_2 = 250 pF. According to the results, the amount of the generated ozone increase with the oxygen flow rate and the applied voltage V_1 and the threshold of the voltage for the ozone generation shifts to higher voltage for higher oxygen flow rate. In case of glow discharge or glow discharge with weak arcing in mixtures of He/O_2 = 2.8/0.2 l/min, the generated ozone increase with increasing of the inductance L (i.e. the steepness of the voltage applied across the main electrodes decreases with the inductance) and saturate at about L~15 μH as shown in Figs. 5. 1 and 5. 2. The arrows shown in these figures show the appearance of weak arcing. The appearance voltage of the weak arcing shifts to lower voltage with the inductance as shown in Fig. 5. 1. On the other hand, at higher oxygen flow rate the discharge includes the glow-to-arc transition with the intensive arcing and the situation mentioned above is changed, i.e. the amount of generated ozone with L = 0 μH is larger than that with L = 3 μH. Generally speaking, when the delay time between the appearance of the glow discharge and glow-to-arc transition becomes long, the intensity of arcing becomes weak and the generated ozone increase as shown in Fig. 5. 3. In almost glow discharge mode, the generated ozone increase with the oxygen flow rate for various applied voltage V_1 at fixed total flow rate

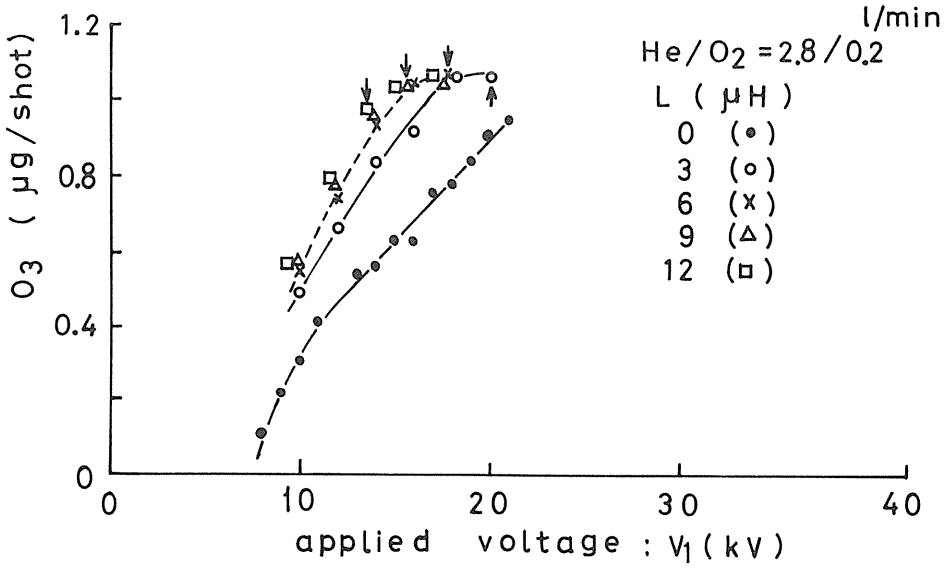

Fig. 5. 1 Generated ozone as a function of applied voltage for various steepness of rise time of applied voltage

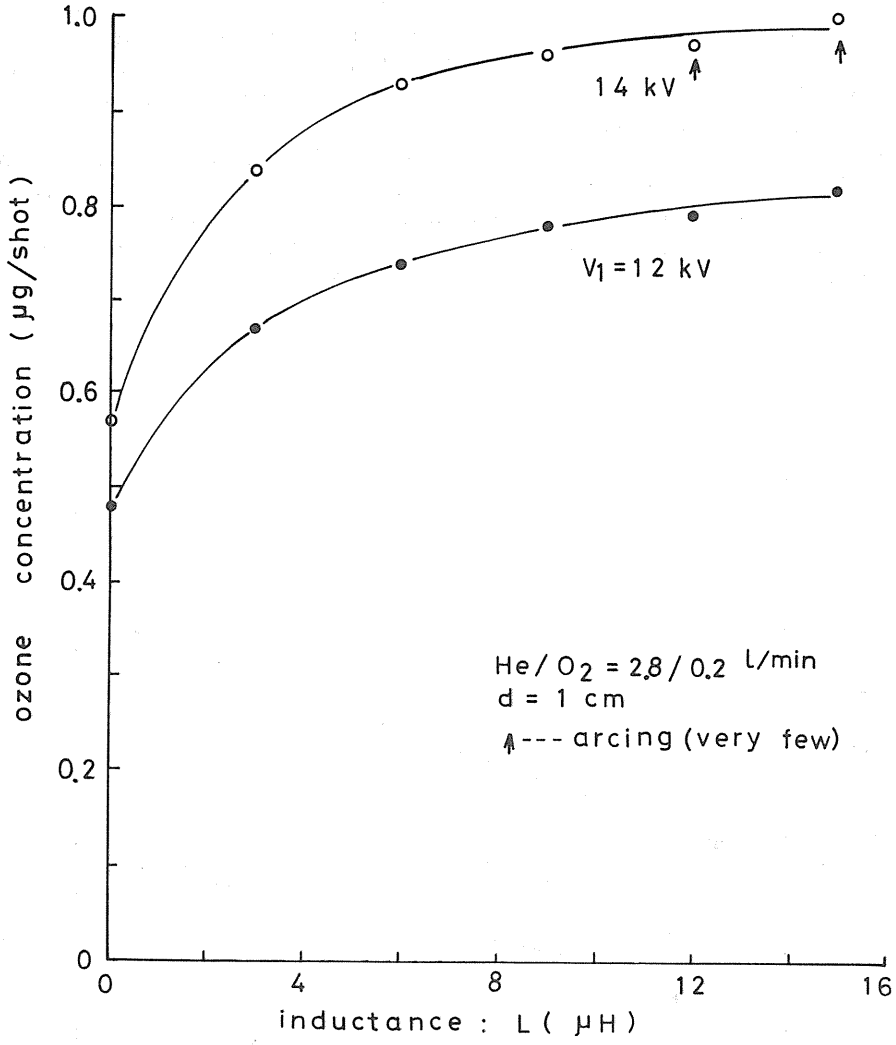

Fig. 5. 2 Generated ozone as a function of inductance

of 3 l/min. The characteristics of ozone generation with dielectrics which is attached on anode have been studied. The size of the dielectrics is 0.35 mm thick, 3 cm wide and 12 cm long. The main gap spacing d and the inductance L are 1 cm and 0 μH respectively. In this case, the discharge volume with dielectrics is considerably large compared with that without dielectrics and it has been confirmed that the amount of generated ozone with dielectrics is more than two times larger in the mixtures of $He/O_2 = 2.8/0.2$ and 2.6/0.4 l/min (Fig. 5. 4). The generated ozone with dielectrics (1.5 cm wide) increase with the applied voltage linearly for the various gap spacing (d = 6–15 mm) as shown in Fig. 5. 5. When the width of dielectrics is changed from 1.5 cm to 3 cm, the slope of increasing line shown in the figure becomes larger (▲→◎). From these results, it is thinkable that there is an effect of dielectric width on the ozone generation. The effect of dielectrics on both

discharge and the ozone generation also has been confirmed in O_2/N_2 mixtures and oxygen only. The diffuse glow discharge is obtained in any O_2/N_2 mixtures and the amount of generated ozone increase both with applied voltage V_1 and with the mixture ratio of oxygen as shown in Fig. 5. 6. On the other hand, the efficiency of the ozone generation (g/kWh) is shown in Fig. 5. 7 as a function of the flow rate of oxygen at $V_1 = 20$ kV, d = 5 mm, L = 0 μH and the total flow rate 2.2 l/min and maximum efficiency of about 240 g/kWh has been obtained. The measured waveforms of the voltage and current across the main electrodes are shown in Fig. 5. 8. The peak value and FWHM (full width at half maximum) of the current are about 100 A and 13 ns respectively. The FWHM is almost same for the various mixtures of O_2/N_2.

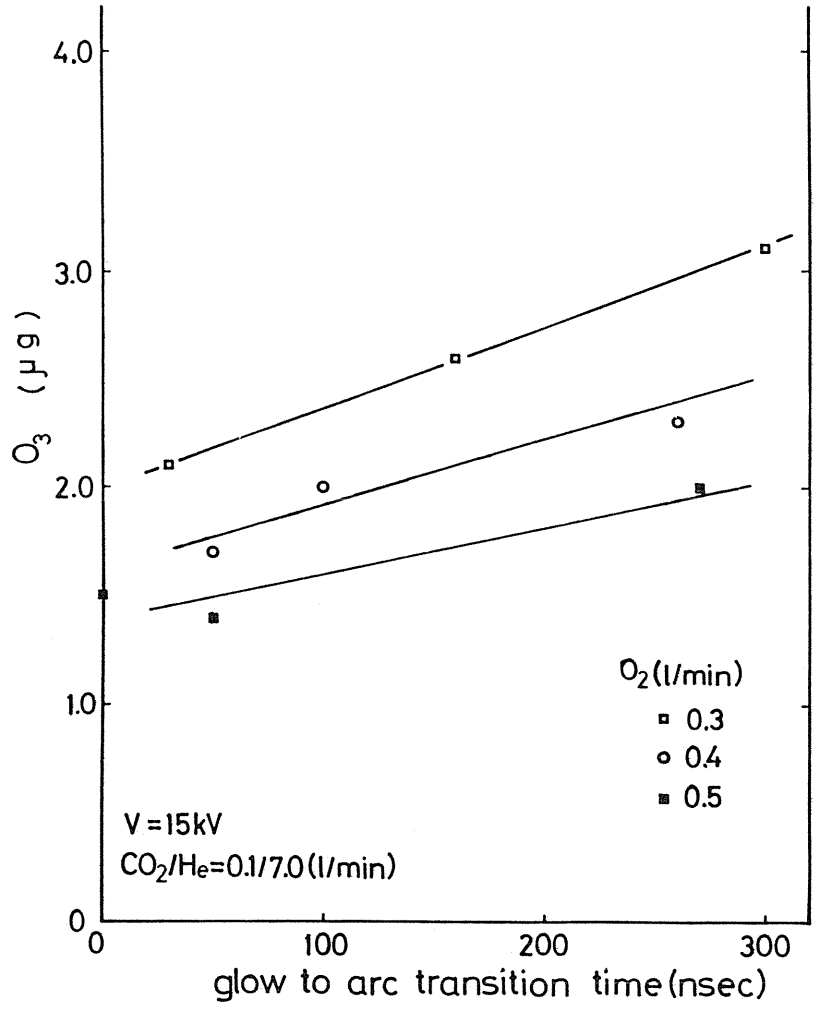

Fig. 5. 3 Generated ozone as a function of glow-to-arc transition time in $CO_2/He/O_2$ mixtures at 15 kV

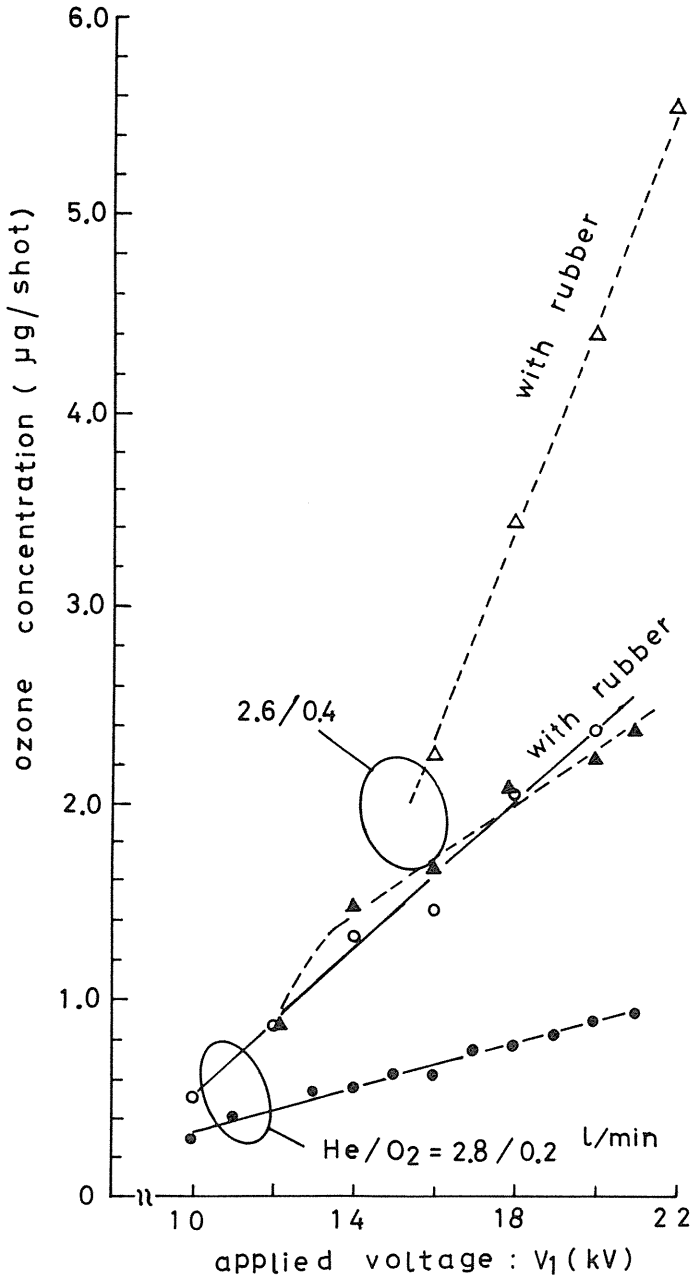

Fig. 5. 4 Ozone concentration as a function of applied voltage with and without rubber used as a dielectric material in He/O_2 mixtures

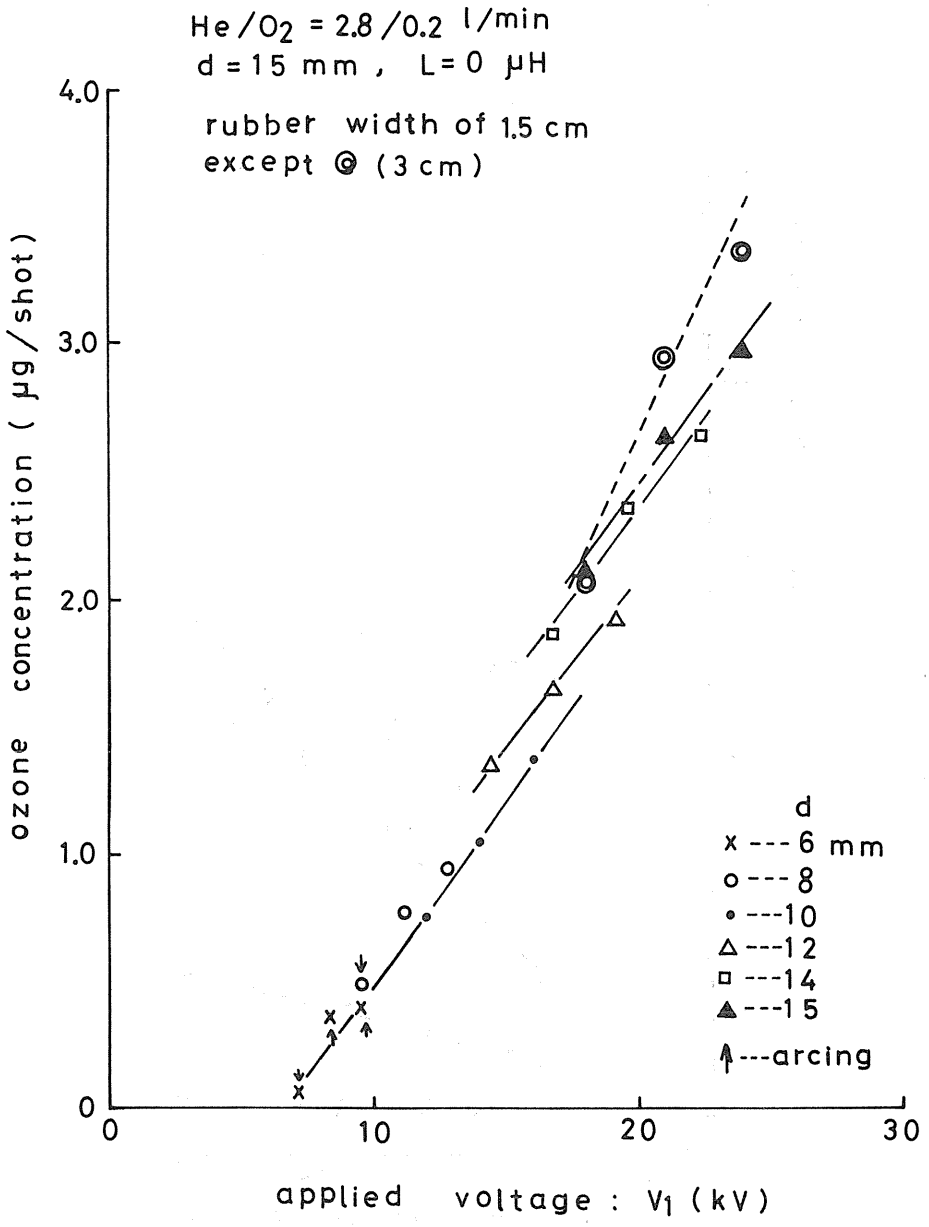

Fig. 5. 5 Ozone concentration as a function of applied voltage for various gap spacing (d=6−15 mm) with rubber as dielectric material whose width is 1.5 cm and 3 cm (◎)

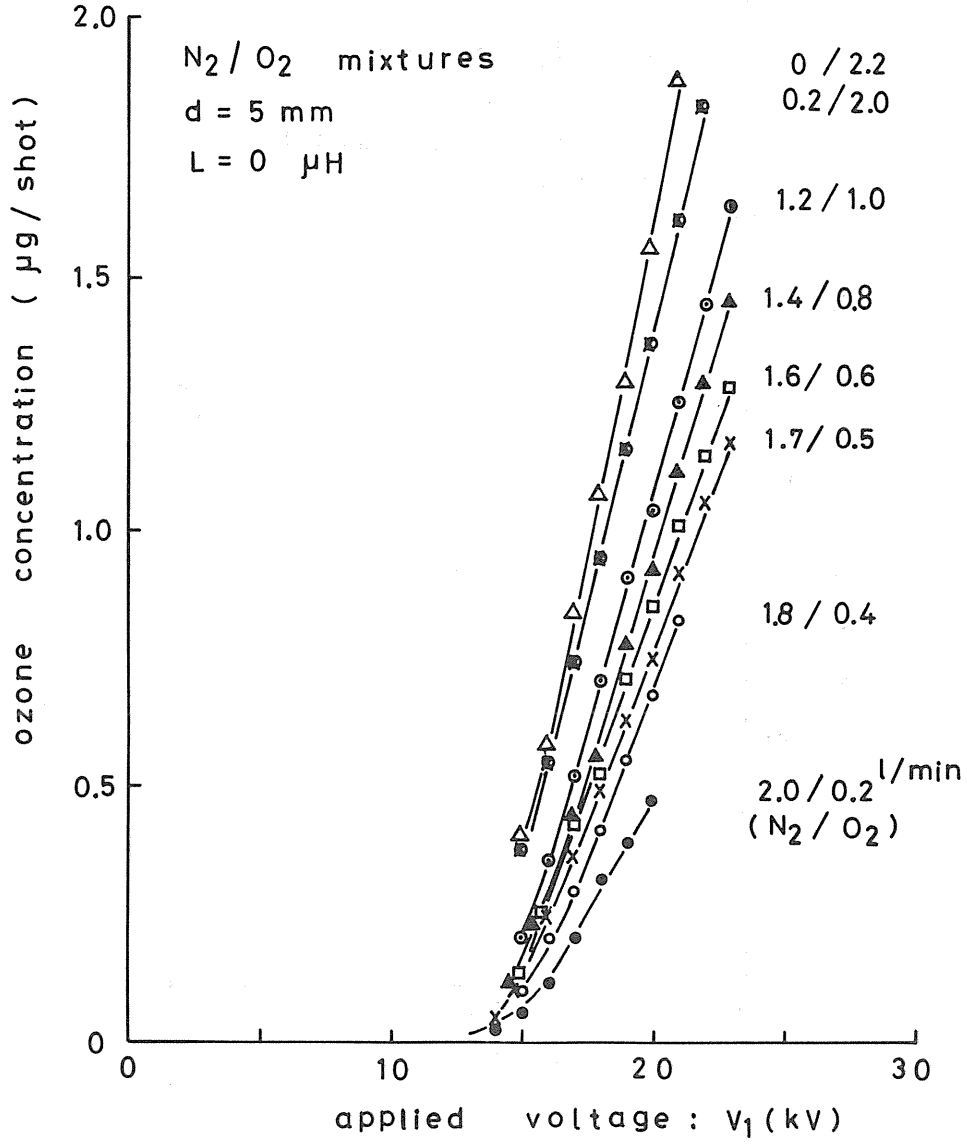

Fig. 5. 6 Generated ozone as a function of applied voltage in the different mixture ratio of N_2/O_2 at constant gap spacing of 5 mm

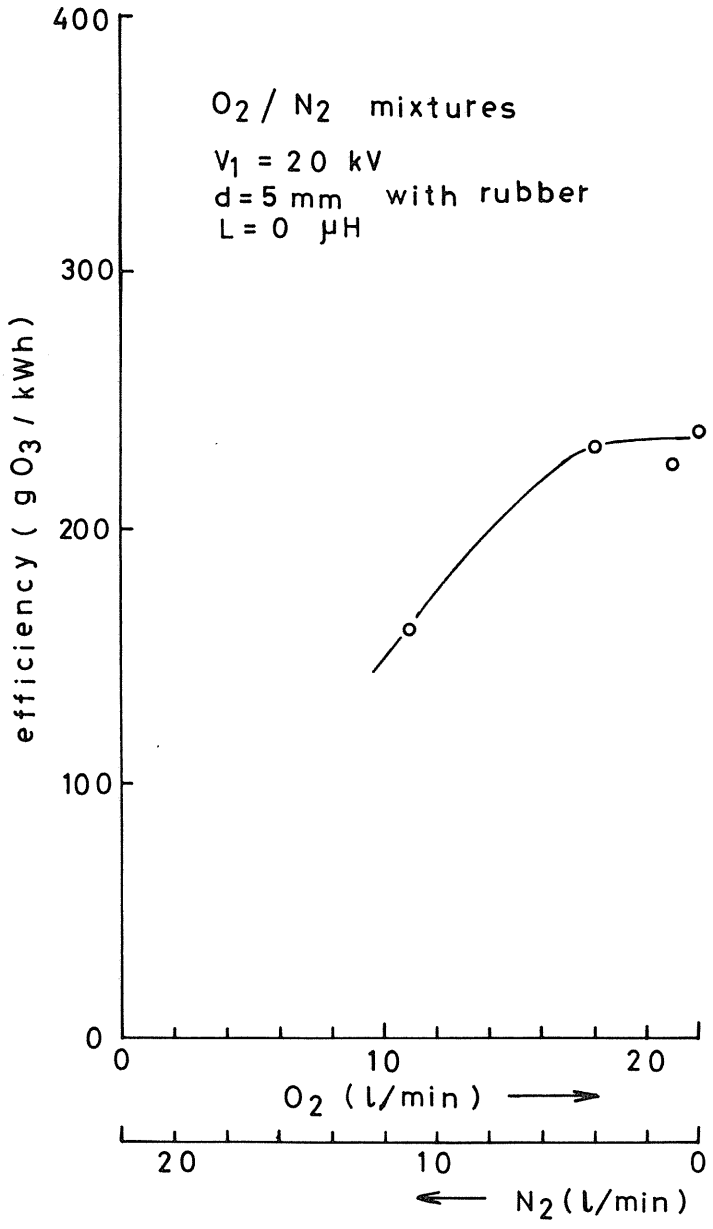

Fig. 5. 7 Efficiency of ozone generation as a function of oxygen flow rate

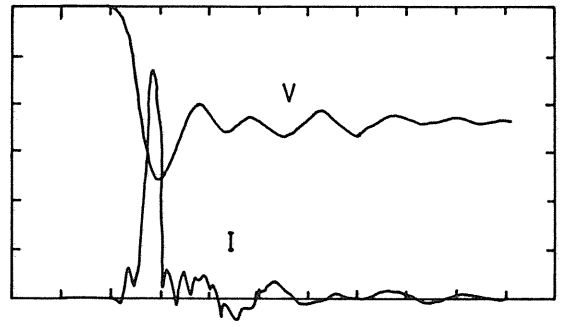

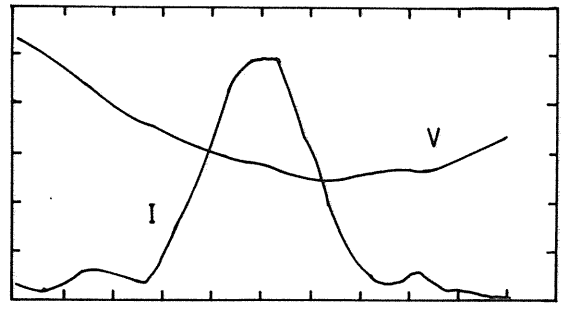

Fig. 5. 8
Waveforms of voltage across the main electrodes and main discharge current in pure oxygen

5. 4. Conclusions

In case that glow discharge is obtained without dielectrics, the generated ozone increase with the inductance L. The glow-to-arc transition with intensive arcing reduces ozone generation. Attaching dielectrics on anode, the discharge volume increases compared with that without dielectrics and the improvement of discharge is also made. Especially, the improvement in O_2/N_2 mixtures is remarkable and the glow discharge is obtained even in the oxygen only. This type of device mentioned above is available for high efficiency ozonizer, producing large amount of ozone, excitation of gaseous lasers, and the generation of the atomic oxygen effectively.

6. Discharge operation with higher repetition[14)]

The He/O_2 mixtures are used in this experiment and the electrical circuit used is shown in Fig. 6. 1. Two capacitors C_0 and C_1 are connected in series and the capacitor C_0 is used to prevent the current from flowing continuously from the power source when the arc discharge appears across the main electrodes. The main gap spacing is 10 mm and the total flow rate is about 7 l/min. The constant applied voltage V_0 is 11.8 kV. The frequency of the discharge ($f = 360$ Hz) is measured by the voltage waveforms on the capacitor C_1. The experimental results are shown in Table 6. 1 and Fig. 6. 2. The produced ozone is maximum in the mixture of $He/O_2 = 7.0/0.2$ l/min due to the effect of both increasing of the oxygen flow rate and the stability of discharge.

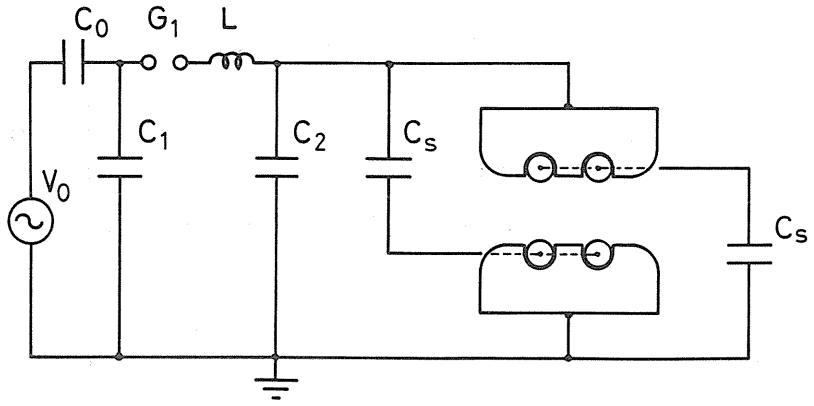

Fig. 6. 1 Electrical circuit for discharge operation with higher repetition rate

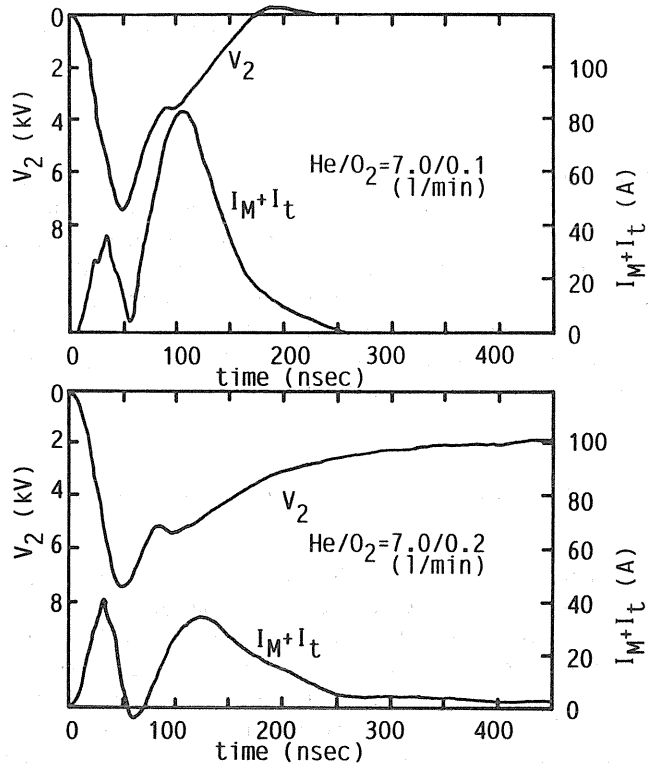

Fig. 6. 2 Observed voltage and current waveforms for different ratio in He/O_2 mixtures

Table 6. 1 Ozone production in He/O_2 mixtures

O2 (l/min)	discharge condition	O3 (μg/shot)
0. 1	glow	0. 13
0. 2	glow and arc (few)	0. 27
0. 3	arc	0. 19

7. Ozone generation in O_2/N_2 mixtures

Though the efficiency of more than 400 g/kWh has been obtained in He/O_2 mixtures, it is superior to use the O_2/N_2 mixtures (finally the air) economically in place of the expensive helium gas. The conditions for the establishment of the stable atmospheric glow discharge in O_2/N_2 mixtures using the double discharge type ozonizer and the ozone generation characteristics are studied.

7. 1. Influence of dielectric material as the cover of the trigger electrode[15]

Both Pyrex and quartz tubes are used for the measurement of the effect of dielectrics and transmittance of the ultraviolet rays. The produced ozone is shown in Fig. 7. 1 as a function of the applied voltage V_1. The produced ozone with quartz tube is much more than that with the Pyrex tube, though the glow-to-arc transition of almost 100% appears.

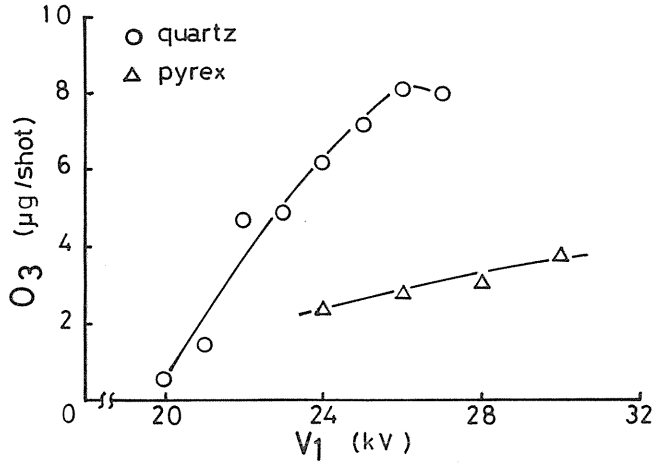

Fig. 7. 1 Influence of dielectric material on ozone production

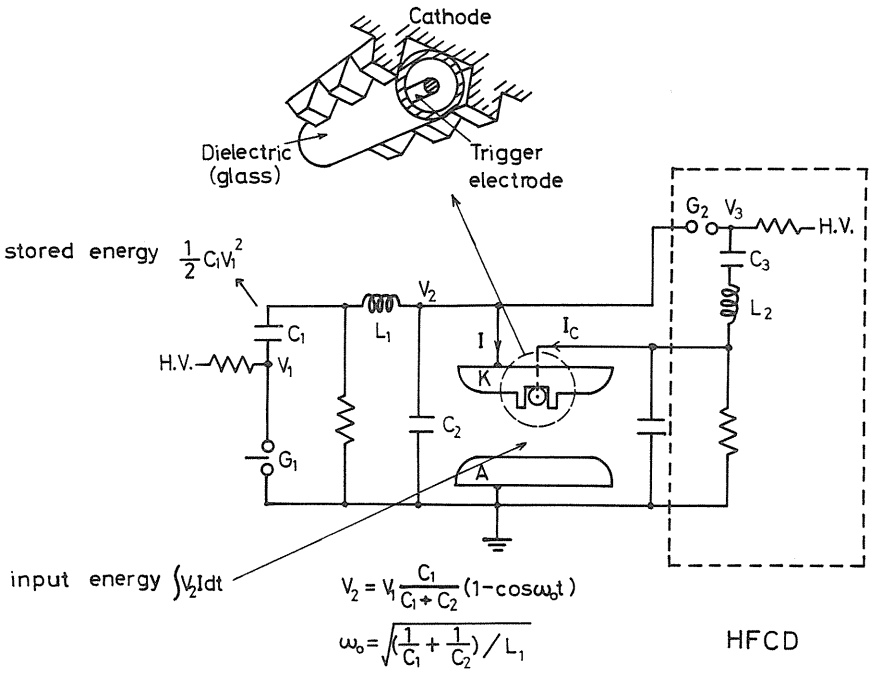

Fig. 7. 2 Electrical circuit of double discharge type ozonizer

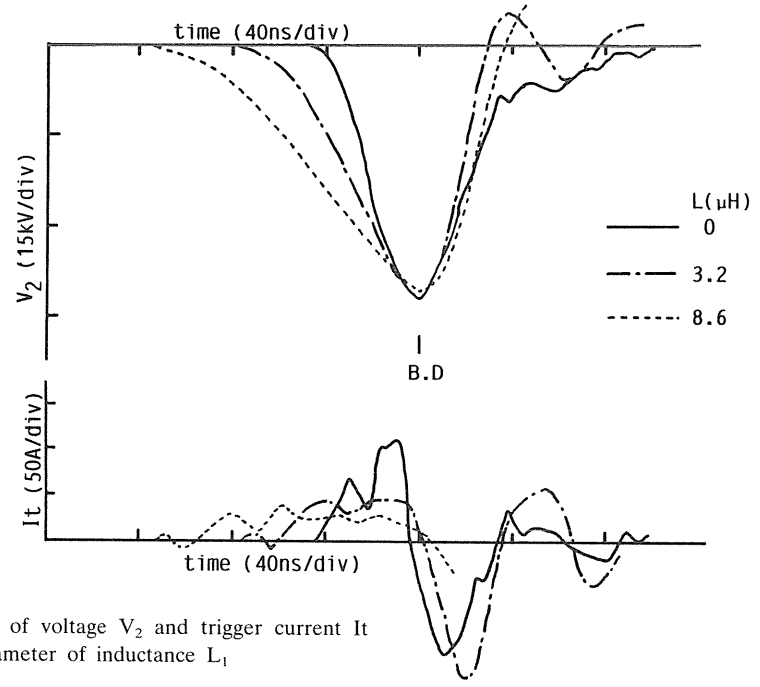

Fig. 7. 3
Waveforms of voltage V_2 and trigger current It as the parameter of inductance L_1

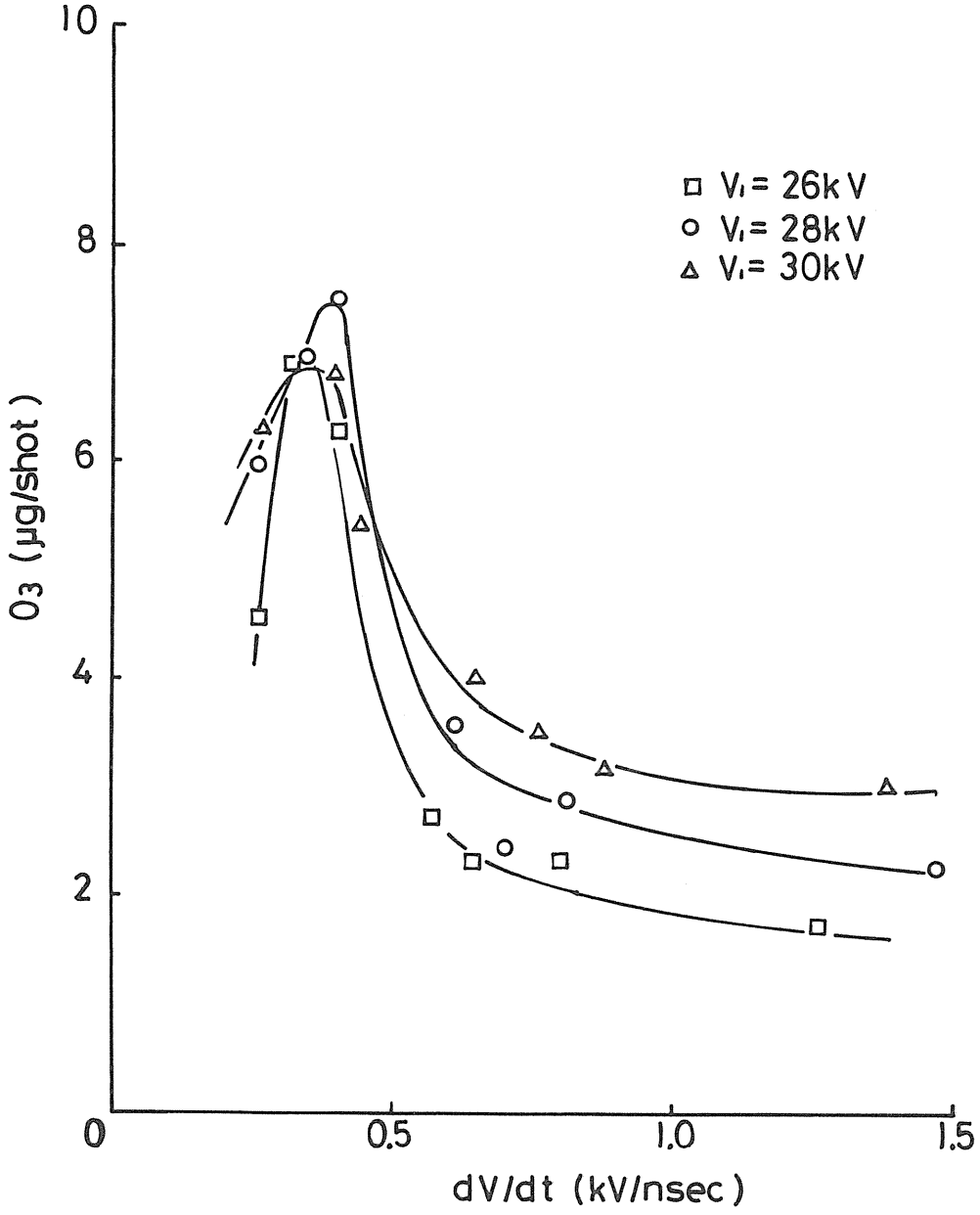

Fig. 7. 4 Produced ozone as a function of dV/dt

No difference of the discharge condition between with Pyrex and quartz tube is observed visually. The effect of the dielectric constant of the tube and the transmittance of uv rays from inside of the tube must be separated in future.

7. 2. Influence of the steepness of the applied voltage

The inductance shown in Fig. 7. 2 is changed up to 21.3 μH to vary the steepness of the rise time. Both applied voltage V_2 and trigger current are shown in Fig. 7. 3 as a parameter of L_1. By changing the inductance L_1, the steepness dV/dt and the delay time $t_{It\text{-}BD}$ of the breakdown after the trigger current starts are varied. The dV/dt is estimated by the value of 20–80% of the breakdown voltage V_b. Both produced ozone as a function of dV/dt and $t_{It\text{-}BD}$ are shown in Figs. 7. 4 and 7. 5. In this experiment, when the value of inductance L_1 is fixed, both dV/dt and $t_{It\text{-}BD}$ are automatically decided and the tendency of them is opposite. So, they must be independently controlled by using series gap G_m as shown in Fig. 1 in the reference 16). When the steepness of the rise time of the applied voltage is increased, the delay time between the pre-ionization and the main discharge is changed automatically. Therefore the delay time is not suitable for the establishment of the glow discharge, the characteristics of the ozone generation is not so good. In this section, the ozone generation with a series gap G_m which is shown in Fig. 7. 6 is introduced.[16] Both the steepness of the rise time of the applied voltage and the delay time are controlled independently by a new electrical circuit which has the series gap G_m as mentioned above.

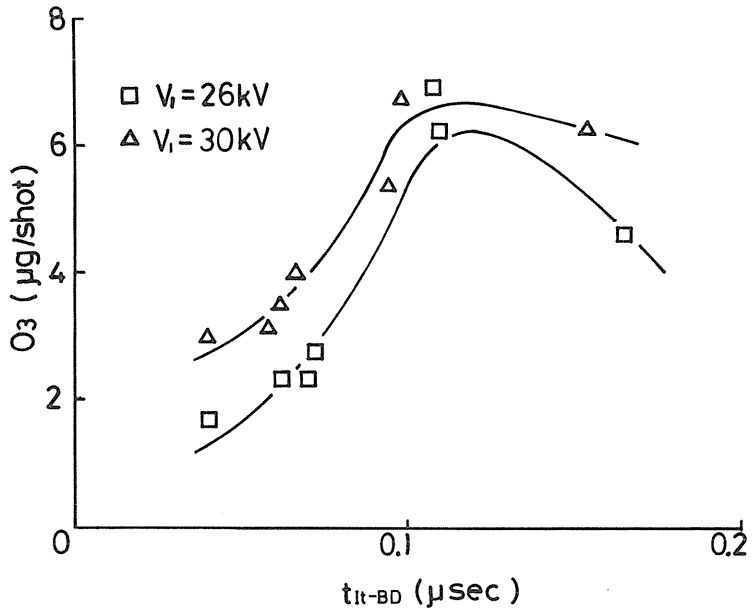

Fig. 7. 5 Produced ozone as a function of delay time tIt-BD

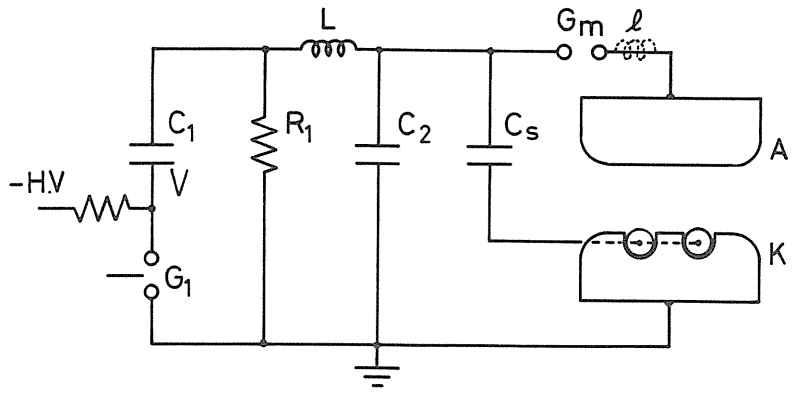

Fig. 7. 6 Schematic diagram of the experimental device

7. 2. 1. Experimental apparatus and procedure

The schematic diagram of the experimental device is shown in Fig. 7. 6. The typical cross section of the discharge is about 3.5 mm × 10 mm and the discharge length (i.e. the direction of gas flow) is about 10 cm long. The gap G_m as shown in Fig. 7. 6 is connected with one of the main electrodes and it is consisted with sphere and plane electrodes. It's gap spacing d_m is variable at atmospheric pressure with N_2 gas or dry air. From the ignition of gap G_1 to the appearance of voltage on capacitor C_2 is the same situation with without G_m.[10] But, although the voltage on capacitor C_2 increases and trigger current starts to flow, the steep voltage does not appear between main electrodes before the ignition of G_m and the steep voltage appears with the ignition of G_m. That is, it is the merit of this circuit that the steepness of the voltage and the timing of the pre-discharge for the initial electrons are independently controlled by the gap G_m. In the experiments, the timing between the pre-discharge and the main discharge is changed by the variation of the gap spacing d_m of gap G_m. Both O_2/N_2 and O_2/He mixtures are used. The voltage and the main discharge current are measured by a high voltage probe (Tektronix P6015) and a shunt (made by Tokyo Transformer Co.LTD) respectively. The amount of generated ozone is measured by the ozone monitor (Ebara Jitsugyo Co.LTD, type EG-2001D) using uv absorption method.

7. 2. 2. Experimental results

The experiments have been done at the fixed gap spacing $d_m = 5$ mm. The circuit parameters shown in Fig. 7. 6 are $C_1 = 3500$ pF, $C_2 = 200$ pF, and $L = 4.4$ μH. The gap spacing of the main electrodes is 10 mm. The results are shown in Fig. 7. 7. The amount of generated ozone with G_m is about three times larger compared with that without G_m at large value of V_1. On the other hand, at lower voltage, the amount of generated ozone with G_m is lower compared with without G_m because gap G_m does not fire frequently and the effective generated ozone per one discharge is estimated to be low. The glow-to-arc transition is 100% for all of the measured points in this experiments.

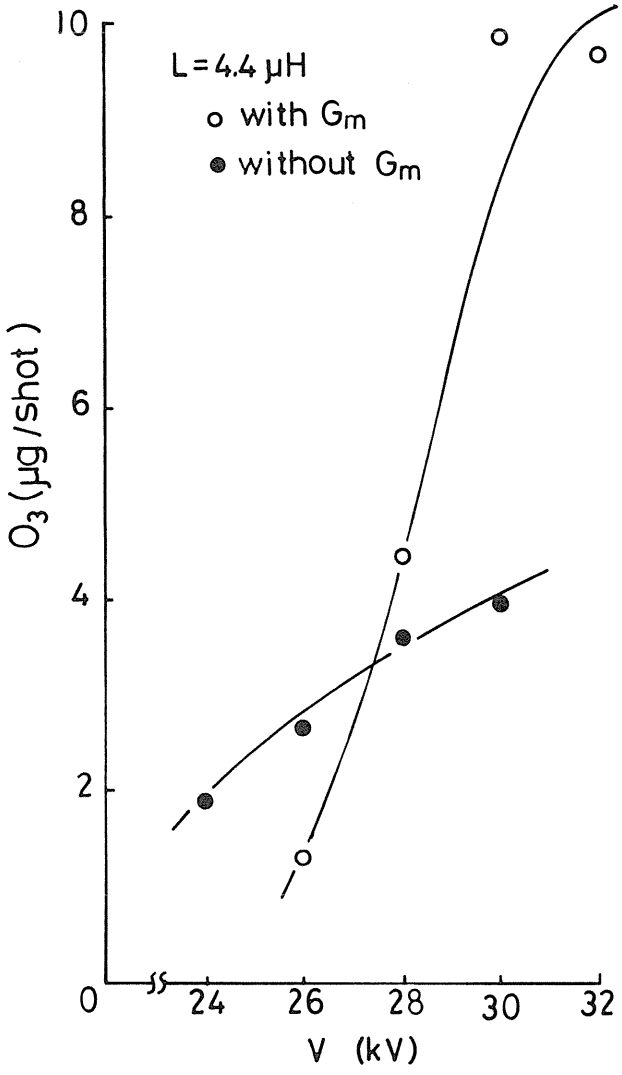

Fig. 7. 7 Generated ozone as a function of voltage with and without series gap Gm

The effect of gap spacing G_m on ozone generation and discharge is studied. The relation between the gap spacing d_m of G_m and the uniformity of the main discharge (i.e. the glow-to-arc transition rate: t.r.) and the amount of generated ozone are measured. These results are shown in Fig. 7. 8. It is understood from these results that the discharge condition is improved and the amount of produced ozone is increased by changing the gap spacing d_m. It is also clear that the amount of produced ozone is related strongly to the uniformity of the discharge. For that reason, it is very useful to use the gap G_m in the double discharge type ozonizer operated with O_2/N_2 mixtures at atmospheric pressure. The inductance l in the main electrical circuit (i.e. C_2-A-K-C_2 as shown in Fig. 7. 6) also affects the ozone generation characteristics due to the lack of the uniformity of the discharge with the increase of the inductance as shown in Fig. 7. 9.

The effect of the steepness of the applied voltage and the timing of pre-discharge on the main discharge condition is also studied. it is studied to obtain the conditions for the

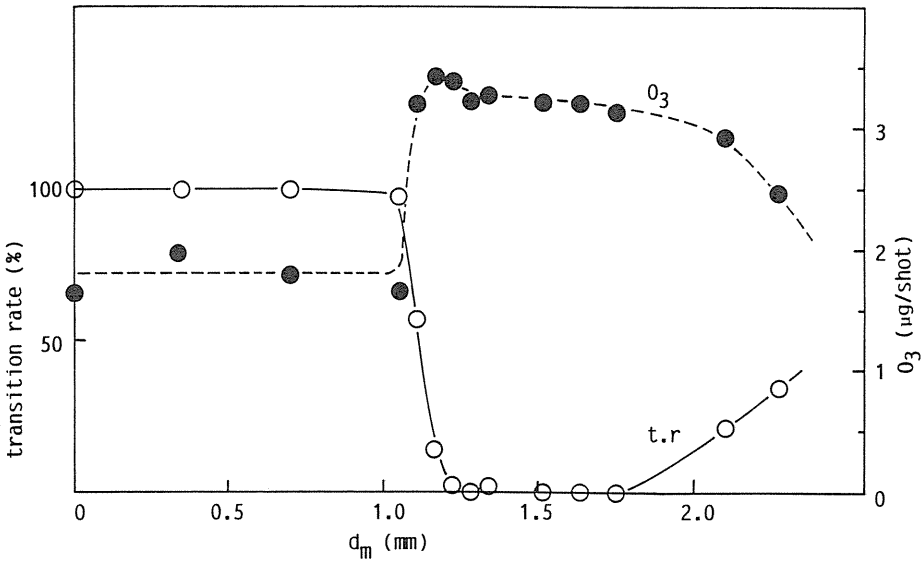

Fig. 7. 8 Generated ozone, glow-to-arc transition rate as a function of series gap spacing d_m

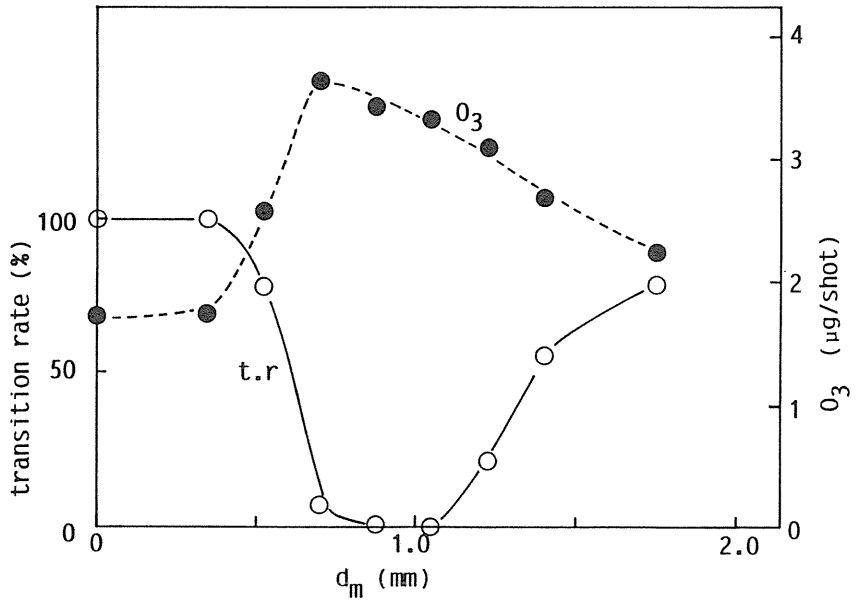

Fig. 7. 9 Influence of the inductance in the main electrical circuit

establishment of glow discharge in O_2/N_2 mixtures at atmospheric pressure. The experiments have been done to combine the following parameters of the electrical circuit, $C_1 = 400,800$ pF, $C_2 = 100$ pF, $C_s = 50,2000$ pF, $L = 0.5,7.0$ μH. A pair of typical voltage and current waveforms measured are shown in Fig. 7. 10. Both the steepness of the voltage dV/dt (kV/ns) and the timing of the pre-discharge $t_{It\text{-}BD}$ (ns) are obtained from these waveforms. The relation between dV/dt and $t_{It\text{-}BD}$, glow-to-arc transition is shown in Fig. 7. 11. The number shown in the figure shows the glow-to-arc transition rate and the positions where the number is written in the figure show the measured points. It is necessary that both conditions of dV/dt = 0.6 kV/ns and $t_{It\text{-}BD} = 30-50$ ns are satisfied to obtain the diffuse glow discharge in O_2/N_2 mixtures at atmospheric pressure.

The stored energy ($= C_1V^2/2$) vs $[O_3]$ (ppm), glow-to-arc transition (%) and the optimum gap spacing d_{op} of G_m are shown in Fig. 7. 12. In this case, dry air with flow rate of 1.5 l/min is used. Both the signs (○) (●) show the measurements of produced

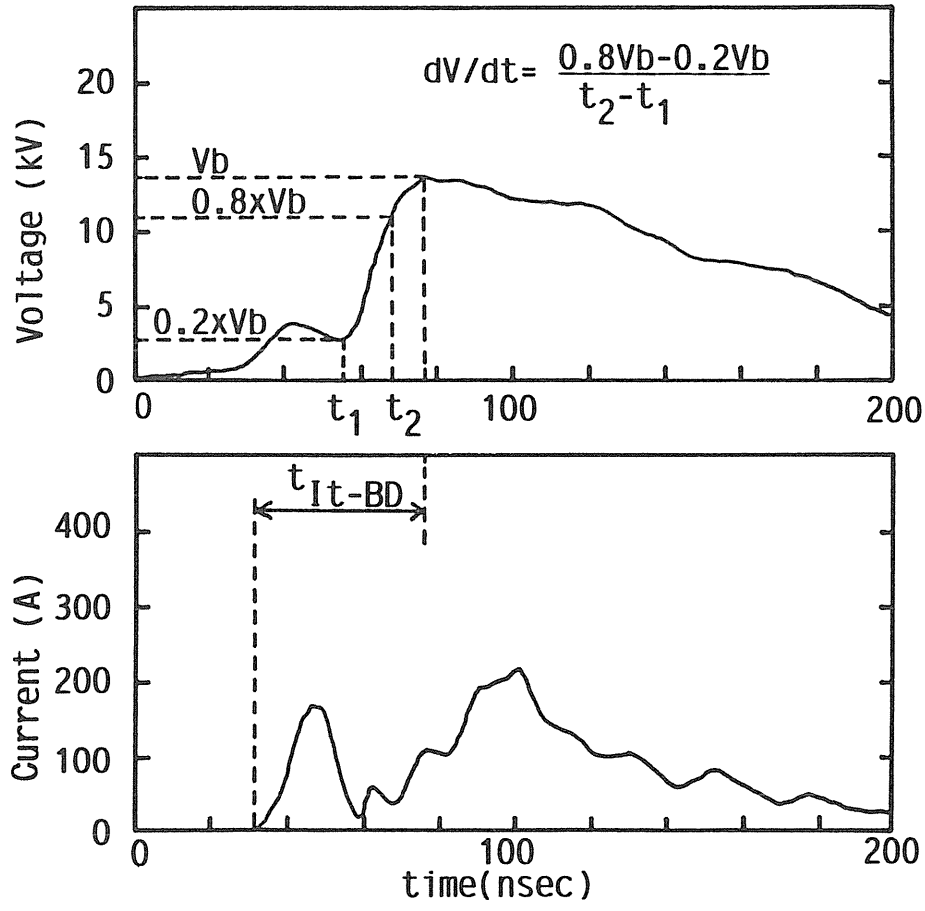

Fig. 7. 10 Typical measured voltage and current waveforms in O_2/N_2 mixtures

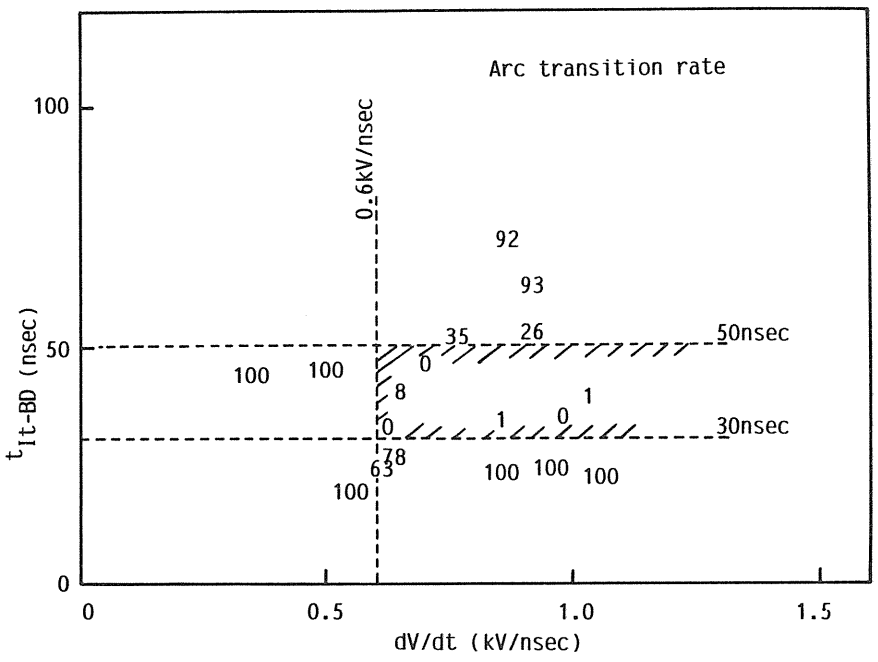

Fig. 7. 11 Relation between dV/dt and tIt-BD, glow-to-arc transition rate

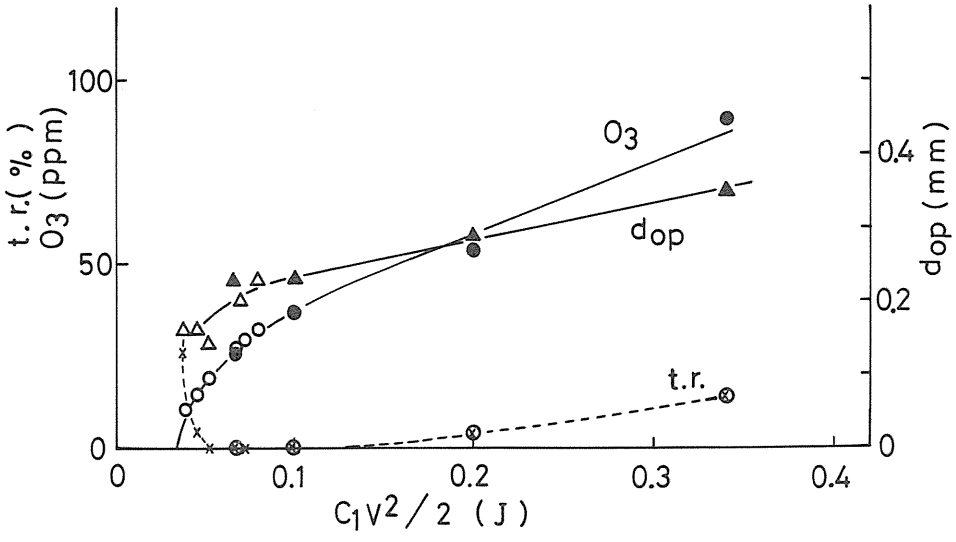

Fig. 7. 12 Ozone concentration, glow-to-arc transition and optimum gap spacing dop of series gap as a function of stored energy

ozone [O_3] (ppm) with the variation of C_1 and fixed voltage V = 28.4 kV, and the measurements with the variation of V and fixed capacitance C_1 = 167 pF respectively. The capacitance of 167–200 pF are obtained for maximum efficiency and in these region, the stable uniform discharge is obtained with free of the glow-to-arc transition.

The stable uniform glow discharge has been established at the repetition rate of 20 Hz using dry air of 1.5 l/min with C_1 = 167 pF, V = 28.4 kV, and C_s = 2000 pF and [O_3] = 520 ppm have been obtained. It is possible to operate at much higher than 20 Hz in dry air at atmospheric pressure from these results.

7. 3. Conclusions

It is found the double discharge is useful for the establishment of atmospheric diffuse glow discharge in both O_2/N_2 and O_2/He mixtures. This method has been applied for the efficient ozone generation and the efficiency of 240 g/kWh for O_2/N_2 mixtures and 400–450 g/kWh for O_2/He mixtures have been obtained. The conditions for glow discharge have been obtained and it has been necessary to be dV/dt > O.6 kV/ns and $t_{lt\text{-}BD}$ = 30–50 ns.

8. Ozone generation by Blumlein type ozonizer[17)]

Characteristics of the Blumlein type ozonizer in O_2/N_2 mixtures are reported here. The block diagram of the ozonizer is shown in Fig. 8. 1. The electronics print board is used as a capacitor. Both electrodes are the copper tube of the diameter of 7 mm and the length of them is 20 cm. The equivalent circuit shown in Fig. 8. 2 is used for the explanation of the operation. At first, two capacitors are charged simultaneously at the voltage V_1, and the gap G is closed, the charge in the capacitor C (right side in the figure) starts to oscillate in the circuit of L and C. The voltage V_2 on the cathode is given by the following equation.

$$V_2 = V_1(cos\omega t - 1),\ \omega = 1/\sqrt{LC} \tag{8.1}$$

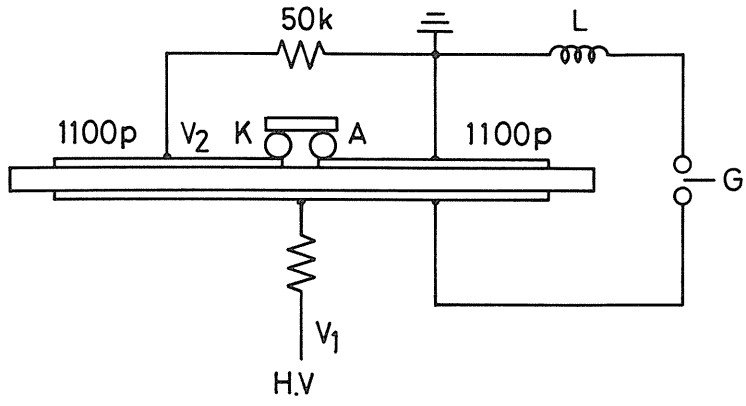

Fig. 8. 1 Schematic diagram of the Blumlein type ozonizer

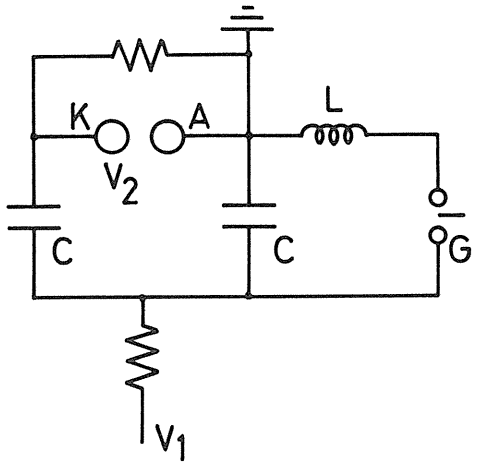

Fig. 8. 2 Equivalent circuit for the Blumlein type ozonizer

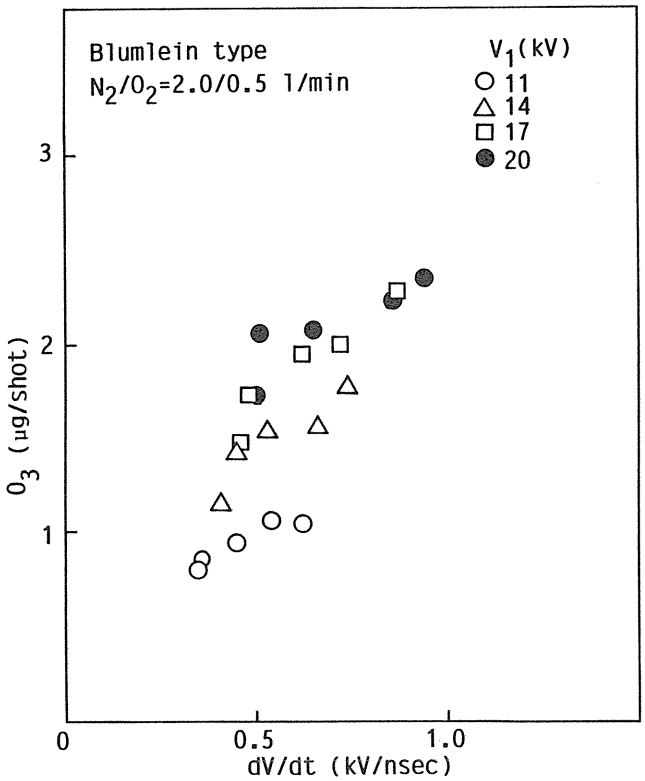

Fig. 8. 3 Generated ozone vs. the steepness of rise time of applied voltage dV/dt as a parameter of charging voltage in N_2/O_2 mixtures

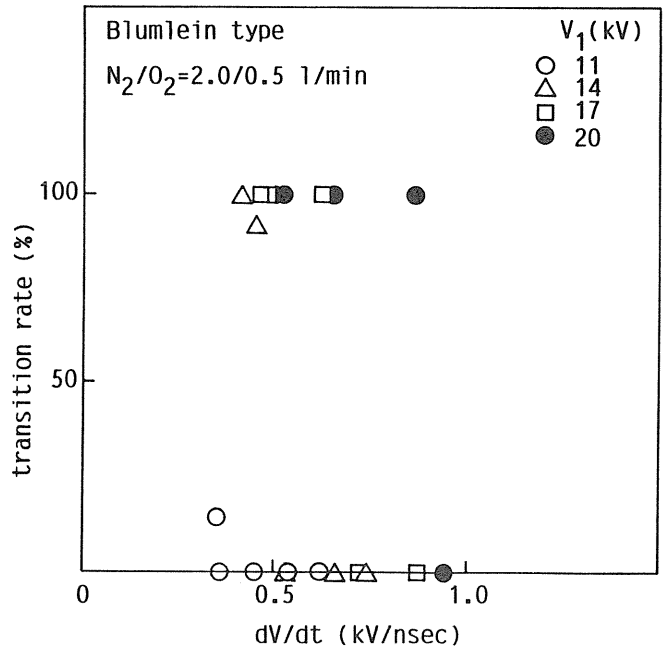

Fig. 8. 4 Glow-to-arc transition rate vs. dV/dt in N_2/O_2 mixtures

The steepness of the rise time of the voltage is

$$dV/dt = -V_1\omega \sin\omega t$$
$$\sim -V_1/\sqrt{LC} \qquad (8.2)$$

here, assumed to be $\sin\omega t \sim 1$.

The inductance L is varied to change the steepness. The amount of generated ozone is shown in Fig. 8. 3 as a function of the steepness dV/dt. The generated ozone increases with the steepness for the various charging voltage V_1. The glow-to-arc transition is also shown in Fig. 8. 4 as a function of the steepness. When the steepness increases, the transition rate reduces and the uniform discharge is easily obtained. The following three factors are considered to be able to obtain the atmospheric diffuse glow discharge without the pre-ionization caused by the pre-discharge in the Blumlein type ozonizer.

i) The surface of the cathode is smooth compared with that of the double discharge type ozonizer which has a groove on the surface.

ii) The discharge obtained by the Blumlein type ozonizer looks like a thin sheet and it is hardly influenced by the weak point on the electrode.

iii) The inductance in the main discharge circuit is small because the main electrodes and the capacitor are connected as a body.

These three factors are successful for the glow discharge in N_2/O_2 mixtures and are effective on the ozone generation.

9. Development of a coaxial cylindrical double discharge type ozonizer

9. 1. Introduction

A new type of the discharge with no dielectric material used between the main electrodes has been proposed to get a large discharge volume at atmospheric pressure.[18)]

Some parameters were found to establish the atmospheric diffuse glow discharge. For example, the rise time of the applied voltage dV/dt and the delay time between the pre-discharge and the main-discharge were required to be greater than 0.6 kV/ns and 30–50 ns respectively. Consequently, the stable glow discharge was obtained for the stored energy in the range of 0.05–0.35 J. Considering these results, the coaxial cylindrical double discharge type ozonizer was made and the characteristics of the ozone production were measured.

9. 2. Experimental apparatus and procedure

The diameter of the outer and inner electrodes is 42 mm and 25 mm respectively. The number of trigger electrode covered with the Pyrex glass tube whose diameter is 3 mm distributed around the inner electrode are twelve and the main gap spacing is 3.5 mm. The length of the ozonizer is about 11cm. The trigger electrodes are connected together and earthed through a capacitor C_s. The dry air is used for the ozone production normally with the flow rate of 2 l/min and the produced ozone is measured by the ozone monitor. The voltage and the discharge current are measured by a high voltage probe and a shunt respectively. The electrical circuit and the cross section of the coaxial cylindrical double discharge type ozonizer are shown in Figs. 9. 1 and 9. 2.

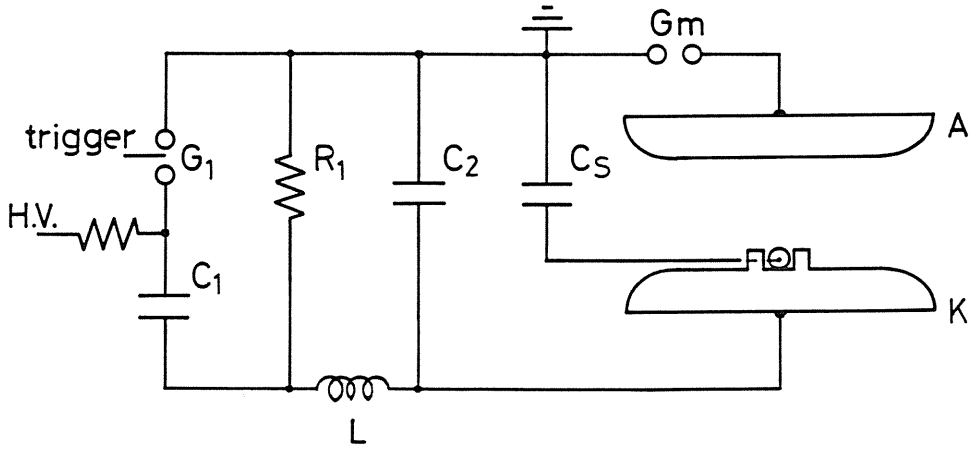

Fig. 9. 1 Electrical circuit of a coaxial cylindrical double discharge type ozonizer

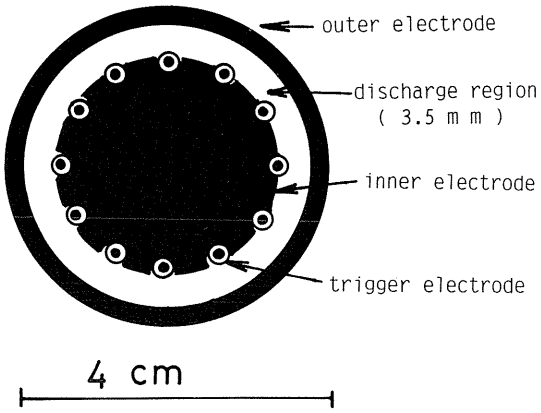

Fig. 9. 2 Cross section of a coaxial cylindrical double discharge type ozonizer

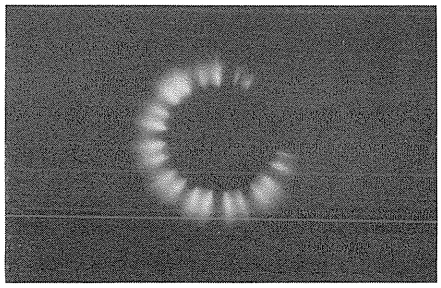

Fig. 9. 3 Time integrated discharge photograph in air at gap spacing of 3.5 mm

9. 3. *Experimental results*

9. 3. 1. *Discharge characteristics*

The breakdown voltage of the gap G_m (V_m) and the cathode (V_k) were measured by the high voltage probe. The discharge photograph observed from the end of the ozonizer and the typical waveforms of the voltage and the discharge current are shown in Figs. 9. 3 and 9. 4 for the variation of the applied voltage on the capacitor C_1. In this case, the gap spacing (d_m) of G_m, capacitance of C_1 and C_s were fixed at 0.47 mm, 250 pF and 100 pF respectively. According to these results, the applied voltage between main electrodes ($V_{AK} = V_K - V_m$) is estimated to be about 5 kV and the average reduced electric field E/p is about 19 V/cm Torr. The rise time of the applied voltage between the main electrodes was 0.3–0.5 kV/ns and the current density on the anode was 3–9 A/cm^2. The voltage of $V_1 = 22$ kV was the critical value for the operation of G_m. Though the cathode voltage was almost constant (~ 15 kV), the main discharge current increased with the applied voltage V_1.

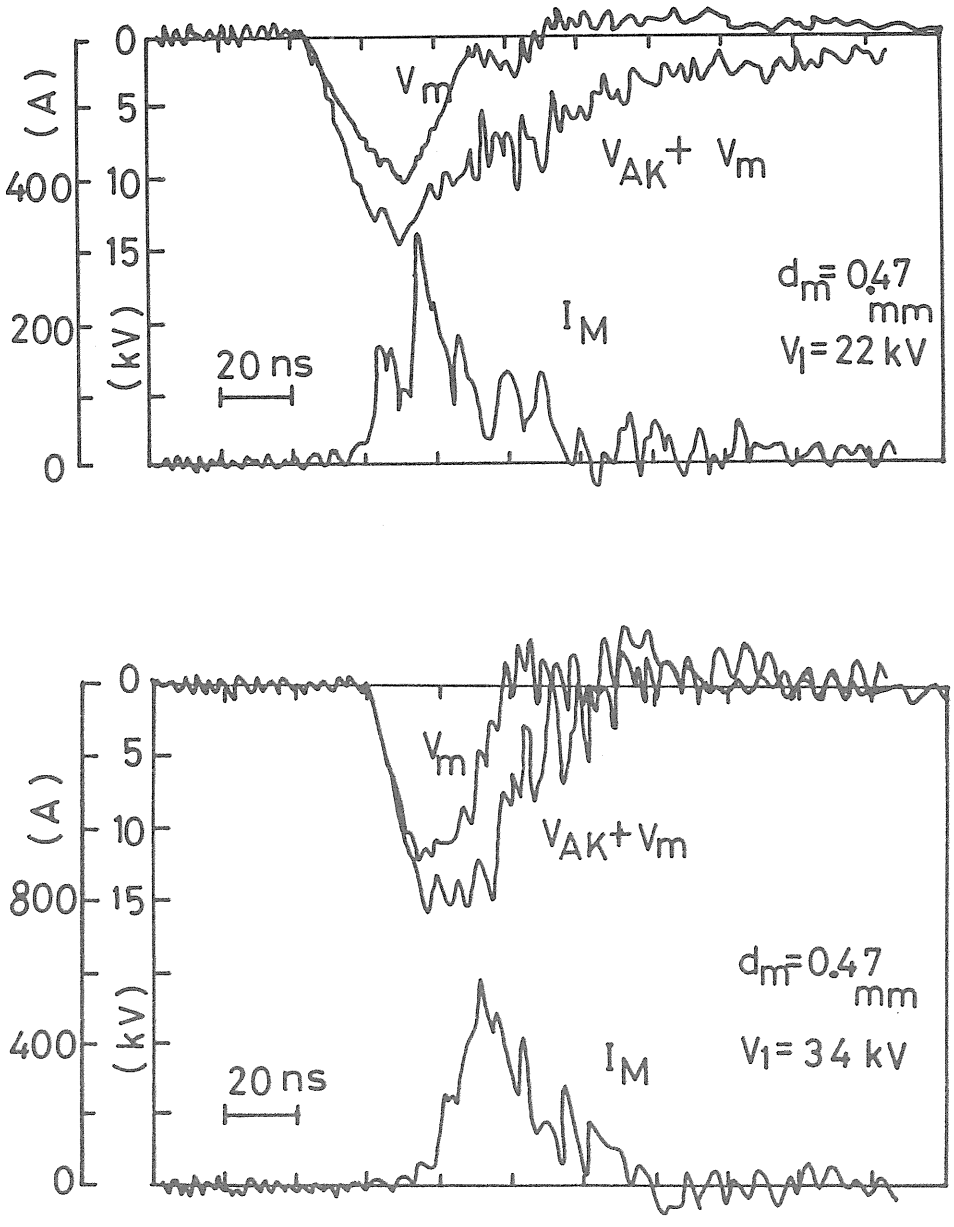

Fig. 9. 4 Typical waveforms of the voltage of series gap G_m, of the cathode and main discharge current for two different charging voltage

9. 3. 2. Ozone production characteristics

At the fixed capacitance C_1 and the flow rate, the produced ozone is influenced with the capacitance C_s connected with the trigger electrodes and the gap spacing d_m. The efficiency of ozone production (= $[O_3]$/[stored energy on capacitor C_1]) and the optimized capacitance C_{so} as a function of the capacitance C_1 with the optimized gap spacing d_{mo} are shown in Fig. 9. 5. The maximum efficiency was obtained with $C_1 = 400$ pF and $C_{so}/C_1 = 0.5$. The produced ozone (= [μg/shot] and [ppm]) and the glow-to-arc transition rate [t.r.] as a function of the frequency of the discharge [f] are shown in Fig. 9. 6. In this experiment, though the diffuse glow discharge was easily obtained up to f = 30 Hz in the air with the flow rate of 2 l/min, but the produced ozone decreased with frequency at 20–30 Hz. On the other hand, the produced ozone as a function of the stored energy on the capacitor C_1 ($= C_1V_1^2/2$) is shown in Fig. 9. 7. The dashed curve in the figure shows the value obtained by the straight line type ozonizer.[16] The ratio of the energy put into both gap G_m ($= E_m$) and the main gap ($= E_{AK}$) to the stored energy decreases with the stored energy as shown in Fig. 9. 8. The error of the measurement is about 25% and the discharge energy varies with the gap spacing d_m as shown in the figure. So far, though the separation of the energy E_m dissipated in G_m from the total energy ($= E_m + E_{AK}$) has been done, the value of E_{AK} is estimated to be 25–30% of the total energy. When the operating frequency of this type of ozonizer was increased up to 100 Hz in air with the

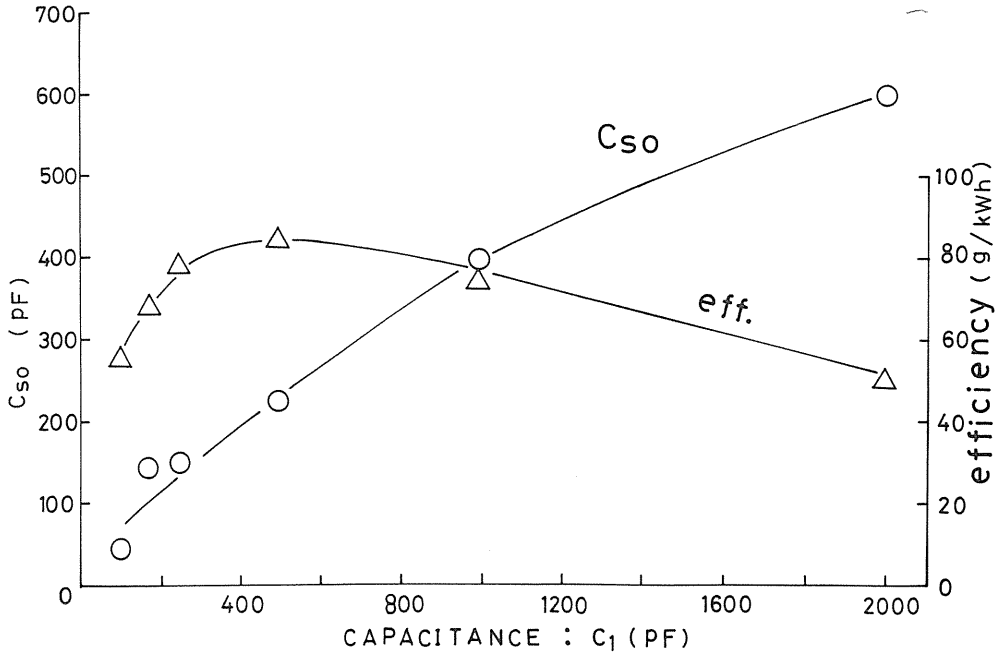

Fig. 9. 5 Efficiency of ozone generation and optimized capacitance C_{so} as a function of capacitance C_1 with the optimized gap spacing

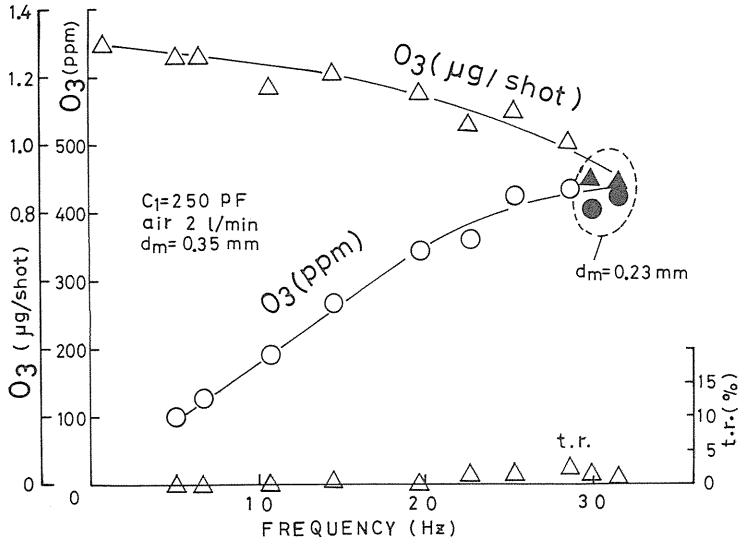

Fig. 9. 6 Produced ozone and glow-to-arc transition rate [t.r.] as a function of frequency of discharge

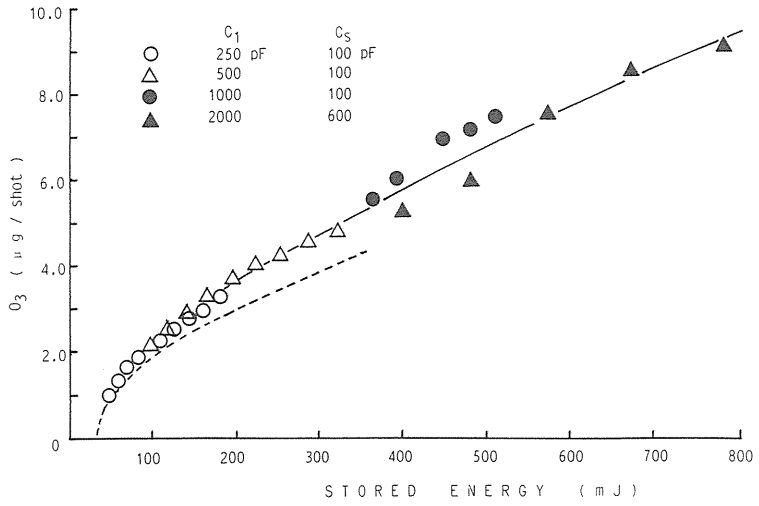

Fig. 9. 7 Produced ozone as a function of stored energy on capacitor C_1. Dashed curve in the figure shows the value obtained by the type of straight line ozonizer for various capacitances

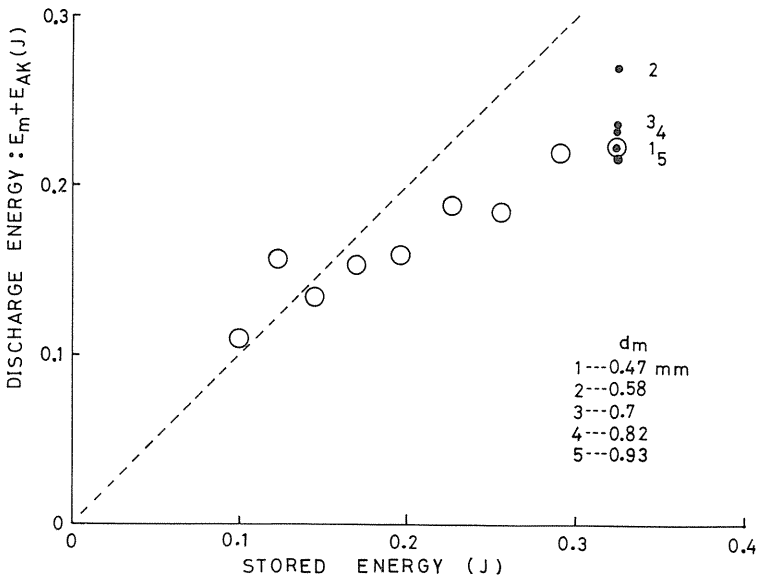

Fig. 9. 8 Energy injected into both series gap G_m and main gap vs. stored energy

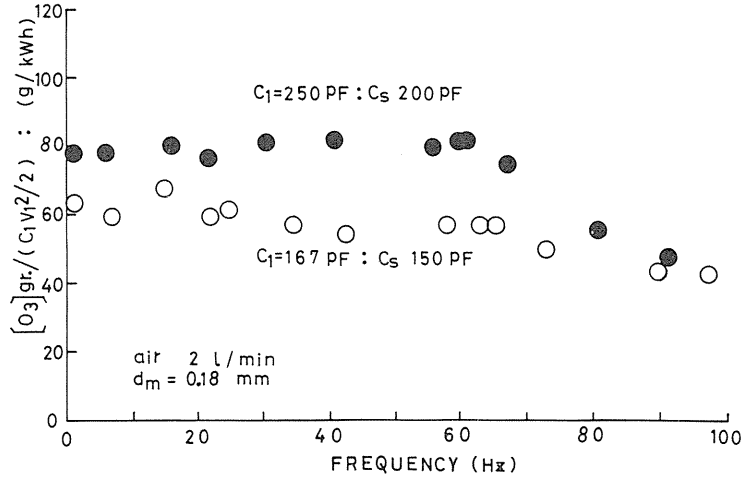

Fig. 9. 9 Efficiency of ozone generation as a function of frequency of discharge

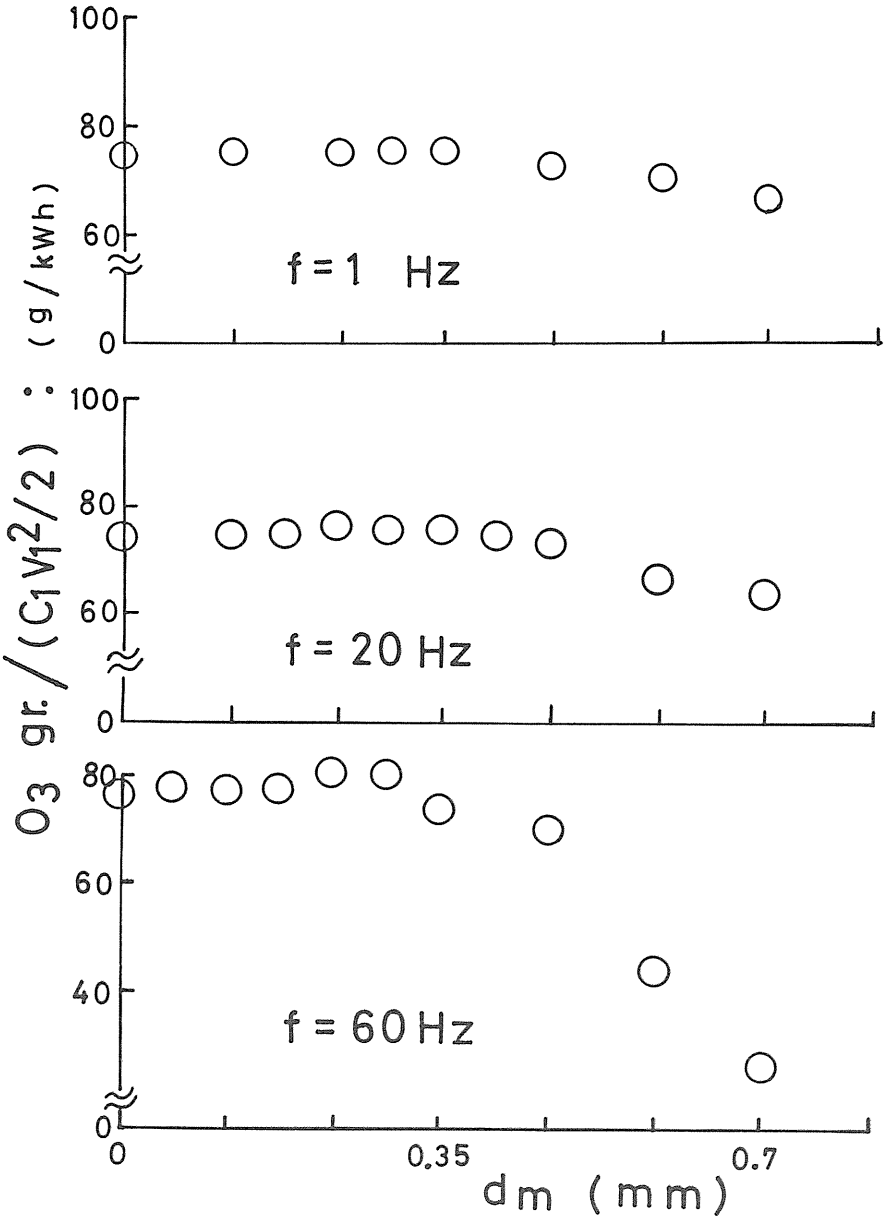

Fig. 9. 10 Series gap spacing d_m vs. efficiency of ozone generation as a parameter of frequency of discharge

flow rate of 2 l/min and $C_1 = 167$ pF ($C_s = 150$ pF) and $C_1 = 250$ pF ($C_s = 200$ pF), the efficiency of the ozone production was almost constant (~ 60 g/kWh and ~ 80 g/kWh respectively) up to f = 60 Hz (Fig. 9. 9). The influence of the gap spacing d_m of the gap G_m on the efficiency was also observed in air with $C_1 = 250$ pF, $C_s = 200$ pF. At the operation with low frequency ($f \leqq 20$ Hz), the efficiency was not changed so much in the range of $d_m = 0$–0.7 mm but, it was decreased rapidly at $d_m = 0.5$ mm at f = 60 Hz (Fig. 9. 10). Though the use of the series gap G_m is not effective on the ozone generation at the lower capacitance ($C_1 < 800$ pF), it is effective at $C_1 \geqq 800$ pF due to the improvement of the discharge and also effective for the ozone generation as shown in Fig. 9. 11. The used parameters are $C_1 = 800$ pF, main gap spacing d = 5 mm, $C_s = 100$ pF, $V_1 = 20$ kV, and the flow rate of air of 2 l/min. The number of trigger electrodes distributed around the surface of the cathode is twelve and the diameter of the dielectrics which covers the trigger electrode is 3 mm. The efficiency of the ozone generation as a function of the capacitance C_1 is shown in Fig. 9. 12, when the main gap spacing d is changed. In this case, the capacitance C_s which is connected to the trigger electrode is optimized. For example, at fixed values of $C_1 = 250$ pF, $V_1 = 20$ kV, flow rate of air = 2 l/min and $d_m = 0$ mm, the generated ozone is measured as a function of the capacitance C_s and the optimum value of C_s is found. Both the breakdown voltage across the main electrode V_{AK} and the input energy into the dielectrics ($= \int v_t(t) I_t(t) dt$) in the trigger circuit also are shown in the figure. Where, $v_t(t)$ and $I_t(t)$ are the voltage between the cathode and the trigger electrode and the trigger current respectively. When the number of the trigger electrode is increased from twelve to twenty four, the efficiency is improved a little at larger capacitance C_1 as shown in Fig. 9. 13.

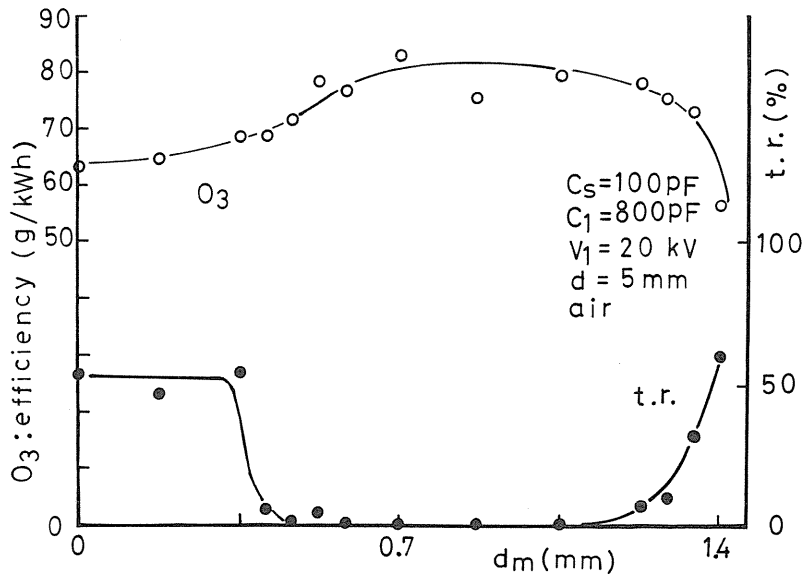

Fig. 9. 11 Efficiency of ozone generation and glow-to-arc transition rate vs. series gap spacing at V_1=20 kV, C_1=800 pF, C_s=100 pF and d=5 mm in air

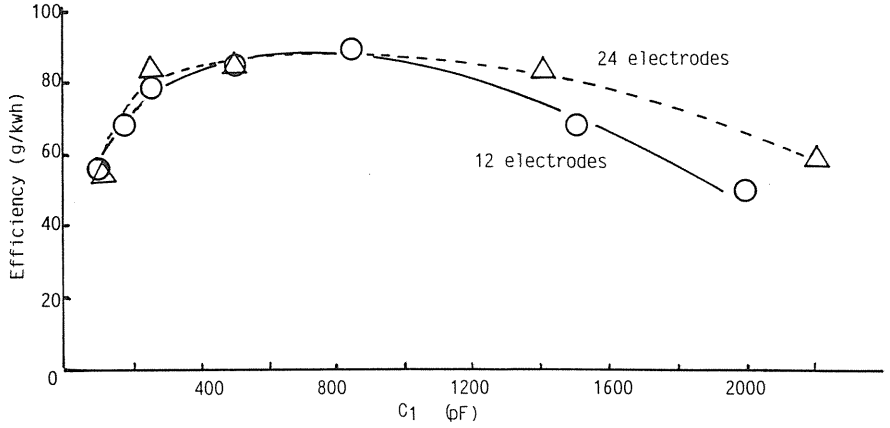

Fig. 9. 12 Efficiency of ozone generation as a function of capacitance C_1 for different number of trigger electrodes

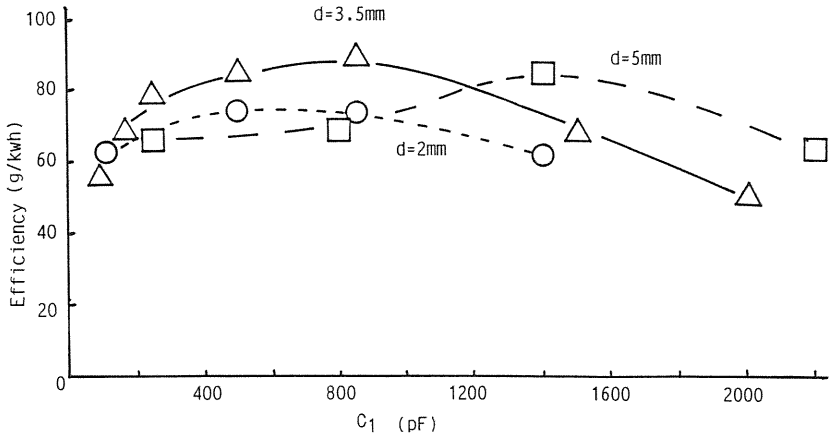

Fig. 9. 13 Efficiency of ozone generation as a function of capacitance C_1 for different main gap spacing (D=2, 3.5, 5 mm)

9. 4. *Conclusions*

The coaxial cylindrical double discharge type ozonizer has been proposed and the characteristics of it have been measured. According to the experimental results, it was confirmed that this type of ozonizer was useful for the efficient ozone production or atomic oxygen.

Acknowledgment

The authors wish to express their appreciation to N. Oyama, Y. Tachioka, M. Hayashi and S. Takase for their technical assistance.

They also are grateful to the members of the ozonizer group of the Fuji Electric Co. Ltd. for the useful discussions.

A part of this work was supported by the Grant-in-Aid for Scientific Research from the Ministry of Education, Science and Culture of Japan. This work was also supported a part by the Institute of Space and Astronautical Science (ISAS) of Japan.

References

1) Salge, J. and Brauman, P., 4th Int. Symp. Plasma Chemistry, (1979)735.
2) Salge, J., Karner, H., Labrenz, M., Scheibe, K. and Braumann, P., 6th Int. Conf. Phenomena in Ionized Gases, (1980)94.
3) Hogan, L.G. and Burch, D.S., J. Chem. Phys., 65(1976)894.
4) Tabata, N., Tanaka, M. and Yagi, S., Trans. IEE Japan, 97B(1977)100.
5) Yagi, S., Tanaka, M. and Tabata, N., Trans. IEE Japan, 97A(1977)609.
6) Tabata, N., Yagi, S. and Tanaka, M., Trans. IEE Japan, 98B(1978)123.
7) Meyer, J.A., Klosterboev, D.H. and Setser, D.W., J. Chem. Phys., 55(1971)2084.
8) Yagi, S., Tanaka, M. and Tabata, N., J. Phys., D: Appl. Phys.,12(1979)1509.
9) Akiyama, H., Takamatsu,T., Yamabe, C. and Horii, K., J. Phys. E: Sci. Instr., 17(1984)1014.
10) Yamabe, C.,Akiyama, H. and Horii, K., 7th Int. Symp. Plasma Chem., Eindhoven, 1(1985)1327.
11) Yamabe, C., Hayashi, M., Tachioka, Y. and Horii, K. , 8th Int. Symp. Plasma Chem., Tokyo, 2(1987)742.
12) Eliasson, B., Hirth, M. and Kogelschatz, U., 7th Int. Symp. Plasma Chem., Eindhoven, 1(1985)339.
13) Yamabe, C., Hayashi, M., Horii, K., and Sakai, E., 5th Technical meeting on Plasma Processing (in Japanese), (1988)37.
14) Yamabe, C., Takase, S., Horii, K., Sakai, E. and Tanaka,K., 2nd Japanese Symp. Plasma Chem., Nagoya (1989)167.
15) Yamabe, C., Takase, S., Hayashi, M., Horii, K., Sakai, E. and Tanaka, K., 2nd Int. Symp. High Pressure Low Temp. Plasma Chemistry, Poland (1989)39.
16) Yamabe, C.,Hayashi, M., Horii, K. and Sakai, E., 9th Int. Conf. Gas Discharges and their Applications, Venezia, (1988)407.
17) Hayashi, M., Yamabe, C. and Horii, K., Annual Meeting of Tokai chapter, IEE, (1987)15.
18) Yamabe, C., Takase, S., Horii, K., Sakai, E. and Tanaka, K., 9th Int. Symp. Plasma Chem., 2(1989)745.